Synaptic Connectivity in Micropatterned Networks of Neuronal Cells

Dissertation
zur Erlangung des Grades
"Doktor der Naturwissenschaften"

am Fachbereich Biologie
der Johannes Gutenberg-Universität
in Mainz

Angela Katrin Vogt
geboren in Sindelfingen

Mainz 2003

There's plenty of room at the bottom.

<div align="right">R.P. Feynman</div>

1. Introduction

The presented thesis describes the formation of synaptically coupled neuronal networks on micropatterned substrates. In the introductory chapter, an overview over this work will be given as well as some background information on the subject of neuronal physiology and neuronal patterning. Part 1.1 will explain the motivation for the chosen approach and describe how the work fits into the context of other efforts conducted in the field. Part 1.2 will give an outline of the questions that were addressed and summarise the major findings while part 1.3 will describe how the thesis is organised. In part 1.4, some general facts on the subject of neuronal physiology that are important for the understanding of the conducted experiments will be presented. Part 1.5 will deal with the specific topic of neuronal patterning and part 1.6 with preceding work performed in this group that was of importance as a starting point for this thesis.

1.1 Motivation

Men ought to know that from the brain, and from the brain only, arise our pleasures, joys, laughter and jests, as well as our sorrows, pain, griefs and tears. Through it, in particular, we think, see, hear, and distinguish the ugly from the beautiful, the bad from the good, the pleasant from the unpleasant[...].

attributed to Hippocrates, fifth century B.C. [Kandel, 2000]

The brain as the central organ responsible for mental processes like consciousness, perception, memory and emotion has attracted the interest of scientists for centuries. However, investigation of brain function is impeded by the overwhelming complexity of this organ: A human brain on average consists of 10^{11} neurons that are connected through approximately 10^{14} synapses. The detailed analysis of neuronal signalling *in vivo* is therefore an extremely difficult if not impossible task. The story is complicated even further by the presence of about 10^{12} glia cells that for a long time were thought to play a merely supportive

role in providing nutrients and structure to neurons. Recently, these cells began to emerge as being involved in signalling processes themselves [Kast, 2001].

The analysis of brain function has been performed on different complexity levels: On the one end of the scale lie different tomography techniques that are used to image physiological activity of different brain areas. These investigations have been useful in assigning specific mental actions, such as the processing of visual or auditory stimuli, to particular parts of the brain. The other extreme is represented by studies of single neurons in the cell culture. From work on the single cell level, much has been learned about principles of neuronal signal formation and conduction.

Several approaches have been taken to bridge the gap between the analysis of single cell behaviour on the one hand and neuronal signalling in the whole brain on the other hand. Starting in the early 1970s, several groups began to grow networks of neuronal cells on extracellular recording devices such as field effect transistors (FETs) or multielectrode arrays (MEAs) [Thomas, 1972; Gross, 1977; Pine, 1980; Jimbo, 1993; Thiebaud, 1997; Ingebrandt, 2003]. These allowed to record electrical signals from some of the cells in the network (namely those sitting on the sensitive parts of the recording device) for hours and days. Many insights into network behaviour and the development of correlated activity patterns have been gained through these studies. However, the networks grown on extracellular recording devices are still too complex to gather information on the behaviour of single synapses. In other words, the resolution at which a network can be analysed is still too low for the investigation of many aspects. Also, the forming network architecture cannot be manipulated, such that it is not possible to explore the impact of different connectivity patterns on network behaviour. Network architecture and principles in neuronal interconnectivity are believed to be crucial in the formation and shaping of rhythmic activity [Muller, 1997; Misgeld, 1998; Manor, 1999].

Addressing these issues, the approach of patterned neuronal cell culture emerged. Patterned cell culture is performed by using structured surfaces that direct neuronal adhesion and
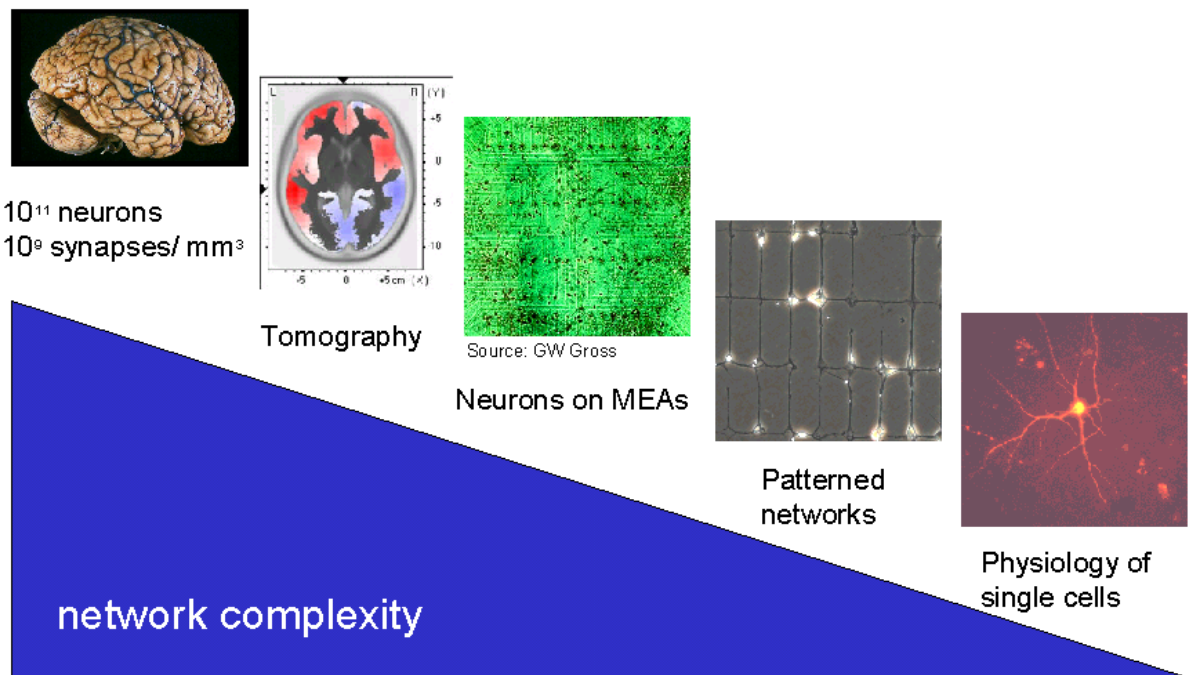
connectivity to predefined areas and pathways. With this approach, the formation of neuronal networks of a dramatically reduced complexity is feasible (Figure 1-1). Such networks are very useful in the study of synapse behaviour, as no input from outside of the investigated circuit overlays the signals. The interference by such signals is described as a problem in many *in vivo* studies, and some investigators apply drugs to silence particular synapse types in order to investigate others [Varela, 1999]. As the application of drugs can have multiple side effects, this approach is somewhat problematic.

A system in which neurons comply with the predefined network geometry while being physiologically intact and connecting through chemical synapses as they would under *in vivo* conditions is an ideal model system for the behavioural analysis of neuronal networks.

Neuronal patterning has been attempted by many groups, but it has been proven difficult to achieve a high compliance to the pattern without interfering negatively with cell behaviour. Most highly compliant networks are reported on very young cultures, which are too immature for electrophysiological experiments, while those groups who report electrophysiological activity and synapse formation have a reduced compliance with the pattern, such that uncontrolled connectivity results.

The presented thesis achieved the formation of neuronal networks highly compliant to an underlying micropattern, which is stable over two to three weeks, allowing the formation of synaptic connections.

Studying Neuronal Networks on Different Levels of Complexity

10^{11} neurons
10^9 synapses/ mm^3

Tomography

Neurons on MEAs
Source: GW Gross

Patterned networks

Physiology of single cells

network complexity

Figure 1-1: *In vivo* forming neuronal networks are difficult to study because of their enormous complexity. Different approaches have been taken to unravel signal transduction between neurons and investigate network behaviour: Tomography techniques and extracellular recordings of randomly forming networks on the one hand and physiological studies on single cells on the other hand. An innovative approach lies in the growth of neuronal networks on micropatterned substrates, which allow single cells to connect in a highly controlled fashion. This technique allows the study of synapses on the single cell level.

1.2 Outline of Investigations

The presented thesis describes the formation of functional neuronal networks on an underlying micropattern. Small circuits of interconnected neurons defined by the geometry of the patterned substrate could be observed and were utilised as a model system of reduced complexity for the behaviour of neuronal network formation and activity.

The first set of experiments was conducted to investigate aspects of the substrate preparation. Micropatterned substrates were created by microcontact printing of physiological proteins onto polystyrene culture dishes. The substrates displayed a high contrast between the repellant background and the cell attracting pattern, such that neurons seeded onto these surfaces

aligned with the stamped structure. Both the patterning process and the cell culture were optimised, yielding highly compliant low-density networks of living neuronal cells.

In the second step, cellular physiology of the cells grown on these substrates was investigated by patch-clamp measurements and compared to cells cultivated under control conditions. It could be shown that the growth on a patterned substrate did not result in an impairment of cellular integrity nor that it had an impact on synapse formation or synaptic efficacy. Due to the extremely low-density cell culture that was applied, cellular connectivity through chemical synapses could be observed at the single cell level.

Having established that single cells were not negatively affected by the growth on patterned substrates, aspects of network formation were investigated. The formation of physical contact between two cells was analysed through microinjection studies and related to the rate at which functional synaptic contacts formed between two neighbouring cells. Surprisingly, the rate of synapse formation between physically contacting cells was shown to be unaltered in spite of the drastic reduction of potential interaction partners on the micropattern.

Additional features of network formation were investigated and found consistent with results reported by other groups: A different rate of synapse formation by excitatory and inhibitory neurons could be reproduced as well as a different rate of frequency-dependent depression at excitatory and inhibitory synapses. Furthermore, regarding simple feedback loops, a significant enrichment of reciprocal connectivity between mixed pairs of excitatory and inhibitory neurons relative to uniform pairs could be demonstrated. This phenomenon has also been described by others in unpatterned cultures [Muller, 1997] and may therefore be a feature underlying neuronal network formation in general.

Based on these findings, it can be assumed that inherent features of neuronal behaviour and cellular recognition mechanisms were found in the cultured networks and appear to be undisturbed by patterned growth. At the same time, it was possible to reduce the complexity of the forming networks dramatically in a cell culture on a patterned surface. Thus, features of

network architecture and synaptic connectivity could be investigated on the single cell level under highly defined conditions.

1.3 Organisation of this Thesis

This work is organised in three major parts. Part one gives an introduction to the subject of cellular patterning as well as to some basic features of neurobiology essential to understand the conducted experiments. Part two describes and explains the methods and techniques that were applied. Part three presents and discusses the acquired results. These start with the characterisation of micropatterned substrates and the optimisation of the cell culture conditions (chapters 3 -5). Next, electrophysiological measurements were carried out to characterise the cells growing on patterned substrates (chapter 6). In the last two chapters (7 and 8), aspects of cellular connectivity and network behaviour in a simplified system are described. Chapter 9 will summarise the acquired results and provide an outlook for future experiments.

1.4 Neuronal Physiology

The following paragraphs briefly describe some aspects of neuronal physiology that are of importance for the understanding of the conducted experiments. For more detailed descriptions, the reader is referred to the literature [Kandel, 2000; Nicholls, 2001; Hille, 2001].

1.4.1 Resting Potential

Maybe the most striking feature about neuronal cells is their electrical excitability. In the resting state, a neuron displays a negative potential with respect to the surrounding tissue. This potential is due to the following two factors: First, to a difference in ionic composition between the cytoplasm and the extracellular fluid and second, to ion specific channels in the cell membrane.

Several ion species experience a steep concentration gradient between inside and outside of the cell. The most important ones are Sodium, Chloride and Calcium which are more abundant outside of the cell and Potassium which is strongly enriched within the cell. The concentration differences are created and maintained by membrane integral ion pumps. The most prominent one among these is the Na^+-K^+ exchange pump which exchanges three intracellular Sodium ions for two extracellular Potassium ions under the consumption of ATP. In addition to active pumps, the membrane contains a large variety of channel proteins that are passively permeable to different ion species. Most of these channels are regulated, but some are also open in the resting state. The majority of these are selectively permeable to Potassium. Through these channels, potassium is able to flow out of the cell along the concentration gradient, resulting in a loss of positive charge from the cell. A much smaller number of Sodium channels is open at rest, allowing a small amount of Sodium to flow in. However, as the permeability for Sodium is far lower than that for Potassium, a negative potential within the cell builds up, eventually holding back Potassium ions through electrostatic forces. The third type of channels open at rest is selective for Chloride, which again contributes to the negative membrane potential by flowing into the cell. Thus, every ion species experiences two competing forces, an electrical driving force depending on the potential across the membrane and a chemical one depending on the concentration gradient

(Figure 1-2). For a single ion species, the potential at which the equilibrium between the two forces is reached can be calculated using the Nernst Equation:

$$E_x = \frac{RT}{zF} \ln \frac{[X]o}{[X]i}$$

E_x = Equilibrium Potential for the ion x
R= Gas constant
T= absolute temperature
z= valence of the ion X
F= Faraday's constant
[X]o= Concentration of X outside the cell
[X]i= Concentration of X inside the cell

Equation 1-1: Nernst equation

The Nernst Equation can be used to calculate the resting potential in cells in which only one type of channel is open at rest and thus only one type of ion species contributes to the resting potential. This is the case in glia cells, which only open Potassium channels in the resting state. When more than one ion species contributes to the resting potential as it occurs in neurons, the relative permeabilites of the membrane for each type of ion need to be taken into account. The resting potential can then be calculated with the Goldman Equation:

$$V_m = \frac{RT}{F} \ln \frac{P_K[K]o + P_{Na}[Na]o + P_{Cl}[Cl]i}{P_K[K]i + P_{Na}[Na]i + P_{Cl}[Cl]o}$$

V_m= Membrane potential
$P_{K/Na/Cl}$= Relative permeability of the membrane for the K/Na/Cl

Equation 1-2: Goldman equation
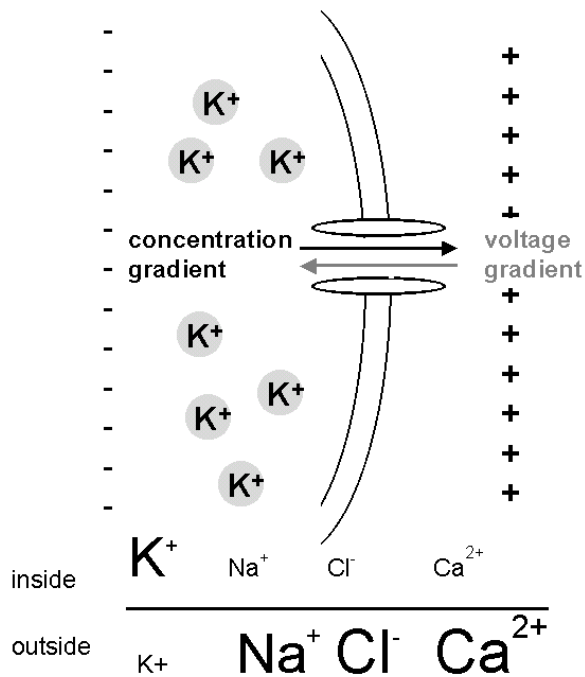
Figure 1-2: Creation of the resting potential (scheme). Some ion species experience a steep concentration gradient over the cell membrane (listed in the lower part of the picture); in the cartoon, only Potassium is depicted for simplicity. Potassium selective channels are open in the resting state, allowing this ion to leave the cell following the concentration gradient. As no other ion species can pass the channel, the loss of positive charge cannot be compensated for such that a negative potential builds up. Equilibrium is reached when the potential difference exerts the same force on the Potassium ions as the chemical driving force arising from the concentration gradient. Clearly, the membrane potential can change drastically when additional channels permeable to other ion species are opened.
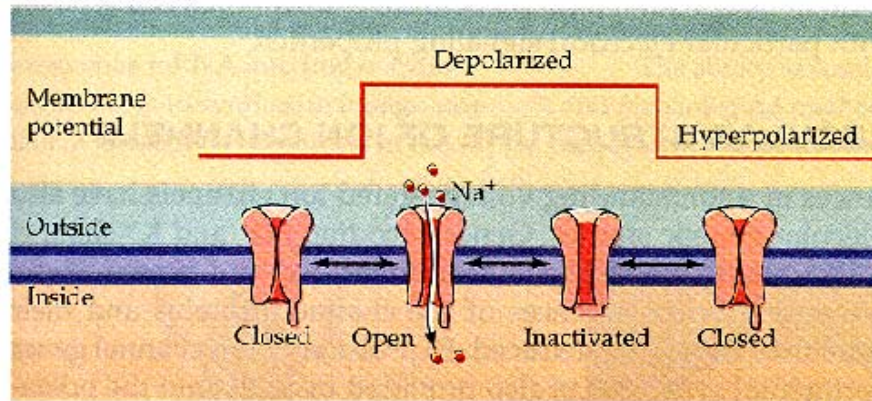
1.4.2 Action Potentials

The ability of neurons to initiate and propagate electrical signals in the form of transient changes in the membrane potential (action potentials) is due to the activity of regulable ion channels. An action potential is initiated through depolarisation of the neuron by an external stimulus. When the neuron is depolarised above a critical threshold, voltage-sensitive Sodium channels in the membrane open. This opening dramatically changes the membrane permeability for Sodium which flows into the cell and causes a steep rise in the membrane potential resulting in a spike which is called an action potential. Thus, depolarisation represents a positive feedback loop as it induces further depolarisation. However, the mechanism is self-limiting as the Sodium channels automatically close after about 2 ms

12

independent of whether the membrane is depolarised or not. After one cycle of opening and closing, the Sodium channels are refractory, which means that they can not be activated. This state is only overcome through repolarisation of the membrane, thus, repeated activation of the channels requires intermittent repolarisation. An additional mechanism limiting the duration of an action potential lies in a particular type of voltage-gated Potassium channels (called the delayed-rectifier) that opens upon depolarisation but with a slower time course than the Sodium channel mentioned above. In contrast to the voltage-gated Sodium channel, this type of Potassium channel only closes upon repolarisation of the membrane, thus ensuring that the cell returns to the resting potential. After an action potential, the original relative concentrations of Sodium and Potassium are reestablished by the Na^+-K^+ exchange pump. Figure 1-3 shows the contributions of Sodium and Potassium channels to the different phases of an action potential.

Action potentials can be propagated along the axon of a cell. This occurs without a loss in signal amplitude: An action potential initiated at one point of the axon passively depolarises the neighbouring membrane area through electrotonic conduction. Membrane patches in close vicinity can be depolarised sufficiently to activate voltage-gated Sodium channels and thus induce a second action potential through the positive feedback mechanism described above. This second action potential again depolarises neighbouring patches allowing the signal to be propagated without losses even along long distances. Backpropagation is impeded through refractoriness of Sodium channels after firing. When the signal arrives at the end of the axon, the signal can be passed on to the next cell through a synapse.
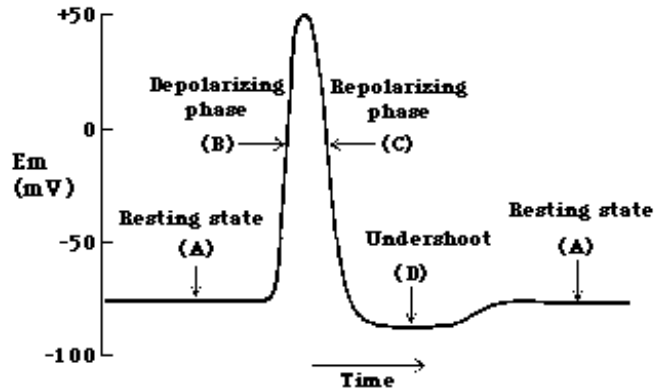
Na⁺ CHANNEL
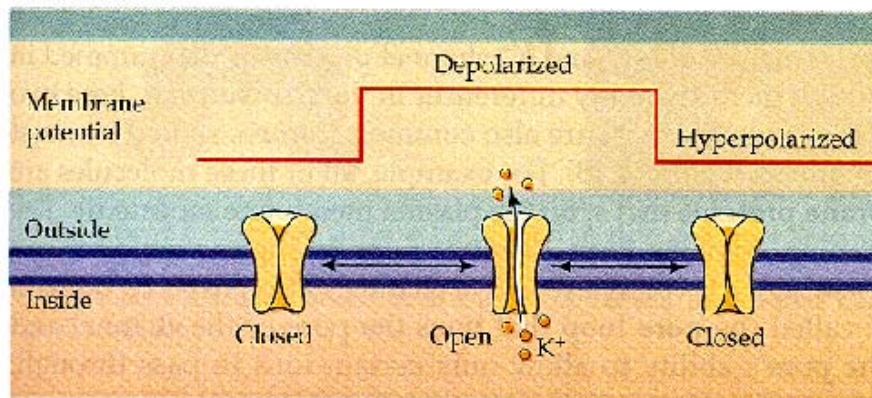
A)

B)

Figure 1-3: Conductance changes in the cell membrane during an action potential. A) Upon a depolarising stimulus, voltage-gated Sodium channels open, allowing positive charge to flow into the cell. This channel inactivates after several milliseconds. A second type of voltage-gated membrane channel, which is permeable to Potassium, opens shortly after the Sodium channel and remains open throughout the depolarisation. The opening of this channel leads to a loss of positive charge from the cell and thus favours repolarisation. B) The different phases of an action potential. The depolarising phase (B) is attributed to the opening of voltage-gated Sodium channels which leads to a steep rise in the membrane potential. The repolarising phase (C) is due to the closing of Sodium channels and concurrent opening of voltage-gated Potassium channels. The undershoot phase (D) is characterised through closed Sodium channels while the Potassium channels are still open. The resting state is achieved again when the voltage-gated Potassium channels are closed. Adapted from [Kandel, 2000].

14

1.4.3 Synapses

Two major types of synapse have been described, electrical and chemical synapses. These two types are clearly distinct in structure and functionality. Electrical synapses, which are also called gap junctions, consist of a pore spanning the lipid bilayer of two adjacent cells. This pore (also termed "connexon") has an internal diameter of about 2 nm and thus is large enough for many ions and small metabolites to pass. Each connexon is composed of six subunits arranged in a circle. Identical sets of six subunits in the two cells are paired to form one channel as shown in Figure 1-4. Gap junctions have multiple functions in the organism, the conduction of electrical signals between excitable cells being only one. Electrical synapses between neurons serve to transduce signals directly with almost no time delay and are therefore involved in actions that need to be fast, like flight reflexes. Additionally, electrical connectivity plays an important role in the synchronisation of oscillatory activity in the brain [Galarreta, 1999]. Most electrical synapses are symmetrical in structure, such that signal conduction occurs equally well in both directions although curiously, the first description of an electrical synapse was made on a rectifying channel that conducted signals only in one direction [Furshpan, 1959].
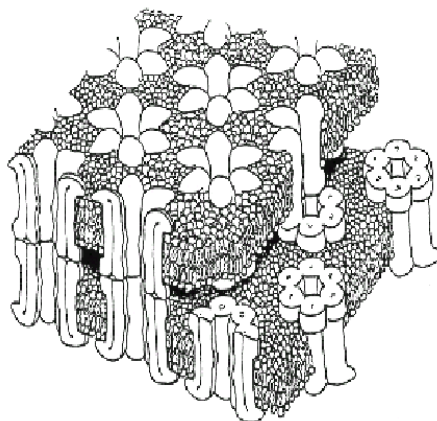
Figure 1-4: Gap junctions consist of two sets of six protein subunits arranged in a circle in the connected cells. Identical subunits are apposed to form one conductive channel (after [Makowski, 1977]).

15

The second major type is the chemical synapse. Typically, chemical synapses form between the axon of the presynaptic cell and a dendrite of a second postsynaptic cell. This structure does not allow the direct flow of current as the two cells are separated through a gap of about 30 nm, the synaptic cleft. A chemical synapse is strictly asymmetric, such that signalling occurs in a unidirectional fashion from pre- to postsynaptic cell only. When an action potential travelling down the axon of the presynaptic cell reaches the presynaptic terminal, transmitter molecules are released into the synaptic cleft. This behaviour is mediated through voltage-gated Calcium channels in the presynaptic terminal that are activated by the incoming action potential. Calcium influx in turn is the trigger for transmitter-filled synaptic vesicles to fuse with the presynaptic membrane and release transmitter molecules into the synaptic cleft. These can bind to receptors in the postsynaptic cell and thus activate them, as depicted in Figure 1-5. Signal transmission at a chemical synapse occurs with a time delay of several ms which arises due to the time it takes to release the synaptic vesicles from their anchorage in the cytoskeleton and to fuse with the presynaptic membrane.
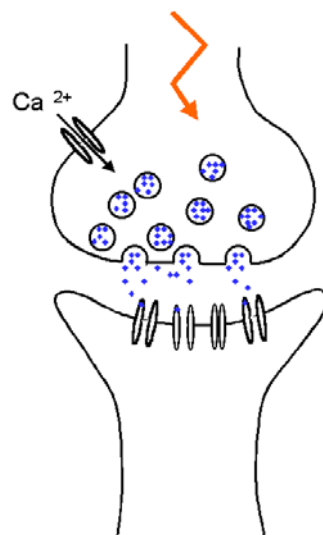
Figure 1-5: Chemical synapse. An incoming action potential in the presynaptic terminal activates voltage-gated Calcium channels, inducing an influx of Calcium. The Calcium signal triggers the fusion of synaptic vesicles with the presynaptic membrane, releasing stored transmitter molecules into the synaptic cleft. These can bind to receptors in the postsynaptic cell. Ionotropic receptors consist of ion channels that typically open upon ligand binding. This opening leads to an ion flux which can de- or hyperpolarise the postsynaptic cell, depending on which types of transmitter and receptor are present at the synapse.

Different types of synapses exist that use different types of transmitter. Ionotropic receptors (as opposed to metabotropic receptors which couple to intracellular signalling systems and are not considered here) represent ion channels that typically undergo a conformational change upon transmitter binding, which leads to their opening. Depending on the ion species the channel is permeable to, channel opening can either depolarise or hyperpolarise the postsynaptic cell. Therefore, chemical synapses are classified as either excitatory (when channel opening induces depolarisation) or inhibitory (when hyperpolarisation is transmitted). The synapses formed by one neuron always use the same type of transmitter.

The major excitatory transmitter applied in the central nervous system is glutamate, the major inhibitory transmitters are γ-aminobutyric acid (GABA) and glycine. The ionotropic GABA receptor ($GABA_A$) as well as the receptor for glycine are selectively permeable to anions, of which Chloride is the most prominent. Thus, the opening of this channel hyperpolarises the cell (although under special circumstances, e.g. after repetitive activation, the intracellular Chloride concentration may shift, such that the reversal potential for Chloride becomes more positive than the resting potential. In this case, an opening of Chloride channels causes depolarisation. Similarly, GABA has been shown to behave as an excitatory neurotransmitter in the embryonic brain, where the relative concentrations of intra- and extracellular Chloride are different from the adult organism [O'Donovan, 1999]).

Different subtypes of ionotropic glutamate receptors with different permeabilities have been described. These can be divided into two major classes, characterised by the compounds that can act as selective inhibitors on these receptors: NMDA receptors (which are named after their specific agonist N-methyl-D-aspartate NMDA), that can be blocked by the drug APV (2-amino-5-phosphonovaleric acid) and non-NMDA receptors, which can be subdivided into kainate and α-amino-3-hydroxy-5-methyl-4-isoxalone proprionic acid (AMPA) receptors, again named after specific agonists. Non-NMDA receptors are specifically blocked by 6-Cyano-7-nitroquinoxaline-2,3-dione (CNQX). NMDA and non-NMDA play very different

roles in synaptic signal transmission, which depend strongly on their gating mechanisms. The non-NMDA receptors transmit the majority of the postsynaptic current: This group of receptors is permeable to both Sodium and Potassium. Channel opening upon glutamate binding leads to an ion flux that in sum causes postsynaptic depolarisation.

NMDA receptors display two distinguishing features: First, they only open upon glutamate binding when the cell is depolarised concomitantly. This is due to an extracellular Magnesium ion which blocks the pore at a negative membrane potential, but which is expelled electrostatically from it when the membrane is depolarised. The NMDA receptor therefore only participates in the later phase of a strong depolarising signal, when membrane depolarisation has been achieved through the action of non-NMDA receptors.

Second, the channel is permeable not only to Sodium and Potassium, but also to Calcium. Intracellular concentrations of free Calcium are about four orders of magnitude lower than free Calcium in the extracellular fluid, therefore an opening of Calcium permeable channels causes a strong influx of this ion, which significantly changes the concentration of intracellular Calcium. In addition to its immediate function of a charge carrier, Calcium can act as a second messenger. Calcium signals triggered by NMDA receptors are thought to be important in synaptic plasticity, which will be described in the next subchapter.

1.4.4 Synaptic Plasticity

Neuronal networks are by no means a static structure. Although synapse formation occurs predominantly during early phases of development, neuronal circuits are constantly being refined throughout an organism's lifetime. This occurs both on the level of synapse formation or elimination and on the level of variations in synaptic strength. The ability of single synapses to modulate their strength in an activity-dependent fashion is a prerequisite for

learning and memory formation. Although a fascinating topic, the mechanisms leading to the multitude of observable synaptic modifications are only understood to a limited extent.

Modulations in synaptic strength can arise on different levels and timescales: Changes occurring directly after the applied stimulus and persisting for a relatively short period of time are called short-term changes (as opposed to long-term changes which will be discussed shortly). Depending on whether the modulation causes an increase or decrease of the postsynaptic signal, these changes are termed facilitation / augmentation or depression. Short-term changes are known since the 1950s [delCastillo, 1954] [Mallart, 1967].

Synaptic facilitation is observed when the presynaptic neuron is subjected to a short train (5-10 pulses) of stimuli in rapid succession. Test stimuli applied shortly after the train induce a postsynaptic potential that is substantially higher than that seen before stimulation, an effect that was shown to be due to increased transmitter release [delCastillo, 1954]. This increase was later attributed to residual Calcium remaining in the presynaptic terminal between the pulses, such that intracellular Calcium built up during the stimulus train. As transmitter release correlates with both the steady-state and the transient concentration of Calcium, residual Calcium potentiated transmitter release probability [Katz, 1968]. (Calcium binding to the release machinery functions in a cooperative manner. Therefore occupancy of one binding site in the steady-state, which may occur at an elevated concentration of Calcium, facilitates binding upon a Calcium spike induced by an action potential [Thomson, 2000]). Synaptic facilitation decays in the range of several tens to hundreds of milliseconds.

A similar but longer lasting effect is synaptic augmentation. Augmentation is also Calcium dependent and inducible by conditioning trains of stimuli. Its induction is believed to be due to an accumulation of Sodium and Calcium (which both enter the presynaptic terminal with an action potential). As Calcium is – among other mechanisms – removed from the cell through Na^+-Ca^{2+} exchange, accumulation of Sodium slows down the extrusion of Calcium

from the cell, resulting in a sustainment of the elevated Calcium concentration, which explains the longer persistence of augmentation as opposed to facilitation [Thomson, 2000].

The one lasting longest among the "short term changes" is the so called posttetanic potentiation, which can be induced by longer trains of stimuli (in the range of several thousand pulses). Again, the result is a strengthening of the postsynaptic signal, which – in contrast to facilitation which decays within several hundred milliseconds and augmentation which decays after seconds– can last for minutes to hours and also has a slower onset. Similarly to facilitation and augmentation, the effect is presynaptic in origin and dependent on Calcium entry to the presynaptic terminal [Rosenthal, 1969], although the mechanism is not completely understood. An interesting hypothesis suggests that a transient saturation of the cellular Calcium buffer systems (mainly the endoplasmatic reticulum and mitochondria) in the presynapse leads to an elevation of the concentration of free Calcium for a longer period than that seen after single action potentials [Kandel, 2000]. Calcium is an important second messenger in eucaryotic cells. In neurons it acts on a number of different target molecules apart from those involved immediately in vesicle release. While the Calcium spike typically induced through a single action potential is too short in duration for an interaction with most of these targets, a sustained elevation allows their activation. Downstream targets of Calcium include a large range of signalling molecules such as Calcium / Calmodulin dependent protein kinase (CaMKII). This enzyme has been shown to be involved in both posttetanic potentiation [Ohno, 2002] and in several forms of long-term synaptic plasticity, which are discussed below [Elgersma, 2002]. Other targets that have been implicated in synaptic plasticity are Calmodulin itself [Bi, 2001] and Calcineurin [Bi, 1998].

The phenomenon contrary to facilitation, synaptic depression, can also be induced by repetitive stimulation and occurs only in strong synapses with a large quantal transmitter release. The underlying mechanism is not clear but also seems to be presynaptic in origin. The fact that a large amount of transmitter release is necessary for its induction led to the

assumption that synaptic depression may be caused by a depletion of releasable synaptic vesicles in the presynaptic terminal [Mallart, 1968; Thomson, 2000].

Short-term changes have mostly been investigated in the peripheral nervous system although they have also been described in the brain [Nicholls, 2001]. Long-term changes on the contrary are predominantly studied in the hippocampus where they have been described first [Bliss, 1973]. These can last for hours to days and are widely believed to be a key feature in the cellular basis of learning and memory formation [Malenka, 1999].

Long-term potentiation (LTP) and long-term depression (LTD) occur as a result of correlated or uncorrelated activity of two coupled neurons. A mechanism that strengthens synapses between synchronously active neurons was first postulated by the psychiatrist Donald Hebb in 1949: "When an axon of a cell A is near enough to excite cell B or repeatedly takes part in firing it, some growth or metabolic change takes place in both cells such that A's efficiency, as one of the cells firing B, is increased" [Hebb, 1949]. These rules later were extended, generalised and mathematically formulated to the "Hebbian rules" of synaptic modification [Bienenstock, 1982].

Experimentally, LTP was described for the first time in the 1970s through the famous work of Bliss and Lomo [Bliss, 1973] who were able to show that repetitive activation of glutamatergic synapses in the hippocampus of an anaesthetised rabbit resulted in an increase of the postsynaptic potential that lasted for several hours. Since then, the concept of activity dependent synaptic modifications strengthening connectivity between synchronously firing neurons and attenuating connectivity between asynchronously firing ones, has been enormously refined, revealing time windows critical for LTP / LTD induction as well as spatial specificity and associative features [Bi, 2001].

In spite of an enormous interest in the subject, the exact mechanisms leading to LTP or LTD are only partially understood. Even the seemingly simple question whether the effect leading to an increase of the transmitted signal stems from changes on the presynaptic or the

postsynaptic side is still being debated [Sanes, 1999; Kullmann, 1995; Lopez, 2001; Madison, 1991]. Investigators favouring a presynaptic mechanism believe that that the amount of transmitter released per incoming action potential is increased as it occurs in facilitation and augmentation [Zakharenko, 2001; Thomson, 2000], while those in favour of a postsynaptic mechanism report evidence for the recruitment of extra AMPA receptors (which mediate most of the postsynaptic current) to the postsynaptic density during LTP [Shi, 1999; Takumi, 1999; Lledo, 1998].

It is possible that both mechanisms contribute to the effect; in addition, the seemingly contradictory findings may partially be explained by the fact that different types of LTP exist which appear to be mediated differently. Most investigators agree that in the mammalian nervous system, there are at least two (and possibly more) different forms of LTP occurring in different cell types and involving distinct mechanisms [Malenka, 1999]. The first of these types, which was first described in the CA1 region of the hippocampus [Schwartzkroin, 1975], but later found in other brain areas as well [Nicoll, 1995] is dependent on the activation of postsynaptic NMDA receptors. NMDA receptors are a subtype of glutamate receptors that in contrast to the non-NMDA receptor are blocked at the resting potential, as explained in chapter 1.4.3 . They can only be activated by glutamate binding when the cell is concurrently depolarised by a separate stimulus relieving this block. NMDA receptors can therefore be regarded as coincidence detectors sensing synchronous activity of the pre- and the postsynaptic neuron which fits well with the predictions of Hebb's rule. An intriguing feature about NMDA receptors is that they are permeable to Calcium, which can act as a second messenger as described before. Calcium influx through NMDA receptors has been shown to be critical in the induction of LTP [Lynch, 1983].

The second form of LTP was first described in mossy fibres [Alger, 1976], which arise from dentate granule cells and form synapses with CA3 pyramidal cells region of the hippocampus. Therefore, this form is often called mossy fibre LTP although it has also been described in

peripheral synapses [Minota, 1991] but, interestingly, not in any other brain area so far [Nicoll, 1995]. Mossy fibre LTP has been shown to be independent of NMDA receptor activation, postsynaptic depolarisation and Calcium concentration in the postsynaptic terminal [Harris, 1986]. Instead, it appears to be mediated through Calcium entry to the presynapse and on the second messenger cAMP [Weisskopf, 1994].

Based on these findings, it is tempting to assume that NMDA receptor dependent LTP, which requires postsynaptic Calcium entry is also expressed through postsynaptic modifications, while the mossy fibre LTP, which depends on presynaptic Calcium entry would be mediated through presynaptic modifications. However, although electrical signals are transmitted unidirectionally from pre to postsynapse only, intercellular signalling molecules distinct from the transmitter molecules employed by the synapse have been reported that are transduced in a retrograde fashion from post- to presynapse [Bon, 2003; Makram, 1997; Sanes, 1999; Fitzsimonds, 1997], such that a signal initiated in the postsynapse can have an impact on the presynapse. Retrograde signalling has been shown several times to play a role in the context of LTP / LTD: Ganguly et al. found that postsynaptic NMDA receptor activation has an impact on voltage-gated Sodium channels (and thus on the firing threshold) in the presynapse [Ganguly, 2000] while Brocher et al. were able to demonstrate that postsynaptic Calcium influx is critically involved in a presynaptically mediated LTD mechanism [Brocher, 1992]. Thus, the induction of an effect in either the pre- or the postsynapse does not necessarily imply that it is also mediated through modifications in the same cell.

The induction of LTD curiously is also mediated through a Calcium dependent mechanism. It has been suggested that the amount and / or kinetics of Calcium signals are critical in determining whether potentiation or depression is induced.

The effects of synaptic plasticity described above all refer to the early phase of LTP (which occurs minutes and hours after activation). It should be noted that longer lasting changes (long-lasting LTP (L-LTP)) can also be induced that are stable for weeks and months. These

are dependent on transcriptional activation and the synthesis of new proteins. Of central importance in this context is the transcription factor cAMP / Ca^{2+} response element (CRE) binding protein (CREB) [Poser, 2001]. As this thesis did not investigate synapses in a timescale allowing transcriptional activation, L-LTP will not be reviewed here further.

Although most studies on LTP have been performed at glutamatergic synapses in the hippocampus, LTP and LTD have also been shown to occur in other brain areas such as the cortex [Kirkwood, 1993; Otsu, 1995]. Interestingly, LTP and LTD have been shown to be inducible in inhibitory synapses by the same protocols able to stimulate excitatory synapses [Shew, 2000; Ouardouz, 2000].

Most work on LTP induction has been done on the intact brain or slices thereof. Although this approach is extremely interesting in many respects, particularly with regard to the analysis of the interaction of defined cell types in specific brain areas, the enormous complexity of the mammalian brain makes the isolated observation of single synapses impossible. In many instances, pharmacological treatments were necessary for LTP induction in order reduce the input from other brain areas [Kirkwood, 1995]. An interesting approach for the investigation of synaptic plasticity on the single cell level was taken by Poo and colleagues, who induced LTP and LTD in very low density neuronal cultures. The neurons formed small isolated networks such that single synapses could be stimulated and analysed in patch clamp measurements [Bi, 1998; Bi, 1999; Ganguly, 2000; Fitzsimonds, 1997]. A similar approach was taken in this thesis on the small circuits grown on the micropattern and will be presented in chapter 8.

1.5 Neuronal Patterning

The approach of patterned cell cultures has been taken by several groups through different methods and pursuing a range of different aims. The following paragraph gives an overview over the history and the applications of cell patterning.

Being able to guide cellular migration and / or outgrowth by features of the underlying substratum is a promising approach in many scientific disciplines. It can be applied in tissue engineering or pharmaceutical screening as well as for the elucidation of fundamental biological questions regarding the question how cellular alignment and guidance function in the living organism. Different approaches have been taken to align cells to a microstructure. On the one hand, it is known since the 1960s that cells orient themselves with respect to topographical structures of the surface [Rosenberg, 1963; Curtis, 1997; Curtis, 1998; Merz, 2002]. On the other hand, chemical guidance cues have proven a high potential of guiding cellular adhesion and outgrowth; the investigation of this feature started around the same time as topographical patterning [Carter, 1965; Letourneau, 1975]. Of particular interest in this context were experiments that offered conflicting topographical and chemical cues to see which parameters determined the relative strength of a guidance signal [Britland, 1996].

In chemical patterning, cells are seeded onto a surface which offers permissive areas supporting adhesion while the rest of the surface is cell repellant. If the two surface types are to coexist in close vicinity, a high contrast is necessary in order to keep cellular adhesion restricted to the permissive parts.

A variety of different methods are available for the realisation of chemical patterns. One of the most prominent works in this field was performed by Kleinfeld et al. [Kleinfeld, 1988], who used photolithography to pattern silane surfaces with different types of permissive organic molecules. The group was able to show that neuronal cells preferably attached to areas patterned with amine groups, while adhesion to alkane chains was not supported. A

related technique was applied by Corey et al. [Corey, 1991], who performed patterning by laser ablation, such that protected areas retained a coating of polylysine, while the amine groups were lost from the irradiated areas.

Alternatively, patterns of organic molecules can be applied through microcontact printing, a technique that uses an elastomeric stamp to transfer the permissive molecules to an unpermissive background. The technique was originally developed by Kumar and Whitesides [Kumar, 1993] and has been used successfully in a range of studies [Wheeler, 1999; Scholl, 2000; Lauer, 2002]. As one of the central techniques applied in this study, it will be described in detail in chapter 2.3.

The systems described so far apply patterns of synthetic or natural adhesion molecules to a synthetic, highly cell repellant backgrounds in order to create a high contrast between the two areas and achieve a high compliance of cell adhesion. This is desirable in applications which aim at the creation of a patterned cell culture as such. An alternative application for patterned surfaces is more focused on the investigation of processes that are responsible *in vivo* for the guidance of cells. Such approaches apply stripes of different adhesive molecules in order to analyse which route is more attractive e.g. for outgrowing axons when two permissive choices are available [Lemmon, 1992].

Since the focus of this thesis lied in the creation of simplified neuronal networks to study synapse formation and behaviour in simplified circuits, a synthetic hydrophobic background was utilised. A variety of physiological and unphysiological adhesive molecules was applied by microcontact printing, thus including the investigation of physiological guidance cues into the study.

1.6 The Preceding Project

It was described in part 1.1 that the goal of the presented thesis lies in the creation of functional neuronal networks on micropatterned substrates. Since this work was performed in direct continuation of the PhD thesis of Dr. Lars Lauer [Lauer, 2001], it seems appropriate to briefly describe aspects of his work as the starting point of the work presented here, pointing out ideas that were adopted and others that were changed.

One of the major achievements of the quoted thesis was the optimisation of a patterned surface for the confined growth of neuronal cells. As a background, hydrophobic and thus cell repellent polystyrene culture dishes were used, onto which a pattern of the extracellular matrix protein laminin was applied by microcontact printing. The geometry of the grid pattern was optimised for the accurate placement of neurons to the desired adhesion areas: The nodes of the grid were made large enough to allow the adhesion of just one neuronal cell body. The lines of the grid had to be sufficiently broad to support the outgrowth of neurites, but thin enough to prevent cell bodies from adhering to them. This was accomplished with nodes ranging from 12-14 μm in diameter and lines with a width of 4-6 μm.

The applied cell culture protocol used neurons from the brain stem of embryonic rats. Thin slices of this brain area were immersed into cell culture medium, allowing neurons to migrate out of the slice onto the patterned surface, where they formed new connections with their respective neighbours on the pattern.

A strong confinement of neurons to the applied pattern could be demonstrated. The neurons were found to couple through gap junctions, but only very few formed chemical synapses. Since the presence of chemical synapses in a network is required to study network plasticity - which is the major aim of the project - this was the primary obstacle to be overcome in subsequent projects.

Aiming at a higher yield of chemical synapses, reasons for their lack in the described system were looked for. The following points were considered:

- Interactions of neurons with the extracellular matrix have been shown to have a profound impact on cellular development and even synapse formation [Letourneau, 1994; Son, 1999; Reichardt, 1991]. In this context, the question arose whether laminin, a protein known to favour axonal over dendritic development [Chamak, 1989; Lein PJ, 1989; Cestelli, 1992], is suitable for the growth of neuronal networks with a balanced amount of axons and dendrites. One part of this work therefore examines the impact that different inking solutions used in microcontact printing had on synapse formation.

- The brain stem may not be the most suitable brain region for the study of synaptic plasticity. The brain stem is continuous with the spinal cord and also organized similarly on a functional level. It serves to mediate sensations and motor control and is also involved in the coordination of some reflexes. Neurons of the brain stem tend more to innervate other areas of the brain - relaying incoming information - rather than to form synapses among each other. Since the aim of this project is the *in vitro* reconstitution of interconnected networks of cells mimicking signal processing and memory formation, it seemed reasonable to use cells from a brain area concerned with these functions *in vivo*. Therefore, in the presented study cortical cells were used.

- The cell culture medium used may not be ideal. Brewer at al [Brewer, 1993] determined the optimal concentration of several medium components for neuronal cell culture. Some of these concentrations were far different from the ones in the described system (e.g. $FeSO_4$, which was reported to be cytotoxic at concentrations above 0.2 µg/ml was present at 0.8 µg/ml). These culture conditions may have impaired cellular function sufficiently to prevent synapse

formation. In the presented work, the protocol recommended by Brewer et al. was applied, which also included a switch from brain slice to dissociated cell culture.

Since the confinement of neurons to the micropatterned surface had successfully been achieved, the patterning process and pattern geometry were adopted without changes.

Cell culture conditions were modified as described above: Cortex rather than brainstem was used as well as a different medium and cell culture protocol. Additionally, the suitabilities of different inks for micropatterning were evaluated.

These changes in combination with the established patterning method made it possible to grow highly geometrically confined neuronal networks of cells that were interconnected through electrical as well as through chemical synapses.

2. Applied Methods and Materials

The following chapter introduces the reader to the different techniques that were applied in this thesis. Each subchapter will first describe the principle of the applied method and then list the details relevant to the performed experiments.

2.1 Electrophysiology

Electrophysiological measurements on neurons comprise the main part of this thesis. Therefore, some background on electrophysiology in general will be given. After briefly describing historical aspects, the principle of electrophysiological measurements will be explained focussing on details relevant to this work.

2.1.1 Historical Perspective

Although the electrical excitability of some living cells has been recognized for centuries and central concepts about electrical excitation and signal propagation by neurons were already stated around the turn of the twentieth century [Hermann, 1905; Hermann, 1872; Bernstein, 1902], it was not until the "heroic period of classical biophysics" 1935-1952, that the central role of ion fluxes and membrane permeabilities in the creation and conduction of electrical signals by nerve cells could be established experimentally.

An early description of cellular excitation came from Cole and Curtis in the 1930s [Cole, 1938; Cole, 1939], who measured impedance of single cells and integrated their findings into an equivalent circuit. From their work they concluded that the cytoplasm of each cell is highly

conductive for electrical current while the surrounding cell membrane at rest has a very low conductance which increases dramatically during excitation. This is a central finding in early electrophysiology, although Cole and Curtis did not yet link this increase in conductance to an opening of ion channels. The notion that the flow of ions is involved in electrical excitation came in 1949 through the famous work of Hodgkin and Katz [Hodgkin, 1949] who measured the effect that variations in the concentration of Sodium in the bath solution had on the shape of action potentials in the squid axon. In close agreement with their hypothesis that the inward current during the rising phase of the action potential was carried by Sodium ions flowing into the cell, they found that the action potential rose less steeply and had a smaller maximum when the concentration of Sodium in the bath was decreased.

Most early electrophysiological experiments were performed on the giant axon of the squid, which was an ideal model system because its size permitted its isolation and manipulation with relative ease. Up to 1949, action potentials and their propagation were mostly measured in isolated axons by intracellular recordings at two separated points along the axon. This was performed by inserting two microelectrodes into the axon and applying a current pulse through one pipette while recording the evoked action potential through the second.

A major breakthrough in electrophysiological methods came with the development of the voltage clamp technique by Hodgkin, Huxley and Katz [Hodgkin, 1952; Hodgkin, 1949]: Rather than applying current pulses to the cell and measuring the resulting voltage signal over the cell membrane, the method allowed to hold the membrane voltage at an experimentally defined value and record the currents that were evoked in response to changes in the membrane potential. This method for the first time allowed to quantitatively measure the amount of current flowing across the membrane upon depolarisation. Moreover, it allowed Hodgkin and Huxley to separate the observed currents into individual components carried by different ion species. This work later led them to the formulation of the Hodgkin-Huxley model which describes the permeability changes in the neuronal membrane occurring during

an action potential. This model, which explained electrical excitability through ion gradients and voltage-dependent permeability mechanisms, is one of the most central discoveries in modern physiology and Hodgkin and Huxley received the Nobel Price for this work in 1963. Another milestone in electrophysiology (also leading to a Nobel Price, in 1991) was the development of the gigaseal and patch clamp technique by Neher and Sakmann in 1976 [Neher, 1976]. In this technique, a fire polished glass pipette with a very fine tip (the internal diameter is about 1 μm) is tightly sealed to the membrane of a living cell. The seal was called gigaseal because it has a resistance in the range of several Giga Ohms. The membrane area that is trapped by the pipette tip and therefore amenable to recording is so small that currents from single ion channels can be measured. This was a revolutionary achievement, as it presented one of the first occasions at which the behaviour of single biological molecules could be followed stably over hours with a sub-millisecond resolution. Much was learned about the mechanisms and kinetics of channel gating from these studies.

Patch clamping can be performed in a variety of different forms to address a wide range of topics. As it was the central technique applied in this thesis, the following subchapter will describe it in some detail.

2.1.2 The Patch Clamp Technique

The first step in a patch clamp experiment is the gigaseal formation developed by Sakmann as described in the previous paragraph. Starting from the gigaseal, four different recording configurations are feasible, depicted in Figure 2-1. Recording directly after gigaseal formation represents the cell attached mode. In this configuration, minute currents flowing between the pipette solution and the cytoplasm through the one or few single ion channels trapped in the pipette tip are recorded (A). Such small amounts of current are only detectable with a very tight seal between the rim of the pipette and the membrane, such that no current leaks out. In

the inside-out conformation, the membrane patch trapped in the pipette tip is pulled off the cell but remains sealed to the pipette. The side of the membrane that normally faces the cytoplasm is now open to the surrounding bath solution (B). Dipping the excised membrane patch into different solutions allows to measure the effect that particular compounds have on the ion channels in the patch. If in contrast after gigaseal formation the cell patch is ruptured by applying negative pressure, measurements in the whole cell configuration can be performed. This mode integrates the total current flowing over the channels in the membrane surface of the entire cell. In the whole cell conformation, there is no barrier between the cytoplasm and the pipette solution, and therefore an exchange of solutes can take place. For this reason, the intracellular patch solution has to be isoosmotic to the cytoplasm and contain similar concentrations of the cytoplasmic ion species. The last conformation is the outside-out conformation, which is achieved by pulling the pipette out starting from the whole-cell configuration, again excising a patch of membrane. In contrast to the inside out configuration, the side of the membrane facing the bath solution is now the side normally found on the outside of the cell.

As the whole-cell configuration was used in the experiments presented here, only this conformation will be described further and the term "patch clamp technique" will be used in the sense of the whole cell mode.
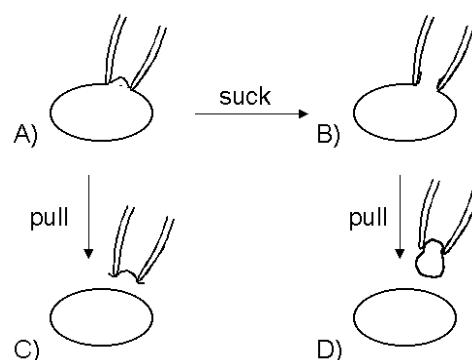
Figure 2-1: The four possible configurations of a patch clamp measurement. A) Cell attached mode B) Whole cell mode C) Inside out mode D) Outside out mode

2.1.2.1 The Experimental Setup

Before performing a patch clamp experiment, patch pipettes need to be made. This is achieved under the use of a micropipette puller: Glass capillaries are inserted into this device such that the middle of the capillary can be melted with a heating filament. Upon melting, the two ends of the capillary are abruptly pulled apart yielding two pipettes with very fine tips. A pipette is then filled with intracellular patch solution and a silver chloride electrode is inserted into the back end. The electrode is mounted onto an amplifier head that in turn is fixed to a micromanipulator unit, as shown in Figure 2-2. Through this micromanipulator, the patch pipette can be moved with a high precision such that the tip can under microscopic control be approached closely to the membrane of the cell of interest. Over a silicon tube connected to the pipette, negative pressure is applied sucking the membrane into the pipette and thus forming a gigaseal. In a second step, the cell is opened by applying another pulse of negative pressure; this step ruptures the membrane patch trapped by the pipette tip and thus opens the cell to the pipette. As both the intracellular patch solution and the cytoplasm are highly conductive, a direct electrical connection between the cell and the recording electrode is established.

A reference electrode is inserted into the bath solution that surrounds the cell. While the intracellular patch solution is similar in ionic composition to the cytoplasm, the bath solution resembles the extracellular fluid in a living organism. This is very important, as cellular signalling depends heavily on concentration differences of several ion species between the cell and the surrounding fluid. When this difference is not maintained by the experimental conditions, neuronal behaviour may be seriously altered.
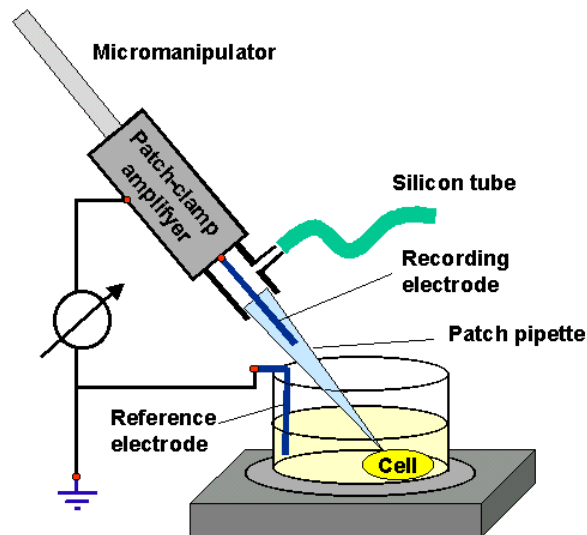
Figure 2-2: Patch clamp setup (scheme). A silver chloride electrode is inserted into a patch pipette filled with intracellular patch solution. The electrode is mounted onto an amplifier head which in turn is fixed to a micromanipulator unit. This unit allows to move the pipette with a high precision such that the tip can be closely approached to the cell membrane. Through a silicon tube, pressure or suction can be applied to the pipette. A reference electrode in the bath solution closes the electrical circuit.

Ideally, the seal between cell and the patch pipette is very tight, such that very little leak current can flow directly between the recording electrode in the patch pipette and the reference electrode. Instead, current in this electrical circuit has to flow through pores in the cell membrane. The cell membrane itself is composed of a lipid bilayer and therefore represents a very poor conductor. Membrane resistance can vary dramatically depending on how many of the different pore proteins are open.

Figure 2-3 schematically depicts the electrical circuit represented by a patch clamp experiment: Current flowing between the two electrodes first passes the resistance of the pipette, R_{pip} (which is in the range of several Mega Ohms as the tip diameter is very fine). Additionally, the pipette represents a capacitor which in the equivalent circuit is displayed in parallel with the pipette resistance. The next element in the circuit is the access resistance, R_{acc} (the small opening connecting cell and pipette results in a notable resistance results at the interphase), followed by the resistor represented by the cell membrane, R_{mem}. As mentioned before, this resistance is very variable and depends on the opening state of the membrane channels. As a thin insulating layer, the cell membrane additionally acts as a capacitor, C_{mem}.

35

The capacitance of a neuron depends on the total size of its membrane and is usually in the range of 10-40 pF. In the equivalent circuit, the membrane capacitance is depicted parallel to the membrane resistance. The capacitance of both the pipette and the cell membrane would normally distort a patch clamp recording considerably as every experimentally applied current pulse designed to induce a voltage step in the cell also charges the capacitors. Therefore, the current that flows at the beginning and the end of a voltage step is not proportional to the membrane resistance. In modern patch clamp setups, both capacitances can be compensated by the appropriate software such that only the current corresponding to the ion flux over the membrane is displayed.

A)   B)
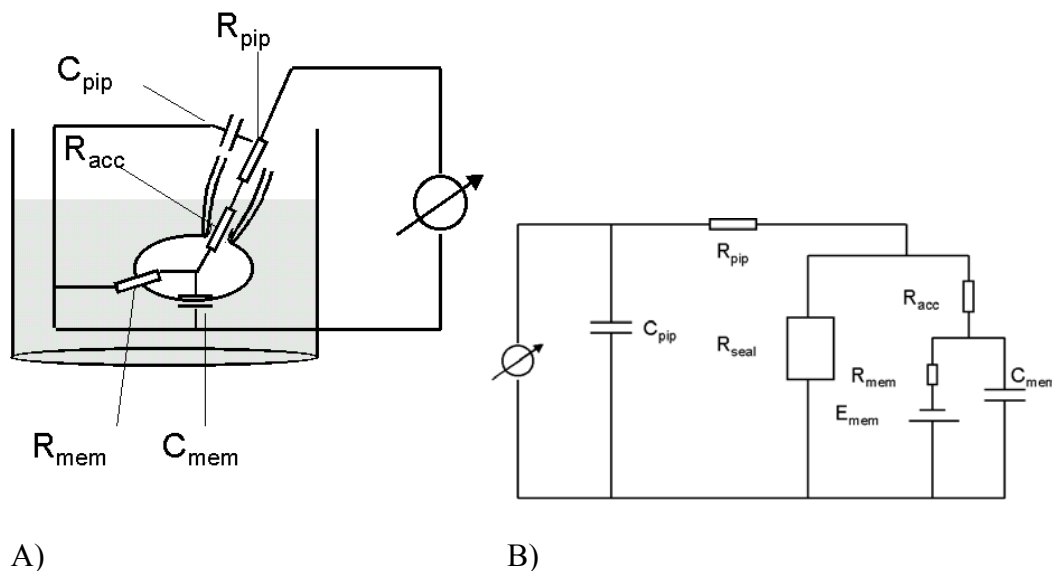
Figure 2-3: Schematic depiction of the electrical circuit represented by a patch clamp measurement (A) and the corresponding equivalent circuit (B). Current flows through the pipette which represents a resistor (R_{pip}) and a capacitor (C_{pip}) in parallel. A small leak current flows directly from the rim of the pipette to the reference electrode, passing the seal resistance R_{seal}. Ideally, R_{seal} is very large to keep the leak current at a minimum. The major fraction of the current flows through pores in the membrane after passing the access to the cell (R_{acc}). As these pores are regulable, the membrane resistance R_{mem} is very variable. As a thin lipid bilayer, the membrane additionally represents a capacitor (C_{mem}). Having passed the membrane, current reaches the reference electrode inserted into the bath solution. For reasons of clarity, the seal resistance R_{seal} is omitted in A).

In a patch clamp experiment, two measuring modes are feasible, the current clamp (CC) mode, in which the experimentator applies current pulses while the impact on the membrane voltage is monitored, and the voltage clamp (VC) mode, in which the membrane potential of the cell is controlled externally while the induced currents are recorded.

The CC mode interferes relatively little with the physiological behaviour of the cell: Current pulses, typically depolarising ones, are injected into the cell. First, the negative membrane potential is passively discharged the way that would be expected for a vesicle representing a resistor with a fixed resistance and a capacitor in parallel. However, as soon as the membrane potential reaches the firing threshold, it develops in a non linear fashion through the opening of voltage-gated Sodium channels. This result in the firing of an action potential (AP) as it would in the living organism (see chapter 1). A typical CC measurement is shown in Figure 2-4.
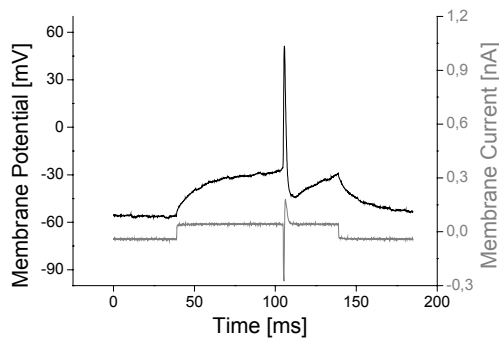
Figure 2-4: Typical current clamp experiment. A current pulse (shown in grey) is applied to the cell which is first passively depolarised until the membrane potential reaches the firing threshold and an AP is evoked. The deviation from the rectangular pulse in the current trace results from the fact that the amplifier can not fast enough compensate the changes in membrane conductance that arise through the opening of voltage-gated Sodium channels.

In contrast, the VC mode applies experimental conditions restricting cellular behaviour strongly: In this configuration, the membrane potential is held at a value defined by the experimentator through a control amplifier. The firing of APs, which relies on fast changes of the membrane potential, is therefore prevented. Typically, voltage steps are applied that hyperpolarise or depolarise the cell in a stepwise fashion. Voltage-sensitive channels in the cell membrane open upon depolarisation above threshold, dramatically changing the membrane resistance and allowing the flow of ions across the membrane. These changes in membrane resistance would normally lead to further depolarisation. The feedback mechanism of the control amplifier compensates this by injecting a current of equal magnitude of

opposite direction to keep the membrane potential at the command value. As the compensating current injected by the amplifier is directly proportional to the current flowing over the membrane, recording the amplifier current allows the deduction of the amount of current that flowed over the membrane in response to the applied voltage step.

Figure 2-5 shows a typical voltage-clamp measurement: The cell is depolarised stepwise by clamping it to different voltages. At hyperpolarising and subthreshold depolarising steps, only the amount of current flows that is proportional to the corresponding voltage step as the membrane resistance is constant. However, as soon as the cell is depolarised above threshold (Figure 2-5 C), additional channels open and a non linear behaviour in the form of a strong inward current is observable (by convention, inward membrane currents are considered negative and shown as downward deflections, while outward membrane currents are depicted as positive [Hille, 2001]). This current is carried by Sodium ions flowing into the cell (see chapter 1). The opening of the Sodium channels is responsible for the upstroke at the beginning of an AP; in a CC experiment the Sodium influx would lead to further depolarisation. The recording also shows the closing of the channels that occurs after about 2 ms independent of whether the membrane is still depolarised or not.

In the recorded signal, a second component is observable which is due to the Potassium current; this is best observable in Figure 2-5 D. Upon depolarisation, a type of Potassium channel distinct from that open in the resting state is activated. This type – which is called delayed rectifier - serves to repolarise the membrane after an AP. It opens upon depolarisation with a slight delay after the Sodium channel and remains open until the resting membrane potential is reached again. Repolarisation is prevented experimentally in the voltage clamp mode, therefore the channel remains open throughout the duration of the pulse while the Sodium current flows only transiently.
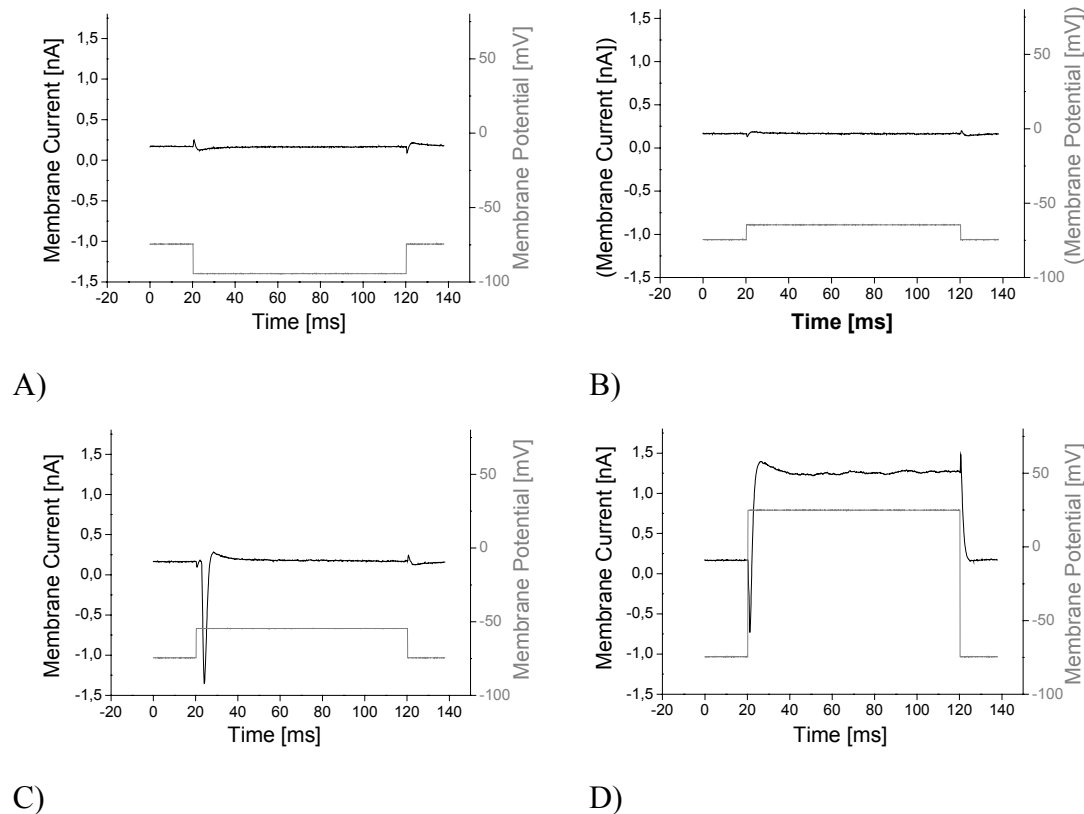
Figure 2-5: Typical VC measurement. To clamp the cell at a hyperpolarising (A) or slightly depolarising (B) membrane potential, a rectangular current proportional to the voltage step is injected by the control amplifier. Depolarisations above threshold however lead to a non linear behaviour as the membrane resistance changes due to the opening of voltage-gated Sodium channels. This results in a strong transient inward current (C). Stronger depolarisations reveal a second component of the induced membrane current: While the inward current occurs only for a brief period, the following outward current (which is mediated through voltage-gated Potassium channels) is sustained throughout the duration of the depolarising pulse. The recording was performed on a cortical culture on a control substrate coated with polylysine, DIV 15. Voltage steps: A) –20 mV, B) +10 mV C) +20 mV D) +100 mV. All measurements started with the cell clamped at -74.4 mV (the uneven value results from the subtraction of the liquid junction potential, see 2.1.2.2.1.)

For Patch clamp recordings, the following material was used:

A patch clamp setup with three amplifier heads was purchased from Heka Elektronik (EPC9/3). The amplifier heads were mounted onto stepper-based micromanipulator units (Mini 25, Luigs&Neumann); manipulation was performed under an IX 50 microscope (Olympus). Borosilicate patch pipettes (1810016, Hilgenberg) were pulled using a micropipette puller (P-97, Sutter Instrument Company).

The extracellular solution contained (mM): KCl, 5; NaCl, 150; $MgCl_2$, 1; HEPES, 10; $CaCl_2$, 2.5; Glucose, 10; pH 7.4, adjusted with 1M NaOH. The intracellular solution (mM): K

Gluconate, 125; KCl, 20; $CaCl_2$, 0.5; $MgCl_2$, 2; HEPES, 10; EGTA, 5; ATP, 4; pH 7.4, adjusted with 1M KOH; all chemicals were purchased from Sigma.

A subset of experiments was conducted with a low-EGTA solution as describeded in chapter 8. The extracellular solution in these experiments contained (mM): KCl, 3; NaCl, 145; $MgCl_2$, 2; HEPES, 10; $CaCl_2$, 3; Glucose, 8; pH 7.3, adjusted with 1M NaOH.

The intracellular solution (mM): K Gluconate, 136,5; KCl, 17,5; NaCl 9; $MgCl_2$, 1; HEPES, 10; EGTA, 0,2; pH 7.2, adjusted with 1M KOH.

Unless stated otherwise, VC experiments were performed by clamping the cell to -74.4 mV (this uneven number results from the subtraction of the liquid junction potential from the reading of the patch clamp amplifier, see 2.1.2.2.1) and applying a series of 100 ms pulses at a frequency of 1.25 Hz. After two hyperpolarising pulses (clamping the cell to −94.4 mV and − 84.4 mV respectively), one pulse with zero amplitude followed after which the cell was successively depolarised by pulses increasing by 10 mV per step. A total of 13 pulses was applied such that the maximal depolarisation clamped the cell at +25.6 mV.

CC experiments were typically performed by applying 10 current pulses of 1.3 nA at a frequency of 0.8 Hz. Before the application of each pulse, the cell was slightly hyperpolarised by a 25 ms pulse of −0.2 nA.

A subset of experiments described in chapter 8 used a paired stimulation protocol for the induction of LTP / LTD in synaptically coupled cells. These protocols first gave 10 test stimuli of 50 ms and 1 nA alternatingly to the two cells; again each pulse was preceded by a hyperpolarising step of 25 ms and −0.2 nA. The interval between the stimulation of the two cells was 1.225 s, the interval between two pulses applied to each cell 2.5 ms (such that the stimulation frequency was 0.4 Hz). Next, a train of stimulating pulses followed. Both cells were stimulated with a total of 60 pulses equivalent to those in the test series at a frequency of 1 Hz. Pre and postsynaptic cell were stimulated with a time delay of 10 ms. The LTP protocol

stimulated the presynaptic cell first while the LTD protocol first stimulated the postsynaptic cell. Only the test stimulus trains were recorded. 2-4 cycles of test and stimulating pulses were applied. The protocol ended with a series of test pulses.

2.1.2.2 Information Extracted From Patch clamp Measurements

2.1.2.2.1 Single Cells

Patch clamp measurements of neuronal cells can be used to investigate many aspects about neuronal physiology. The first piece of information to be gained in the beginning of a measurement is the membrane capacity of a patched cell, which is a measure for cell size. Second, the resting membrane potential can be measured, which can be taken as an indicator of physiological integrity.

Care must be taken at this step as the recorded potential needs to be corrected because of an artefact arising with the measurement: The potential over the cell membrane is recorded as the potential difference between the recording electrode inserted into the cell and the reference electrode in the bath. Before recording, a reference point must be defined at which the potential difference is zero. This point is taken when the pipette is immersed in the bath solution before the cell is approached. Theoretically, at this point no potential difference should be recordable between the two electrodes as the resistance of the bath solution is negligible because of its high salt concentration. The mentioned artefact arises due to the different ionic composition of the intracellular patch solution (which, as described before, is similar to the cytoplasm) and the bath solution (which is designed to resemble the extracellular fluid). The ions that experience a concentration gradient between the two compartments move into or out of the pipette by diffusion. Since ions of different radii are present in the two solutions that accordingly show different mobilities, they do so at different

rates. This results in a potential building up as soon as the pipette is immersed into the bath which is called the liquid junction potential. When the voltage reading is set to zero in this configuration, the recording after cell opening is off the real value by the liquid junction potential. The liquid junction potential for any two solutions can be calculated with the appropriate software. For the experimental conditions applied here, it was calculated with the Junction Potential Calculator developed by Axon Instruments, Inc. It was determined to lie at 14.4 mV. This value was subtracted from all recorded resting potentials.

The third type of information to be gained on single neurons lies in their ability to fire action potentials. A neuron can be induced to fire APs through the application of current pulses in the CC mode as described in the previous paragraph. Parameters like the firing threshold and the firing frequency upon particular stimuli can be determined in current clamp mode experiments. In the VC mode in contrast, the Sodium and Potassium currents flowing upon depolarisation can be quantified. They can be taken as a measure for the amount of voltage-gated Sodium and Potassium channels in the membrane. Normalising maximal induced Sodium and Potassium current with respect to the membrane capacity allows to deduce the density of these channels in the membrane. Additionally, VC measurements show the gating kinetics of these channels.

In chapter 6, physiological parameters of cells grown on a micropattern and on control dishes are compared to determine whether the growth on a pattern has an impact on cell physiology. The parameters described above serve as criteria: The membrane capacity as a measure for the size of the cells, the average resting potential as an indicator of the physiological state as well as maximal Sodium and Potassium currents per surface area in response to a defined series of voltage-steps. However, the main focus of this thesis lies in the analysis of synaptic connectivity between neurons, an aspect that is investigated under the use of double and triple measurements. These measurements will be described next.

2.1.2.2.2 Double and Triple Patch Clamp Measurements for the Detection of Synapses

When two or three amplifier heads are available at one setup, several cells can be patched in parallel. Synaptic connections can be identified by stimulating one of the cells and monitoring whether an induced action potential has an effect on the other cells. The presence of a functional synapse manifests itself through a signal arriving at the non stimulated cell with a time delay of several milliseconds upon a presynaptic action potential. Subthreshold depolarisations are not transmitted. When the postsynaptic neuron is held in the current clamp mode, the synaptic signal is recorded as a change in the membrane potential; this signal is called a postsynaptic potential (PSP). In contrast, when the postsynapse is held in the voltage clamp mode, the postsynaptic current is recorded (PSC).

Three aspects of synaptic behaviour were routinely evaluated in this thesis:

1.) The size of the synaptic response which can be estimated either through the amplitude of the postsynaptic potential or the postsynaptic current, depending on the measuring configuration. This is a very informative parameter, as the strength of a synapse may vary over time and in response to different types of stimuli, e.g. trains of stimuli at different frequencies as discussed in chapter 8. Plotting the development of synaptic strength over time can therefore yield important information on synaptic plasticity.

2.) The rate of synaptic failure. Transmitter release by the presynaptic terminal is probabilistic in nature, which means that it does not occur automatically upon the entry of an action potential to the presynaptic terminal but increases the probability of vesicle fusion. This probability can vary widely under different physiological conditions, resulting in a variance of the postsynaptic signal. When an action potential fails to induce a postsynaptic response altogether, one speaks of synaptic failure [Redman, 1990; Thomson, 2000]. For the characterisation of a neuronal culture, the rate of synaptic failure is a relevant parameter.

3.) The synaptic delay. It was stated in the beginning of this paragraph that a signal

transmitted through a chemical synapse arrives at the postsynapse with a characteristic

time delay. This delay is mainly due to the time it takes for the transmitter vesicles to

be released from their anchorage in the cytoskeleton and to fuse with the postsynaptic

membrane. The delay times described in the literature vary from below 1 ms to 5 or 6

ms and have also been reported to be variable at a single synapse. Delay times of >8

ms are usually due to a polysynaptic connection [Muller, 1997]. This means that the

signal is not transmitted directly from pre to postsynapse but via an unidentified third

neuron. Polysynaptic circuits can be an interesting experimental object for many

topics, but were not addressed in this thesis. Synapses displaying a delay time of more

than 8 ms were therefore excluded from evaluation.

A)   B)
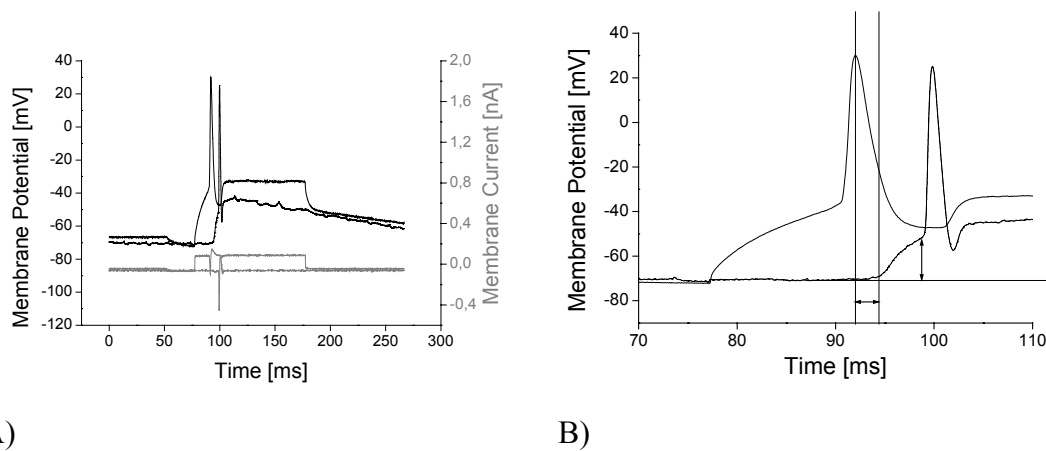
Figure 2-6: Synapse detection in patch clamp measurements. A) Typical measurement of a synaptic connection. Note that only one neuron (solid line) is stimulated by a current pulse (grey solid line) while no external stimulus is applied to the second neuron (dotted lines). The synaptic connection is strong enough to elicit a postsynaptic AP. B) Enlargement of A). Two types of information can be extracted from this measurement: The synaptic delay (horizontal arrow, left) and synaptic strength (vertical arrow, right). The rate of synaptic failure is determined by counting the events in which no synaptic signal was transmitted.

2.1.2.2.2.1 Determination of the Synapse Type

Chemical synapses can be divided into two major groups: Excitatory synapses that depolarise the postsynaptic cell and inhibitory synapses that transmit a hyperpolarising signal. A depolarising signal is mediated through the opening of cation channels in the postsynaptic cell. Their opening leads to an influx of Sodium and an outflux of Potassium which in sum results in a depolarisation of the postsynaptic cell (some receptors are also permeable to Calcium, which flows into the cell and adds to depolarisation). Contrary, inhibitory synapses cause an opening of postsynaptic Chloride channels, which *in vivo* results in an influx of negative charge and thus hyperpolarisation of the postsynaptic cell.

It is important to note that this behaviour is altered in a patch clamp measurement. Generally, the ionic composition of the intracellular patch solution is attempted to be kept as similar as possible to that of the cytoplasm. However, one exception is made from this rule: The concentration of Chloride is chosen higher than that normally present in the cell. This measure has to be taken for a sufficient amount of Chloride in the patch solution to allow communication with the silver Chloride electrode used for recording. This represents a necessary compromise with the attempt of not interfering with cellular physiology by applying physiological concentrations of ions to the intracellular solution.

The increase of intracellular Chloride in a patch clamp measurement has an important impact on inhibitory synapses: As the gradient of intracellular to extracellular Chloride is reduced, the reversal potential for Chloride (which can be calculated with the Nernst equation, see chapter 1) is shifted to a much more positive value. With the patch solutions used in this thesis, the reversal potential is shifted to −30 mV (the value encountered *in vivo* is usually around −60 mV). This means that only at a cellular potential above −30 mV, Chloride flows into the cell, hyperpolarising it when Chloride channels are opened but that below −30 mV Chloride flows out of the cell upon channel opening which causes depolarisation. As the

resting potential of a neuron is usually well below –30 mV, inhibitory synapses in a patch clamp measurement induce postsynaptic depolarisation, making them look extremely similar to an excitatory synapse. The distinction between excitatory and inhibitory synapses in a patch clamp measurement is therefore not as simple as it seems at first.

<u>Methods to Determine the Synapse Type</u>

The easiest way to determine the type of synapse encountered is the application of chemical inhibitors. As excitatory and inhibitory synapses utilise different transmitters that bind to different types of receptors, they can also be blocked in a highly specific fashion by different compounds. Most inhibitory synapses in the central nervous system utilise the transmitter γ-Aminobutyric acid (GABA). GABA-ergic synapses can be blocked by the application of bicuculline. Chemical inhibition with bicuculline is described in chapter 6. In these experiments, bicuculline methiodide (Sigma, B6889) was added to the bath solution to a final concentration of 50 µM as described in the literature [Dallwig, 1999].

The major type of excitatory transmitter applied in the brain is glutamate. Different subtypes of glutamate receptors exist; the majority of the postsynaptic current at glutamatergic synapses is usually carried by the non-NMDA subtype. This subtype can be blocked by 6-Cyano-7-nitroquinoxaline-2,3-dione (CNQX). Chemical inhibition of synapses with CNQX is also described in chapter 6; CNQX (Sigma, C-239) was applied to a final concentration of 20 µM [Honore, 1988].

The experimental setup did not include a perfusion chamber, therefore chemical inhibition was not reversible as the compounds could not be removed from the bath solution during the measurement. In addition, chemical inhibition was time consuming and side effects onto cellular physiology could not be ruled out. Therefore, two additional, non invasive methods for synapse characterisation were applied: The determination of the reversal potential and the analysis of the postsynaptic current.

Determination of the Reversal Potential

As described in chapter 1, the Nernst equation can be used to determine the reversal potential for a given ion species when the concentration gradient between the inside and the outside of the cell is known. The equation assumes that membrane pores are open that are only permeable for this ion species. The reversal potential is that membrane potential at which the electrical driving force equals the opposing chemical driving force such that no net flux of the ion over the membrane occurs.

The approach is also useful in the description of synapses, only that the equation is solved differently: The voltage of the membrane is defined by voltage-clamping the postsynaptic cell throughout the series of experiments at different (but known) values. In addition, the concentrations of the major ions expected to be involved in synaptic actions are known as they are defined through the intracellular and the extracellular patch solution. When the presynaptic cell is induced to fire action potentials, the postsynaptic current can be plotted as a function of the voltage at which the postsynaptic cell was held during the measurement. Such a plot is shown in Figure 2-7. A linear relation can clearly be observed. The reversal potential is the value at which the line crosses the y-axis: At this voltage, an opening of postsynaptic channels induces no postsynaptic current as the net driving force for the involved ions is zero. From the value of the reversal potential, the type of postsynaptic receptor can be deduced. As GABA receptors are primarily permeable to Chloride, the reversal potential of these channels lies close to the reversal potential of Chloride. For glutamatergic receptors, the situation is slightly more complicated, as they are permeable to both Sodium and Potassium but not equally. Under the assumption that Sodium and Potassium are the only types of ion involved in the postsynaptic response, the relative permeabilities for the two species can be calculated after the Goldman equation. In the literature, a value around 0 mV is described for most types of glutamatergic synapses [Hille, 2001].
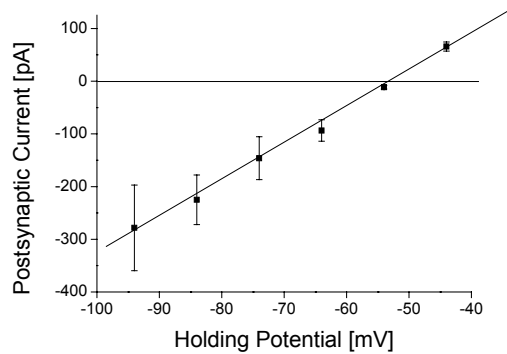
Figure 2-7: Determination of the reversal potential. A series of experiments is conducted in which the presynapse is induced to fire an AP while the postsynapse is voltage clamped at different membrane potentials. A series of 10 pulses is applied for each holding potential and averaged. The potential at which the postsynaptic current is zero can be extrapolated. The shown recording was made on a cortical culture on a PE pattern, DIV 12.
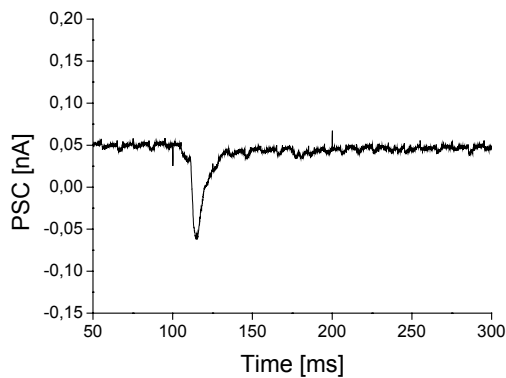
Analysis of the Postsynaptic Current

The third way to characterise a synapse lies in the analysis of the postsynaptic current. As indicated by the different susceptibility to different types of antagonists, the receptors in excitatory and in inhibitory synapses are completely distinct proteins. It is therefore not surprising that their gating characteristics also differ significantly. Both the opening and closing of the channels occur at different rates. In the literature, glutamate receptors of the non-NMDA type and GABA- receptors are mostly distinguished through the rate at which the channels inactivate. This rate is described by the decay constant τ which represents the time between the peak of the postsynaptic current and the return to the half maximal value (Figure 2-8 A). The decay constant for excitatory synapses is mostly described to lie between 1.3 and 6.6 ms, that for inhibitory synapses between 13.6 and 45 ms [Wyart, 2002; Taschenberger, 2000; Liu, 2000; Schneggenburger, 1992; Llano, 1993]. Typical examples of excitatory and inhibitory postsynaptic currents are shown in Figure 2-8 B and C.

The experimental establishment of these two methods for synapse characterisation is described in chapter 6.
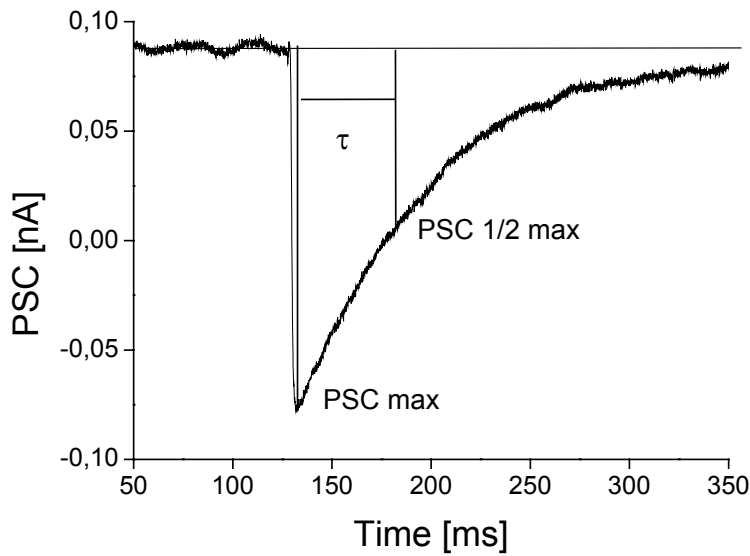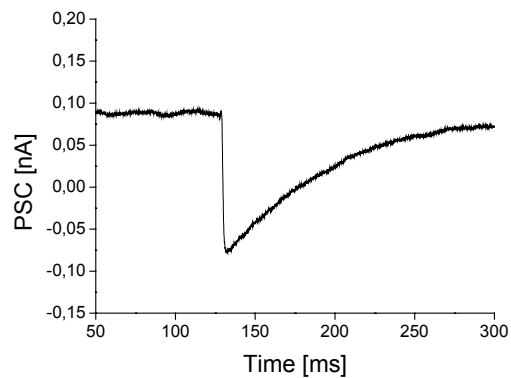
Figure 2-8: Determination of the synapse type by analysis of the postsynaptic current. A) The decay constant τ is determined by measuring the time between the maximum of the postsynaptic current (PSC max) and the return to the half maximal value (PSC ½ max). B) Typical measurement of an EPSC, decay constant 5.8 ms. C) Typical IPSC, decay constant 45 ms.

Figure 2-9 summarises the type of information on synapses that can be obtained from measurements in the CC and in the VC mode. The presynapse was normally held in the CC mode to allow the firing of APs. Depending on the investigated aspect, the postsynapse was held either in the CC or in the VC mode.

Mode	Scheme	Typical Recording	Extractable Information
CC-CC			• delay time • PSP height • postsynaptic APs
CC-VC			• delay time • PSC amplitude • reversal potential • decay constant τ
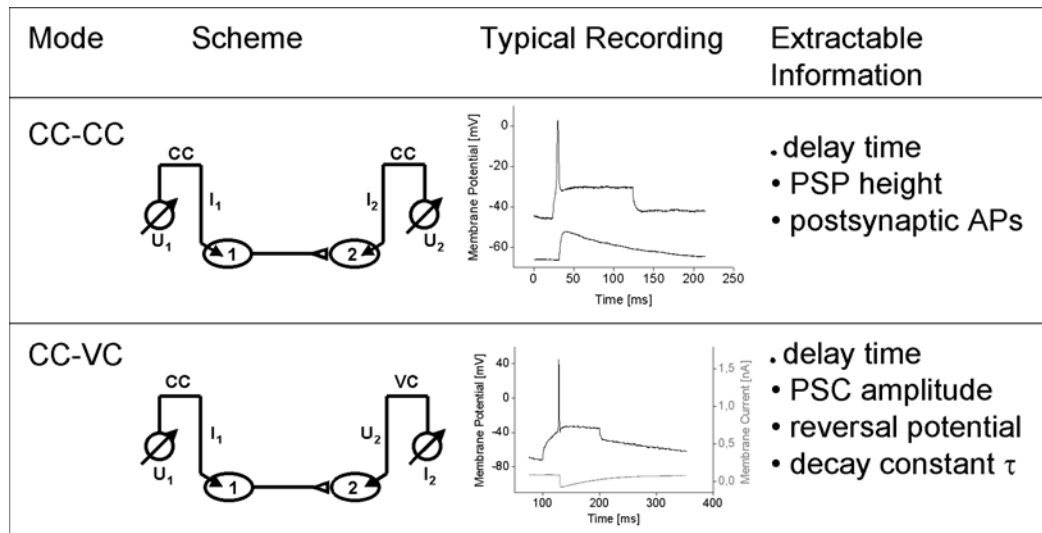
Figure 2-9: Synaptic analysis in the VC and the CC mode. The presynapse was typically held in the CC mode to allow the firing of APs.

2.2 Fluorescence Microscopy Setup

Several experiments involving fluorescence microscopy were performed. The setup for these experiments will therefore be described briefly; it is also shown schematically in Figure 2-10. Samples were observed under an IX 50 microscope (Olympus) equipped with a mercury vapour lamp (IX-FLA, Olympus). Appropriate sets of band-pass, dichroic and long-pass filters were employed to excite and detect the different fluorescent dyes. The bandpass filter is used to select the range of wavelengths adequate for dye excitation from the white light emitted by the mercury lamp. After passing the filter, the light is reflected by a dichroic mirror which directs the selected light onto the sample (a dichroic mirror only reflects light of a defined wavelength while all others are transmitted to the other side of the mirror such that they do not reach the sample). Light reflected on the sample is mostly reflected by the dichroic mirror again such that it does not fall into the detection range of the camera which is located behind the mirror. A longpass filter is placed behind the dichroic mirror that only allows light of a wavelength greater than that of the exciting light to pass and reach the

detection. Since light emitted from a fluorescent molecule always has a wavelength larger than the exciting light because of energy losses, the longpass filter selects for light coming from the substrate as a result of fluorescence events. The spectral response of the filters is designed to observe the fluorescing structures with an optimal signal to noise ratio.

Three sets of bandpass, dichroic and longpass filters were available for different types of dyes applied in this thesis; all were purchased from Olympus:

name	U-MNU	U-MNB	U-MNG
Bandpass filter	BP360-370	BP470-490	BP530-550
exciting wavelength	360-370 nm (UV)	470-490 nm (blue)	530-550 nm (green)
Dichroic mirror	DM400	DM500	DM570
Longpass filter	BA420	BA515	BA590
emitted wavelength	>420 nm (blue)	>515 nm (green)	>590 nm (red)
Applications	DAPI-stained nuclei in immunohistochemistry, (chapter 2.8) Cascade Blue in Microinjection experiments (chapter 2.9)	FITC labeled antibodies in immunohistochemistry, (chapter 2.8) lucifer yellow in Microinjection experiments (chapter 2.9)	Cy3 labeled antibodies in immunohistochemistry, (chapter 2.8) Sulforhodamine in Microinjection experiments (chapter 2.9) and microcontact printing (chapter 2.3.5)

Table 2-1: Overview over the applied filter sets, their properties and applications.
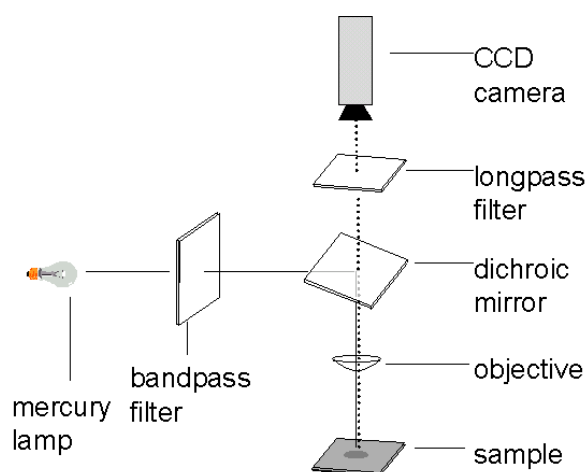
Figure 2-10: The fluorescence microscopy setup (scheme)

2.3 Microcontact Printing

Next to photolithography and laser ablation, microcontact printing is one of the most prominent methods for the application of microstructures to a surface. In this technique, an elastomeric stamp with the desired microstructure is dipped into a solution of organic molecules, allowing these to physisorb to the stamp surface (this process is called inking). The stamp is then dried and placed into contact with the substrate surface, such that the molecules are transferred to the substrate at the contact regions defined by the stamp. The process is schematically depicted in Figure 2-12.

The fabrication of the stamp includes three basic steps: The first consists of the pattern design using a CAD (Computer Aided Design) software. Second, the mould (master stamp), is produced by photolithography. In this step, the designed patterns are photolithographically structured into a photoresist yielding a (negative) topographical image of the pattern. The elastomeric stamp is then prepared by moulding Polydimethylsiloxane (PDMS) against the master stamp.

2.3.1 Structure Design

A subset of the structures designed and tested before [Lauer, 2001] (see chapter 1.6) was used. In accordance with these results, grid patterns with internodal distances of 50 μm and 100 μm were applied; the line thickness ranged from 4-6 μm and node diameters from 12-14 μm. These parameters had been shown already to be optimal for the patterning of neuronal cells and therefore were not varied. In addition, a number of grid patterns containing interrupted lines were applied (presented in chapter 7). For each structure design, wafers of 1 cm^2 were patterned with repetitive units of the respective elementary grid geometry. The exact dimensions of the different types of pattern can be found in the appendix.

2.3.2 Photolithographical Patterning of the Mould

For the creation of a stamp mould (master stamp) containing a topographical image of the designed pattern, a photolithographic technique is applied. A mask containing the desired structure is placed over a photoresist wafer. Exposure of the photoresist results in a photochemical reaction of the areas not covered by the mask. In the following developer step, the photoresist in these areas is removed while the non exposed areas are unaffected. (The described type of photoresist is called positive photoresist, while resists which are removed from the surface in the protected areas and remain where they have been exposed are called negative photoresists. In this project, a positive photoresist was used). Exposure occurred under ultraviolet light; the application of light with a short wavelength is necessary for the realisation of structures in the μm range because of diffraction effects.

The mask used in the process therefore needs to be transparent for UV light in the areas that are to be exposed and intransparent in the areas to be protected. These criteria are met by quartz glass and quartz glass with a thin layer of chromium respectively.

It was mentioned above that for each designed structure, a 1 cm^2 square chip was produced. Borosilicate glass wafers that were 5" in diameter were fabricated as described, containing several separate units with different structures. As a last step, these were separated to single moulds for one stamp each.

The creation of the master stamp was performed in the following three steps:

1) A glass wafer (0.6 mm thick, 5" in diameter, MEMC Electronic Materials) was coated with a 12.5 μm layer of photoresist (AZ 4562, Clarion GmbH) by spin coating. Spin coating is a well established technique for the creation of thin and ultrathin layers. In this method, a drop of photoresist is placed onto the glass wafer. The wafer is then rotated at a high speed such that the photoresist is spread to a thin homogeneous layer by centrifugal force. The resist was dried for 60s at 110° C ("soft bake").

2) The structuring step was performed by pressing the chromium-quartz mask onto the coated surface under the use of a mask aligner (MA-25, Karl Süss GmbH); this method is called contact exposure. Exposure took place with an energy of 30mJ/cm^2. The resist was developed for 30s in the development bath (AZ 726 MIS, Clariant); the reaction was stopped by a washing step with Milli-Q water. In the resulting wafer, the exposed areas, which were the lines and the nodes of the pattern, were present as indentations in the surface. Curing of the photoresist took place subsequently at 110° C for 90 minutes ("hard bake"; this step serves to add extra crosslinks within the photoresist).

3) The separate structured units on the wafer were then separated to platelets of one cm^2 each. Each of these platelets represents a mould for one stamp.

2.3.3 Casting of the Stamp

Polydimethylsiloxane (PDMS), a polymeric material mostly applied as an electrically and thermally insulating silicone glue, was used for stamp fabrication. This material is transparent and initially a viscous liquid. Addition of the appropriate curing agent followed by a heating step allows this material to harden to a rubber-like consistency. The stamps were created by pouring PDMS mixed with the curing agent into small moulds placed onto the master stamps and curing these at 60° C. This is the maximum temperature that can be applied without destroying the photoresist but too low for to achieve sufficient curing of the PDMS. Therefore, the masterstamps were removed from the soft stamps after initial heating and the stamps were hardened in a subsequent step at 110° C. To achieve an easy removal of the stamp from the master stamp, a detergent was applied to the master stamps before pouring the PDMS.

Stamp casting occurred in the following steps:

1) PDMS (Sylgard 184, Dow Corning) was mixed thoroughly with the curing agent (Sylgard 184 curing agent, Dow Corning) in a ratio of 10:1 (volume per volume). The bubbles introduced into the liquid during the mixing step were removed under vacuum.

2.) The master stamp was wet with a drop of 2% SDS (L5750 Sigma Aldrich). After 5 minutes, the SDS was removed and the master stamp dried under a stream of nitrogen.

3.) A plastic mould was placed on top of the master stamp. As a mould, 2 ml Eppendorf cups (Eppendorf) were used. The lid as well as the bottom were cut off yielding an open cylinder.

4.) The evacuated PDMS mixture (about 1 ml per stamp) was poured into the mould placed onto the master stamp. Master stamp and mould were placed into an oven at 60° C for at least 12 hours for initial curing.

5.) The master stamp was removed and the plastic mould cut open with a scalpel to free the PDMS stamp. The final curing step was performed at 110° C for one hour.

1. Pattern design

elementary structure design 100 µm	multiplication of the elementary structure	Arrangement of different structural units on the wafer 3 cm

2. Creation of the photoresist wafer

Application of a drop of photoresist	Spin coating	Drying / "soft bake"

3. Structuring

Exposure	developing	Crosslinking / "hard bake"

4. Stamp fabrication

4. Pouring of the PDMS stamp	Curing	Separation from the mould

Figure 2-11: Schematic description of the fabrication of a PDMS stamp for microcontact printing. The designed structure is transferred to a photoresist wafer by exposure to UV-light through a chromium-quartz mask. Development of the photoresist yields a negative image of the topographical pattern. The PDMS is then poured onto this mould and cured, resulting in a PDMS stamp with the designed structure.

2.3.4 Stamping of Organic Molecules

The principle of the stamping process is very simple: The stamp is dipped into the solution of choice ("inking"), dried and then pressed to the substrate. During this step, the molecules that had physisorbed to the stamp during inking are transferred from the stamp to the substrate. As an ink, a wide range of organic molecules in solution can be used, which makes microcontact printing a very versatile method. In the project presented here, four different types of ink were applied: Laminin (1243217, Boehringer Mannheim), a mixture of laminin and polylysine (MW 70 000- 150 000, P6282, Sigma Aldrich), ECM-gel (E-1270, Sigma Aldrich) and a mixture of ECM-gel and polylysine. Laminin was diluted in PBS buffer (14190-194, GibCo) to concentrations of 50µg/ml or 25 µg/ml (both concentrations worked equally well, so 25 µg/ml was mostly used for economic reasons). Mixtures of polylysine and laminin were also diluted in PBS buffer to concentrations of 12.5 µg/ml each. ECM-gel was diluted in Dulbecco's medium (11880-028, GibCo) (as recommended by the manufacturer), 1:100 (the stock solution contained approximately 10 mg protein / ml). For mixtures of ECM-gel and polylysine, 1 or 10 µg/ml polylysine were added to the ECM-gel solution.

Stamping was performed as explained below:

1.) Before printing, the PDMS stamps were immersed in Milli-Q water for 12-24 hours. This treatment has shown to increase the hydrophilicity and thus the wetting of the stamp. The stamps were then disinfected in 70% ethanol for three minutes, dried and placed into the inking solution. The ink was allowed to adsorb to the stamp for at least 10 minutes.

2.) The stamp was removed from the solution and carefully dried under a stream of nitrogen.

3.) The stamp was pressed onto the substrate, a polystyrene culture dish (35mm in diameter, #627161, Greiner). After 10 seconds, the stamp was removed.

All steps were performed under sterile conditions.

In addition to the stamped areas in the middle of the culture dish, areas at the edge were coated with the inking solution in an unstructured manner. This was done by applying drops of the respective ink and removing them by aspiration after one hour. This measure served to add some extra adhesion areas for the dissociated cells, as described in chapter 4.
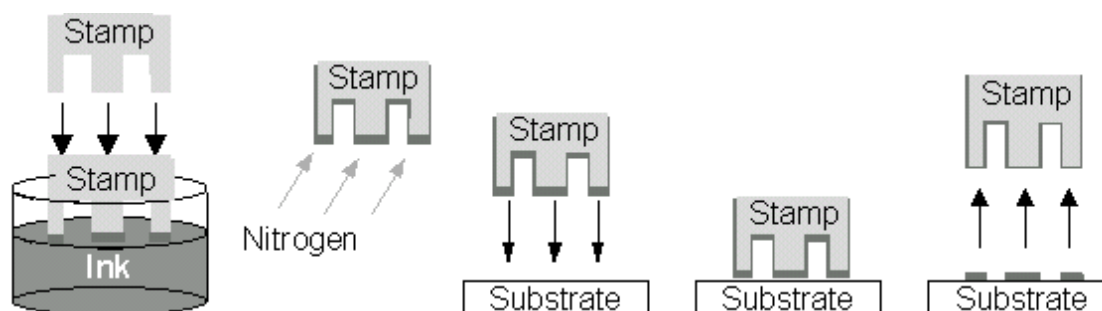
Figure 2-12: The microcontact printing technique (scheme). A PDMS stamp with the desired microstructure is dipped into a solution of organic molecules (termed "ink"). The wet stamp is then dried under a stream of nitrogen and pressed to the substrate surface, leaving the micropattern.

2.3.5 Quantification of Pattern Transfer

In chapter 3, the efficacy of pattern transfer during the printing process is quantified. To this end, the inking solutions were mixed each with 10µg/ml of the fluorescent dye sulforhodamine (Molecular Probes, S-359). Substrates were then printed as usual. The amount of stained inking solution that had transferred to the surface was visualised by fluorescence microscopy using the U-MNG filter set described in 0. Pictures of the substrates were taken (AxioCam color 3.0, Zeiss; 8 bit AD-conversion, exposure time 8s) and evaluated using the grey scale analysis of an imaging software (ImageProPlus). For this evaluation, areas represented by pixels of an intensity 50% or more of the maximum were considered to be covered with protein. The program then counted the number of pixels per picture matching this requirement. 64 pictures per substrate type were evaluated and averaged.
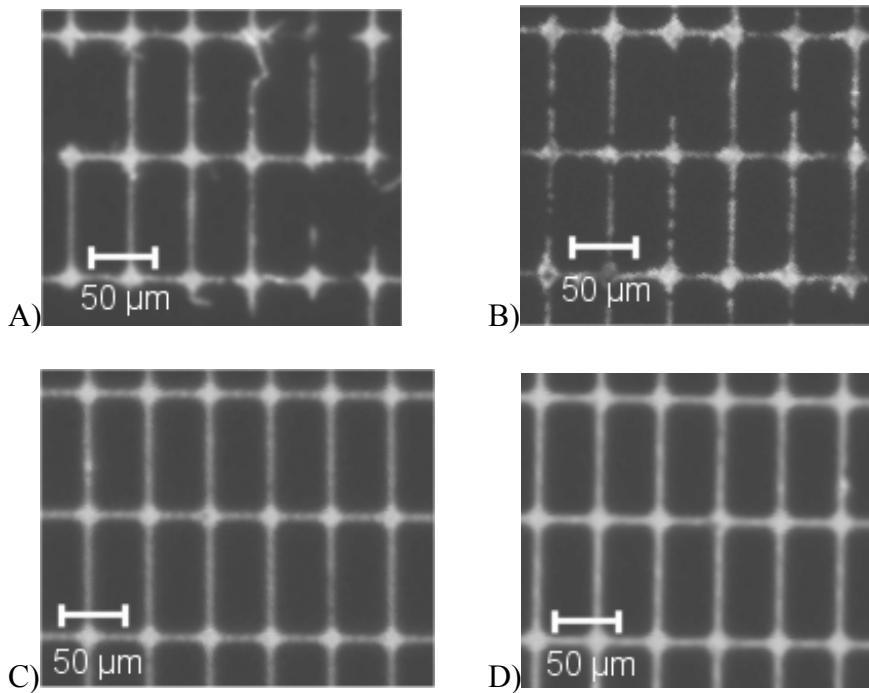
Figure 2-13: Typical pictures of labelled micropatterns as used for the evaluation of transfer. A) Laminin B) PL C) ECM-gel D) PECM

A more detailed analysis of the patterned surfaces was performed by SEM and AFM, two techniques that will be described in the next subchapter.

2.4 Scanning Electron Microscopy (SEM)

The functioning mode of an SEM is schematically depicted in Figure 2-14: An electron gun is used to create an electron beam. This can either be done through thermionic emission (by heating a Wolfram cathode which leads to an emission of electrons) or by field emission (which applies a strong electrical field to induce electron emission). The beam is then focussed in an electrical field and directed onto the sample where the electrons interact with the substrate in a complex manner. The most frequently observed type of interaction are elastic and inelastic scattering. Electrons that are diffracted at the surface or emitted after interaction processes can be detected by a collector and a photomultiplier. The angle at which

electrons are emitted from the probe yield information on the surface topography [Gauer, 1997].
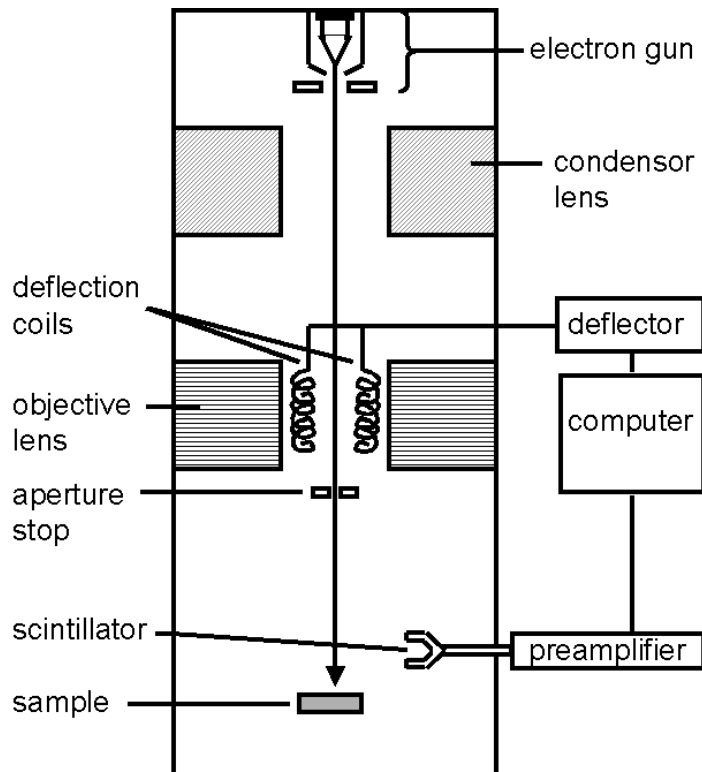
Figure 2-14: Functional sketch of a SEM (after [Gauer, 1997])

SEM imaging was performed at the Forschungszentrum Jülich. A 5 nm gold layer was deposited onto the samples by electron beam evaporation (ESV4, Leibold). Images were made with a field emission raster electron microscope (Gemini 1550, Leitz Electronic Optic).

2.5 Atomic Force Microscopy (AFM)

AFM is a technique that probes surfaces at a resolution of below one nm through a very fine tip with a contact radius of 5-10 nm. This tip is fixed to a cantilever which is about 100μm long. In the contact mode, the AFM tip is brought into contact with the surface applying a defined force while the cantilever moves it laterally. A feedback loop ensures that the force

between tip and surface is kept at a constant value by moving the cantilever up or down. Thus, the displacement of the cantilever through this feedback loop reveals an image of the surface topography. However, the emerging picture can also be influenced by attractive or repulsive surface forces that have an impact on the interaction between surface and AFM tip.

One problem of AFM measurements in the contact mode lies in the fact that the tip moving over the surface may damage soft structures.

Alternatively, AFM can be performed in the tapping mode, which was applied in this thesis. This mode is advantageous for the use on soft surfaces, as the forces applied to the surface are very low. In the tapping mode, the AFM cantilever is brought to a position close to the surface at a distance in the range of several nm and vibrated near its resonance frequency. The tip can penetrate water layers that form on a surface at ambient conditions, tapping onto the surface (hence the name) and revealing structures below the water layer. The resonance frequency depends on the force gradient experienced by the cantilever, which in turn is a function of the distance between tip and surface. Therefore, features about surface topography can be deduced from changes in the resonance frequency. Again, a feedback loop is used that keeps the cantilever at a constant distance from the surface by analysing changes in the resonance frequency. As in the contact mode, features other than topography can have an impact on the emerging picture.
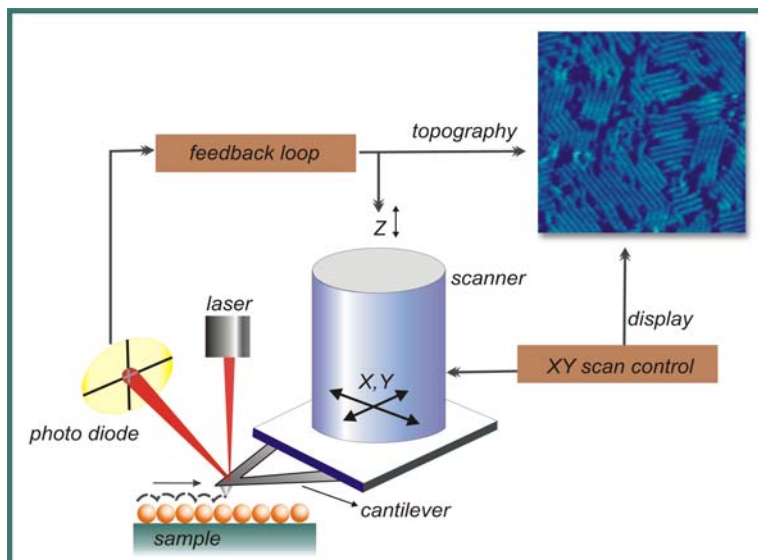
Figure 2-15: Operation principle of a strictly non contact AFM. The AFM tip is moved over the surface, experiencing different types of surface forces, such as steric, electrostatic and van-der-Waals forces. The forces experienced by the tip strongly depend on the distance from the surface. The angle at which the cantilever bends because of attractive forces can be monitored through the angle at which it reflects a laser beam. A feedback loop keeps cantilever deflection and thus tip to surface distance at a constant value by moving the cantilever in the z direction. The cantilever movement through this feedback loop yields an image of the surface topography.
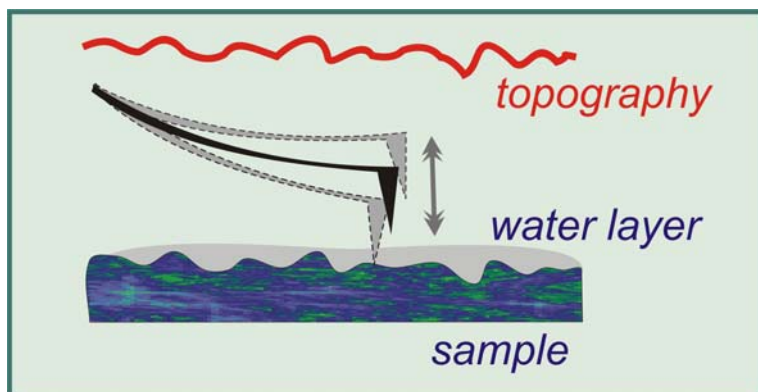
Figure 2-16: AFM measurements in the tapping mode. The cantilever is vibrated near its resonance frequency closely to the surface. As the resonance frequency is dependent on the distance between tip and surface, changes in resonance frequency can be used to obtain information on surface topography. An important feature in this mode is that the tip penetrates the water layer that is always present on the surface of the sample and reveals features under this layer. However, artefacts can arise due to capillary forces.

AFM measurements were performed at Sony international, Stuttgart with a NanoScope, Dimension 3100 (Digital Instruments Veeco Metrology Group) and aluminium coated Silicium tips on a Micro Cantilever from Olympus (OMCL-AC160TS-W2). The resonance frequency was 300 kHz, spring constant 42N/m.

2.6 Neuronal Cell Culture

The possibility to culture neuronal cells outside the living organism was first described around the turn of the last century by Harrison [Harrison, 1907]. Since then, neuronal cell culture has been worked on intensely and represents one of the most central techniques in neurobiology. Currently, a multitude of different protocols is available for the isolation and culture of neuronal cells. One of the first questions an investigator has to ask when deciding to culture neurons is whether to use a dissociated or a slice culture. In dissociated cultures, the tissue organization is disrupted mechanically and / or enzymatically and single cells are seeded onto the substrate. In the slice culture, which was predominantly developed by Gähwiler [Gähwiler, 1981][Gähwiler, 1984b], the brain area of interest is cut into very thin slices which are placed into a tissue culture dish and neurons are allowed to migrate out of the largely intact tissue.

Another basic issue to be addressed is the question which culture medium to use. Many standard formulations add serum as a source of growth factors, hormones and antioxidative agents. The drawbacks of serum containing media are that first, the concentration of the above mentioned components is poorly defined and may vary from lot to lot, second that such formulations only allow neuronal survival above a critical density and third that serum supports the proliferation of glia cells. Glia cells tend to overgrow the neuronal culture as neurons are postmitotic after differentiation and therefore do not proliferate themselves. Protocols applying serum containing media therefore often include the addition of an antimitotic agent like cytosine arabinoside (AraC) in order to limit glia proliferation. Although theoretically, antimitotic agents should have no effect on the postmitotic neurons, several side effects of AraC have been reported such as an impact on differentiation and neurite outgrowth as well as neurotoxicity at higher concentrations [Rebel, 1999].

Several synthetic alternatives to serum containing media exist, the most prominent one being B27-supplemented Neurobasal medium developed in 1993 by Brewer et al. [Brewer, 1993]. This medium contains optimized concentrations of several hormones, amino acids, vitamins and antioxidative agents. The advantages of this formulation are that it does not support the proliferation of glia and that it makes the culture almost independent of cell density. As mentioned above, cellular survival in serum containing media depends heavily of the density of the culture due to autocrine factors released by the cells themselves that need to be present above a minimal concentration. Apparently, it was accomplished to present most of these factors in the synthetic cocktail of supplements in B27 / Neurobasal medium.

During the course of this thesis, two fundamentally different cell culture approaches were used and are compared in chapter 4. Both will be described in the following paragraphs.

2.6.1 Brain Stem Slice Culture

The first approach used a slice culture applying the brain stem as the brain area of choice in a serum containing medium. The protocol, which is an adaptation of the protocol described by Gähwiler [Gähwiler, 1981], included the following steps:

Embryos were recovered from pregnant CD rats at 18 days gestation. Medulla and pons were removed from the embryonic rat brains by a transverse section through the rostral pons. The dissection was performed in HBSS (H-6648, Sigma Aldrich) supplemented with 100 U/ml Penicillin / Streptomycin (P-0906, Sigma Aldrich) and 6 mM glutamine (G-7513, Sigma Aldrich). Coronal slices of the brain stem 250 μm in thickness were cut using a tissue chopper (McILWAIN tissue chopper, model MTC/1, Mickle laboratory engineering Co.LTD). This was done by placing the brain stems onto a sterile piece of filter paper (10311609, Schleicher & Schuell) positioned onto the cutting platform of the chopper and wet with F10 HAMS (N 1387, Sigma Aldrich) containing 5% FCS (F7524, Sigma Aldrich), 4.8 mM glutamine and 100 U / ml Penicillin / Streptomycin (P0906, Sigma Aldrich). After chopping, the slices were rinsed off the filter into a petri dish containing the final culture medium (F10 HAMS, 25% FCS, 4.8 mM glutamine). The dish was placed into the incubator for 4 h, during which time the medium was changed every 60-90 minutes to allow dead cells to detach from the surface. Afterwards, the slices were placed individually into separate substrate dishes (patterned as described in 2.3) using a small surface-polished spatula. A critical amount of culture medium was added, such that the slices would not detach from the surface but that the surface was kept moist. Every 2-3 days, the medium was changed.

2.6.2 Dissociated Cortical Cell Culture

The second protocol used a serum free medium for a dissociated cell culture of cortical neurons. Isolation and cultivation of these neurons occurred as described by Brewer et al. [Brewer, 1993]: Again, embryos were recovered from pregnant CD rats at 18 days gestation. Cortices were dissected from the embryonic brains in Hank's Balanced Salt Solution (without Ca^{2+} and Mg^{2+}, 14170-088, GibCo) containing 0.035% sodium bicarbonate, 1 mM sodium pyruvate, 10 mM HEPES, 20 mM glucose, pH 7.4. Cells were mechanically dissociated by trituration in the above mentioned solution with a fire polished siliconised pasteur pipette. 2 volumes HBSS (with Ca^{2+} and Mg^{2+}, 24020-091, GibCo) 0.035% sodium bicarbonate, 1 mM pyruvate, 10 mM HEPES, 20 mM glucose, pH 7.4 were added to reconstitute divalent cations. For three minutes, non-dispersed tissue was allowed to settle, the supernatant was transferred to a new tube and centrifuged at 200g for 5 minutes. The pellet was resuspended in 1ml Neurobasal Medium (21103-049, GibCo) , 1x B27 (17504-044, GibCo), 0.5 mM L-glutamine (35050-038, GibCo) per cortical hemisphere isolated.

An aliquot was diluted 1:1 with trypan blue (T-8154, Sigma Aldrich) and dye-excluding cells were counted in a Neubauer counting chamber; on average, about 4×10^6 cells were recovered per cortical hemisphere. The remaining cells were diluted in NB medium supplemented as above and plated onto the substrates at a density of 16.000 cells per cm^2. Half of the medium was changed every 3-4 days.

2.7 Evaluation of Cell Adhesion to Different Protein Patterns

In chapter 5, surfaces patterned with different adhesive molecules by microcontact printing are compared with respect to their ability to tether neurons to the pattern.

This comparison was done by seeding equal amounts of neurons (16×10^3 cells / cm^2; the surface of the substrates (polystyrene petri dishes, see 2.3.4) was considered to measure 8 cm^2 (the radius being 1.6 cm, $\pi \times r^2 = 8.04$ cm^2) although only the patterned area of the surface was available for adhesion) to substrates stamped with the different inks. At DIV 11-15, the number of cells growing on the respective pattern was evaluated. This was done first by counting the total number of cells adhering to the substrate per randomly chosen area. These areas were defined by pictures taken under the microscope with a 10x objective. Only single adherent cells were counted while lumps of cells were ignored, as cell lumps on the surface don't represent a genuine adhesion event.

Second, the number of adherent cells per available adhesion site (represented by a node in the grid pattern) was determined. To this end, the amount of transferred pattern per evaluated picture was taken into account. As in contrast to 0, unlabelled inks were used for microcontact printing, the pattern couldn't be visualized by fluorescence microscopy. Nodes available for adhesion were registered when the pattern was visible in the phase contrast picture. Additionally, grid nodes onto which no cell body had attached but which were overgrown by neurites, indicating that the area was permissive for cellular attachment / outgrowth, were regarded as being coated and thus available for adhesion. The number of node points occupied by cells per available nodes was then determined for each surface modification.

2.8 Antibody Staining

In the living organism, antibodies are a central part of the adaptive immune system. Secreted by B-cells, they bind to infectious particles with an enormous specificity, crosslinking several particles and labeling them for degradation by other cells of the immune system. Structurally, an antibody is a Y-shaped molecule, the stem being conserved while the tips of the Y, which are the areas binding to the target, are unique for each antibody.

Apart from playing a central role in the immune response, antibodies in the last 50 years have emerged as one of the most important tools in Molecular Biology and Molecular Medicine where they have in a wide range of applications. Antibodies can be used to detect proteins and small organic molecules with an extraordinary specificity and sensitivity not matched by any standard chemical method. They are also used to label cell types or cellular structures (by binding to proteins specifically expressed in these cells / structures), to purify proteins and even to block protein function. This is possible if the antibody is specifically directed against particular surface structures e.g. the active sites of an enzyme or areas recognised by interaction partners.

Two ways of creating antibodies are feasible, the polyclonal and the monoclonal approach. For the creation of polyclonal antibodies an animal is injected with the substance of interest and after the onset of the immune response, the animal's serum is extracted. It contains multiple types of antibodies directed against different epitopes (structural units displayed at the surface) of the injected material.

The development of monoclonal antibodies was made possible through the work of Georg Köhler and Cesar Milstein and was rewarded with the Nobel Price in 1984. This more complicated technique yields far more specific products: Again an animal is injected with the desired material inducing an immune response. Afterwards B-cells, the cells responsible for the secretion of antibodies, are isolated and cultivated *in vitro*. This step demands the

immortalisation of the cells which is done through fusion with myeloma cells, a cancerous cell type, since activated B-cells have a limited life time. Once an immortalised antibody secreting cell line is created, single cells are isolated. These each give rise to a clone of cells originating from one ancestor and therefore secreting the same type of antibody that binds one particular epitope in the protein.

In immunohistochemistry, antibodies can be used to distinguish between different cell types or to detect the presence of particular cells. This is done by incubating the culture with an antibody specific for a protein that is only expressed by the cell type of interest; this is called the primary antibody. In most cases, the cells are killed and fixed for this purpose, particularly when the antibody is supposed to bind to an intracellular protein. In this case, the cell membrane additionally has to be permeabilised for the antibody (which is a relatively large molecule, usually about 150 kDa) to pass. During the incubation time, the primary antibody is allowed to bind to its target structure, which it does with a high specificity. The cells are then washed thoroughly in order to remove any unbound antibody molecules. In the next step, the so called secondary antibody is added to the culture. The secondary antibody is always a polyclonal one, directed against the serum of the animal that was used to produce the primary antibody. It therefore contains a mixture of antibody molecules directed against different epitopes of the primary antibody. The secondary antibody carries a fluorescent label, the most common ones being Cy3 or fluorescein (FITC). During the second incubation, the secondary antibody is allowed to bind to its target (the primary antibody) and again unbound molecules are removed by washing. As a last step, the nuclei of the cells are stained with 4,6-Diamidino-2-phenyindole (DAPI), a DNA labeling fluorescent dye. Visualisation of the nuclei can be useful to verify whether a given structure represents a whole cell or cell fragments or unspecifically labeled particles.

Under light of the wavelength exciting the fluorescent label, the cellular structures to which the primary and subsequently the secondary antibody are bound can be viewed.

When two different cell types or structures are to be distinguished, two sets of primary antibodies, created in different animals, can be combined and detected with two differently labeled secondary antibodies. Pictures under light exciting the different dyes are taken subsequently and then superimposed to show the distribution of the two cell types or cellular structures.

The consecutive use of a primary and a secondary antibody has two advantages: First, it serves to amplify the signal, since one bound molecule of primary antibody is recognized by several secondary ones. Second, it is cost-efficient as the production of fluorescently labeled antibodies is rather expensive. One labeled secondary antibody can be used for any primary antibody created in a given type of animal.

In this thesis, antibodies directed against the following proteins were applied:

- Neurofilament-M, a cytoskeletal protein specifically expressed by neurons. (Figure 2-17 A). This antibody was used to verify the neuronal identity of the cultured cells and to estimate their abundance relative to glia cells under different culture conditions.

- GFAP (glial fibrillary acidic protein), a cytoskeletal protein specifically expressed by glia cells. (Figure 2-17 B). This antibody was used to determine the amount and physiological state of glia cells.

- Synapsin I, a protein anchoring synaptic vesicles to the cytoskeleton. This protein is expressed at the surface of synaptic vesicles and can thus be used to detect synapses. (Figure 2-17 C). It was applied for the investigation of synapse formation.
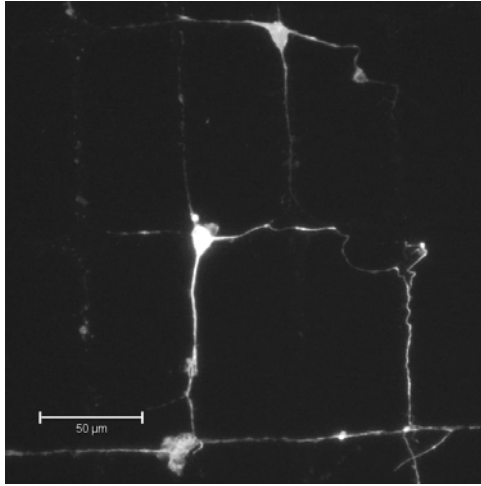
A)
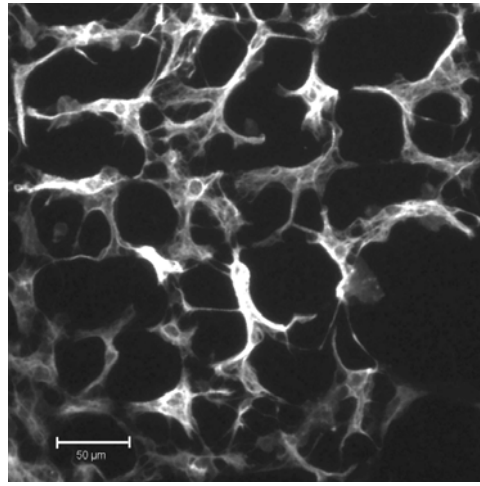
B)
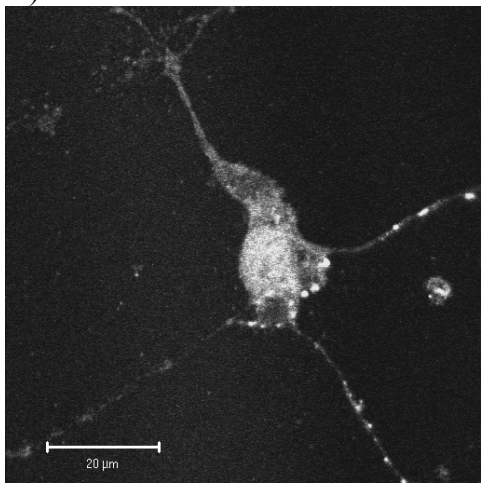
C)

Figure 2-17: Examples of immunohistochemistry experiments performed with the three antibodies used in this thesis. A) anti-Neurofilament-M (substrate: Dissociated cortical culture on ECM pattern B, DIV 7), B) anti-GFAP (substrate: Slice culture on laminin pattern A, DIV 10), C) anti-Synapsin I (substrate: Dissociated cortical culture on PECM pattern G, DIV 5). This picture was taken with a laser scanning microscope.

2.8.1 Applied Antibody Staining Protocol

1) The medium was removed from the culture by aspiration and cells were fixed in 2% paraformaldehyde (P-6148, Sigma Aldrich) for 20 minutes on ice, then washed three times in PBS buffer (14190-094, GibCo)

2.) Permeabilisation of the cells took place in a solution containing 5% acetate (105-12, Sigma Aldrich) in 95% ethanol for 7 minutes at −20°C, followed by three washes with PBS.

3.) The primary antibody was diluted appropriately (rabbit anti-neurofilament-M: AB1987, Chemicon, dilution 1:200, rabbit anti-synapsin I: AB1543, Chemicon, dilution 1:500, mouse anti-glial fibrillary acidic protein (GFAP): MAB3402, Chemicon, dilution 1:10) in PBS containing 10% FCS (F2442, Sigma Aldrich) and 0.02% NaN_3 (S2002, Sigma Aldrich). Incubation of the culture with the primary antibody took place in a humid chamber at room temperature and lasted for one hour. The cells were washed three times in PBS before

4.) incubation with the secondary antibody (Cy3 conjugated donkey anti rabbit, 711-166-152, Dianova and / or FITC (Fluorescein) conjugated donkey anti-mouse, 715-096-150, Dianova, each diluted 1:100 in the same buffer as the primary antibodies) for another hour. The cells were washed three times in PBS.

5.) For staining of the nuclei, an incubation with 0.25μg/ml DAPI (4,6-Diamidino-2-Phenylindole, D 9542, Sigma Aldrich) in methanol followed for 5 minutes. The cells were washed three times.

6.) A drop of mounting medium (S 3023, DAKO), was applied to the substrate, a cover slide was placed on top and sealed at the edges with nail polish (essence fast & last, cosma GmbH). The substrates were investigated using the fluorescence microscopy setup described in chapter 2.2, pictures were taken with an AxioCam color (Zeiss) unless stated otherwise. Some samples were viewed with a Laser Scanning Microscope (LSM-FCS, Version 2.8SP, Zeiss); this is indicated in the figure captions.

2.9 Microinjection of Polar Tracers

Microinjection of polar tracers is a technique used to visualise cellular connectivity. The method exploits the fact that in the course of a patch clamp measurement, a certain exchange of solutes between the intracellular patch solution and the cytoplasm cannot be avoided due to the opening of the cell to the patch pipette (Figure 2-18). If a non toxic, water soluble dye is added to the intracellular patch solution, the dye diffuses into the cell during the course of the measurement. The use of a highly polar dye ensures that it is able to disperse in the cytoplasm but not to cross the lipid bilayer of the cell membrane. It thus remains inside the cell, staining its entire volume including the neurites. When the substrate is illuminated with the excitatory wavelength of the dye, the cell with all its extensions lights up. This allows the investigator to trace which neurites in the network belong to the patched cell. This is not obvious in phase contrast microscopic pictures, since these processes are very fine and intertwine strongly, making it impossible to tell their origin. When more than one cell is patched simultaneously, different dyes can be used to label each cell. Subsequent pictures can be taken with light of the different wavelengths exciting the respective dyes. These can be superimposed to visualise where and how the cells form contacts.

The following dyes were used:

Lucifer yellow (L-453, MoBiTec). This dye absorbs maximally at about 430 nm and emits at 530 nm (yellow / green); it was viewed using the U-MNB filter set described in subchapter 2.2.

Sulforhodamine 101 (S-359, MoBiTec) absorbs at and 430 and 540 nm and emits at 610 nm (red). It could therefore be viewed with the U-MNG or the U-MNB filter set.

Cascade Blue (C-687 MoBiTec) absorbs at 400 nm and emits at about 430 nm, it was viewed with the U-MNU filter set.
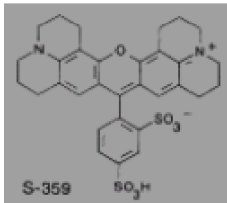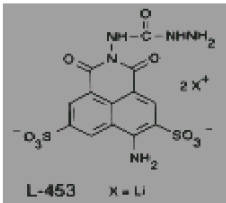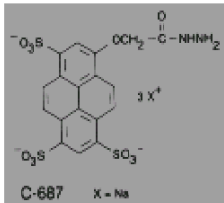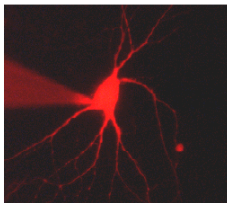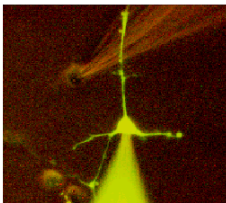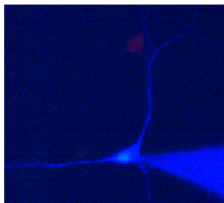
Figure 2-19 shows the molecular structure of the three dyes as well as exemplary pictures.

All dyes were dissolved at 250 μg/ml in intracellular patch solution (see 2.1.2). The stained solution was added to the standard intracellular solution to the very tip of the patch pipette; the cell was then patched as in a standard patch clamp experiment (see part 2.1.2). During the course of the measurement (which on average lasted about 20 minutes), the dye slowly diffused into the cell. Although the dyes themselves are non toxic, their excitation with light of the appropriate wavelength leads to a series of photochemical reactions releasing free radicals which are highly damaging to the cells. For this reason, fluorescence microscopy was always done after electrophysiological measurements were finished.
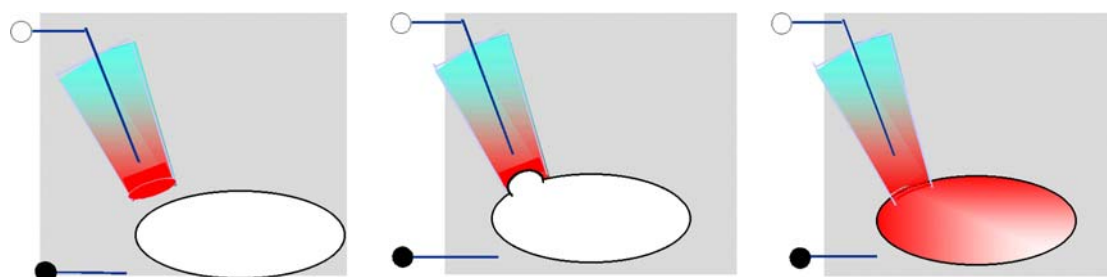
Figure 2-18: Schematic depiction of a microinjection experiment. A patch pipette tip-filled with a polar dye is used as in a standard patch clamp experiment. In the course of the measurement, the dye diffuses into the cell, staining its cytoplasm.

Dye	(A) Sulforhodamine	(B) Lucifer Yellow	(C) Cascade Blue
Absorption	430 nm, 540 nm	430 nm	400 nm
Emission	610 nm	530 nm	430 nm
Chemical structure			
Example			

Figure 2-19: The polar tracer dyes used for microinjection. Up to three cells could be patched simultaneously and injected with a different dye. Separate pictures were taken for each dye under light of the appropriate wavelength. These pictures were later superimposed to visualise areas of physical contact.

2.10 Statistical Evaluation: Predictions on Reciprocal Connectivity

The *in vitro* forming neuronal networks discussed in this thesis are composed of two broad populations of neurons: Excitatory ones on the one hand, that mostly use glutamate as a transmitter and depolarise other cells through synaptic connections. Inhibitory ones on the other hand , using the transmitter GABA, that hyperpolarise their postsynaptic interaction partners. In the nervous system, the balance between excitation and inhibition is crucially important for network activity and function. In this context, studying how excitatory and inhibitory neurons connect and which constellations form is a highly relevant approach to gain an understanding of network behaviour [Bush, 1996; Golshani, 1999; Manor, 1999; Muller, 1997].

In chapter 8, the formation of synapses between excitatory and inhibitory cells is investigated, focussing on reciprocal connections between two cells. The following constellations are possible: Reciprocal inhibitory, reciprocal excitatory and mixed pairs of one inhibitory and one excitatory synapse. The probability for these constellations to occur is calculated here, assuming that the cells connect randomly. Later, these values will be compared to the data obtained experimentally.

As calculations are performed similarly to Müller et al. [Muller, 1997], the approach of this group will be described briefly: First, a representative amount of synapses was measured in the neuronal network under investigation, *in vitro* forming networks from hypothalamic neurons. Next, the average number of synaptic contacts each excitatory and inhibitory neuron formed respectively was estimated. From the respective rates of synapse formation and from the ratio of observed excitatory to inhibitory synapses, the relative numbers of excitatory and inhibitory neurons in the culture could be deduced. Knowing the numbers of excitatory and inhibitory neurons in the system as well as the rate at which they formed synapses, the

probability to encounter the different possible constellations of reciprocal connections could be calculated.

2.10.1 Summary of the Experimental Data Underlying the Calculations

The data used for the following calculations will be presented in chapters 6 and 8. For clarity, the tables summarising the basic findings relevant for these calculations are reproduced in this chapter.

Data underlying the following calculations are:

1.) Numbers of excitatory and inhibitory synapses

As displayed in Table 6-2, on patterned substrates, 30% of the encountered synapses were identified as excitatory, 70% as inhibitory, on controls 38% as excitatory versus 62% as inhibitory. Below, the value to be used is the relative synapse frequency s, which is here defined as the probability of an encountered synapse to be excitatory or inhibitory.

$s_{\text{excitatory\_p}} = 0.30$ (excitatory synapses on patterned substrates)

$s_{\text{inhibitory\_p}} = 0.70$ (inhibitory synapses on patterned substrates)

$s_{\text{excitatory\_c}} = 0.38$ (excitatory synapses on controls)

$s_{\text{inhibitory\_c}} = 0.62$ (inhibitory synapses on controls)

	Total number of characterised synapses	Excitatory Synapses	fraction of total	Inhibitory Synapses	fraction of total
Patterned Substrates	70	**21**	30%	**48**	70%
Controls	13	**5**	38%	**8**	62%
Total	82	**26**	32%	**56**	68%

Table 6-2: Occurrence of excitatory and inhibitory synapses on patterned and on control substrates. In both groups, inhibitory synapses are more abundant than excitatory ones.

2.) Rate of synapse formation by excitatory and inhibitory neurons

Next, the rate at which excitatory and inhibitory neurons form synapses was determined. As non synapse forming neurons could not be identified as either excitatory or inhibitory, the rate of synapse formation had to be calculated indirectly via the rate of branching. The term "branching" was applied by Müller et al. to neurons making more than one synaptic contact. In the presented study, branching was quantified by evaluating triple patch clamp measurements (in which three neurons were patched simultaneously): Neurons making a synaptic contact to just one of the other cells were counted as non branching, neurons connecting to both cells as branching. As displayed in Table 8-1, the likelihood of an excitatory neuron to branch was 20%, whereas the likelihood of an inhibitory neuron to branch was about twice as high, 43%.

	total	branching	non branching	fraction branching
excitatory neurons	5	1	4	20%
inhibitory neurons	21	9	12	43%

Table 8-1: Branching rate of excitatory and inhibitory neurons. Total numbers indicate the number of excitatory and inhibitory neurons identified in triplet constellations

From the rate of branching, the rate of single synapse formation was deduced for each type of neuron. This was done under the assumption that the rate for the formation of the first and the second synapse was the same (the same assumption was made by Müller et al.). Further assuming that first and second synapse formation occur independently of each other, the rate y for the formation of two synapses within an investigated triplet should equal the square of the rate x for the formation of one synapse.

Y is determined experimentally (as the branching rate) and x is calculated as square root therefrom.

Entering the values from Table 8-1, the rate x of synapse formation for excitatory neurons is

$$x_{\text{excitatory\_p}} = \sqrt{0.20} = 0.45$$

and for inhibitory neurons

$$x_{\text{inhibitory\_p}} = \sqrt{0.43} = 0.66$$

(no corresponding values for control substrates were available)

With the relative synapse frequencies $s_{\text{excitatory}}$ and $s_{\text{inhibitory}}$ and taking into account the probabilities $x_{\text{excitatory}}$ and $x_{\text{inhibitory}}$ of the two types of neurons to form a synapse, the ratio of excitatory to inhibitory neurons can be calculated with Equation 2-1:

$$\frac{f_{\text{inhibitory\_p}}}{f_{\text{excitatory\_p}}} = \frac{s_{\text{inhibitory\_p}}}{s_{\text{excitatory\_p}}} \cdot \frac{x_{\text{excitatory\_p}}}{x_{\text{inhibitory\_p}}}$$

$f_{\text{inhibitory\_p}}$ = frequency of inhibitory neurons on patterned substrates

$f_{\text{excitatory\_p}}$ = frequency of excitatory neurons on patterned substrates

$s_{\text{inhibitory\_p}}$ = frequency of inhibitory synapses on patterned substrates

$s_{\text{excitatory\_p}}$ =frequency of excitatory synapses on patterned substrates

$x_{\text{inhibitatory\_p}}$ = rate of synapse formation for inhibitory neurons on patterned substrates

$x_{\text{excitatory\_p}}$ = rate of synapse formation for excitatory neurons on patterned substrates

Equation 2-1

Entering the values presented above yields

$$\frac{f_{\text{inhibitory\_p}}}{f_{\text{excitatory\_p}}} = 1.6$$

or $f_{\text{inhibitory\_p}} = 0.62$ and $f_{\text{excitatory\_p}} = 0.38$

This means that inhibitory neurons on the patterned substrates are more abundant than excitatory ones by a factor of 1.6 and that 38% of the neurons are excitatory, 62% inhibitory.

2.10.2 Probabilities of Different Reciprocal Constellations

From the presented values, the probability of encountering either of the three possible constellations of reciprocal synapses is calculated. This is done by elementary statistical evaluation depicted in Figure 2-20: 8% of the reciprocal synapses found are expected to be reciprocal excitatory after this calculation, 51% are expected to be reciprocal inhibitory and 40% to be mixed.

As discussed in chapter 8 and illustrated in Table 8-2, the values encountered experimentally are strikingly different.

	pattern		control	
	total number	fraction	number	fraction
total number of reciprocal synapses	**11**	**100%**	**4**	**100%**
excitatory - excitatory number	**1** (0.9)	**9 %** (8%)	**0** (0.6)	**0 %** (16%)
inhibitory - inhibitory number	**2** (5.6)	**18 %** (51%)	**1** (1.5)	**25 %** (37%)
excitatory - inhibitory number	**8** (4.4)	**73 %** (40%)	**3** (1.9)	**75 %** (47%)

Table 8-2: Occurrence of different constellations of reciprocal synapses on patterned and on control substrates (bold numbers). The values for the respective constellation expected if synapse formation occurred randomly are depicted in brackets; the calculations leading to the predicted values can be found in chapter 2.10. The formation of mixed constellations is strongly enriched over reciprocal inhibitory ones.

Although reciprocal excitatory synapses occurred at a rate close to the expected value, mixed synapses are clearly enriched over reciprocal inhibitory ones. The occurrence of mixed constellations is higher than expected with a significance of 95%:

Following standard textbooks on statistical evaluation [Sachs, 1983], the lower

95% confidence interval can be calculated after Equation 2-2:

$$\pi_u = \frac{x}{x + (n - x + 1)F} \quad \text{with } F_{\{FG_1 = 2(n - x + 1), FG_2 = 2x\}}$$

Equation 2-2

After R.A. Fisher [Sachs, 1983], $F_{8,16} = 2.59$.

With

n=11 (number of reciprocal synapses)

x= 8 (occurrence of mixed constellation),

$\pi_u = 44\%$

This means that with a probability of 95%, the true fraction of mixed reciprocal synapses in the system is at least 44%. As the value expected under the assumption that synapse formation occurred at random was 40%, the experimental values deviate significantly from this expectation, inferring a mechanism that enriches reciprocal connectivity between mixed pairs of neurons over connectivity between equal cell types.

Analogously, the significance of the deviating occurrence of reciprocal inhibitory synapses can be calculated with Equation 2-3:

With n=11 and x=2,

$$\pi_o = \frac{(x+1)F}{n - x + (x+1)F} \quad \text{with } F_{\{FG_1 = 2(x + 1), FG_2 = 2(n - x)\}}$$

Equation 2-3

$F_{6,18} = 2.66$, therefore $\pi_o = 47\%$

As expected, again, this does not reach the value predicted theoretically, 51%, similarly inferring a significant deviation from the predicted values.

Since no triple patch data were available on control substrates, corresponding calculations for controls can only be performed under the assumption that the rate of branching on controls equals the rate on patterned substrates. (This assumption appears to be justified: In chapter 6.2., the rate of synapse formation on patterned substrates and on controls is compared by

analysing the percentage of patched cell pairs that were synaptically coupled. This percentage and thus the sum of $x_{inhibitatory}$ and $x_{excitatory}$ was found to be the same in both groups).

From $s_{inhibitory\_c} = 0.62$ and $s_{excitatory\_c} = 0.38$ (see Table 6-2) it can be calculated with Equation 2-1 that $f_{inhibitory\_c} = 0.52$ and $f_{excitatory\_c} = 0.48$.

Using the statistical evaluation depicted in Figure 2-20, 16% of the encountered reciprocal synapses are predicted to be reciprocal excitatory, 37% reciprocal inhibitory and 47% to be mixed. Again, the experimental data deviate from the theoretical predictions, showing a preference for the formation of mixed constellations (Table 8-2.) as found on patterned substrates. However, due to the much smaller amount of data, these values do not reach significance.

Another prediction can be extracted from the model: Adding the probabilities of the four possible constellation of non reciprocal, monosynaptic connections to form, it can be inferred that about 58% of all patched pairs of cells are expected to be connected through at least one synapse (see Figure 2-20). This roughly fits the value determined experimentally, which was 49% for both patterned and control substrates (Section 6.2.1.) and can thus serve as a control underlining the validity of the connectivity model used in this chapter.
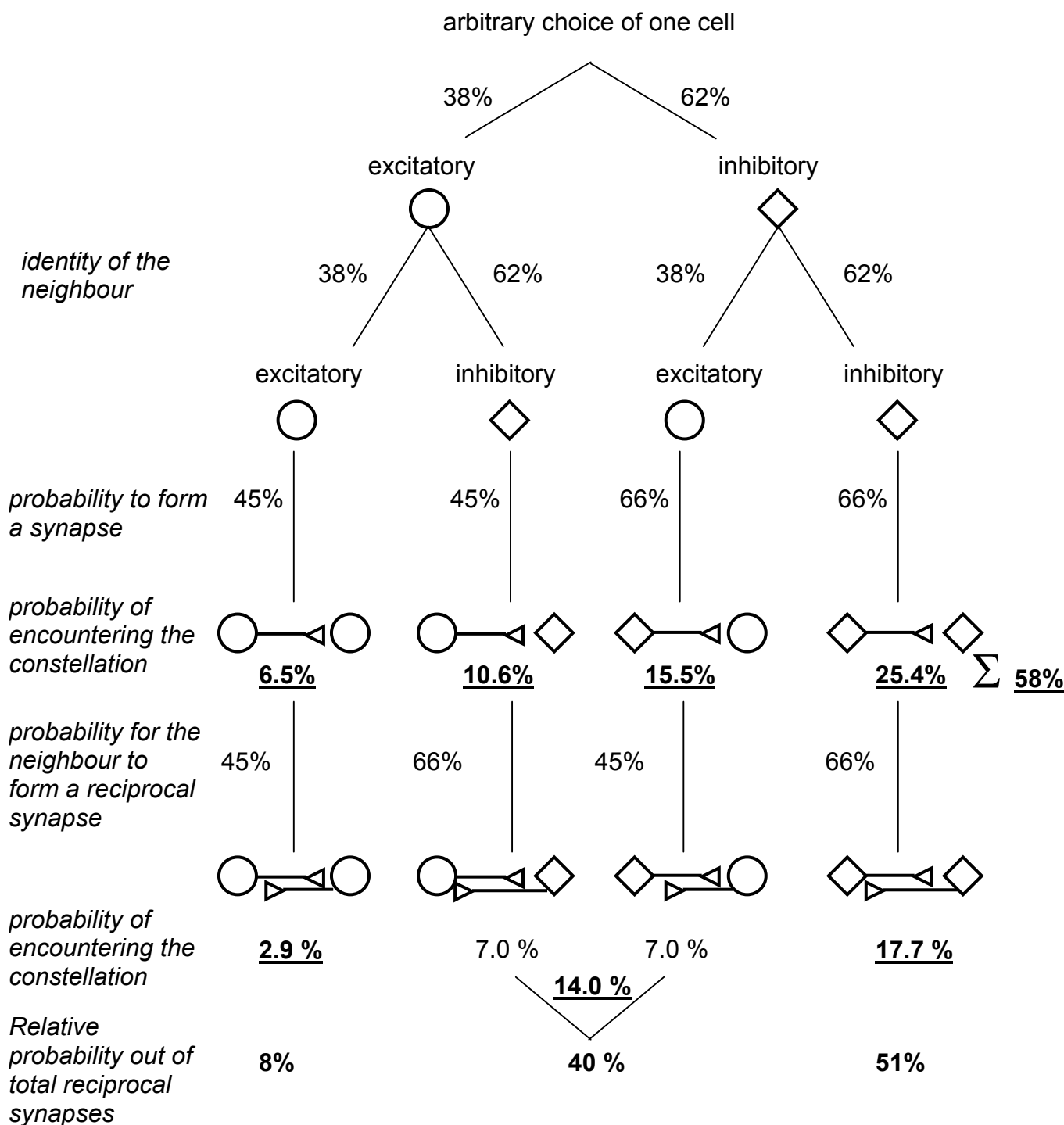
Figure 2-20: Elementary statistical evaluation of the probability to encounter the three possible constellations of reciprocal synapses (for reasons of clarity, non synapse forming neurons were omitted from the scheme). The rate at which the three combinations are expected when patching two cells is calculated by following the branches and multiplying the probabilities for each of the single events. In addition, the expected occurrence of one constellation in relation to the total number of reciprocal synapses is displayed.

The numbers entered into this scheme are the values encountered on patterned substrates, see above. An analogous calculation was performed with the values for control substrates, these were entered appropriately.

3. Substrate Preparation

The following chapter describes the preparation of micropatterned substrates by microcontact printing. The quality of patterns realised with different inking solutions is compared by fluorescence microscopy, SEM and AFM.

3.1 Choice of the Inking Solution

In the past, microcontact printing for the patterning of neuronal cells has predominantly been done with laminin, laminin fragments, polylysine or a mixture of polylysine and laminin as inking solutions [Branch, 1998; Lauer, 2002; Wheeler, 1999; Kam L, 2001; Yeung, 2001; Scholl, 2000]. Laminin was chosen by these groups as a physiological adhesive molecule because it is known to guide neuronal outgrowth *in vivo* [Sanes, 1989] and therefore should be suitable to organise neuronal network formation *in vitro*. Polylysine on the other hand is used as a polycationic polymer known for its potency to attract cells to the surface. However, adhesion to polylysine seems to occur through electrostatic attraction rather than through a biological recognition process (involving specific receptor-ligand interactions), which some people see as a drawback to this system [Banker, 1991; Cestelli, 1992].

Although laminin has been used successfully to pattern neuronal cells in this group and in others, the choice of this protein as an inking solution was reconsidered: The type of surface modification used to allow cell adhesion is not a trivial issue because cellular attachment to particular surface molecules is more than merely a mechanical process. Interactions of cellular receptors with specific extracellular matrix molecules have been shown to have profound effects on morphogenesis, development and even survival of neuronal cells as well as on synapse formation [Chamak, 1989; Lein PJ, 1989; Letourneau, 1994; Son, 1999; Reichardt, 1991]. Such effects are thought to occur mostly through intracellular signalling cascades

triggered by the engagement of cell-matrix receptors. Therefore, it is not surprising that neurons on micropatterned surfaces also respond specifically to the type of substrate coating they encounter: Wheeler et al. found that the cells - when given the choice between differently patterned regions - preferentially extend their dendrites onto polylysine coated regions while axons prefer to grow on a mixture of polylysine and laminin [Wheeler, 1999]. Based on these findings, it seemed interesting to examine the impact that different types of inking solution had on the development and connectivity of neuronal networks grown on micropatterned substrates.

The following inking solutions were compared: First, laminin and polylysine-laminin (referred to as PL) were stamped as in previous experiments. Second, a commercial product called ECM-gel was used, which consists of a protein mixture directly isolated from native tissue without further purification steps. This product was chosen because offering only one purified protein for cell adhesion seems to be rather remote from the *in vivo* situation where the cells encounter a highly complex extracellular matrix consisting of multiple different components. A mixture of ECM proteins of physiological relative amounts appeared to be an attractive alternative to the pure laminin system. ECM-gel contains laminin as a major component and collagen type IV, heparan sulfate proteoglycan, entactin as well some minor components not specified by the distributor. Because positively charged polymers are known to enhance cell adhesion [Makohliso, 1993], ECM-gel mixed with polylysine was included in the investigation. Mixtures containing different amounts of polylysine were tested; since a concentration of 10 µg / ml was the one ultimately employed, only this solution is considered here. Polylysine alone could not be used, because the solution didn't wet the stamp sufficiently to allow printing.

3.2 Quantification of Pattern Transfer

In the comparison of different inking solutions, the first aspect to evaluate was whether they behaved similarly during the patterning process or whether one system had advantages over the others in terms of transfer to the substrate. Pattern transfer was quantified by adding the fluorescent dye sulforhodamine to the respective protein solution before stamping. Labelling the inks with this dye made it possible to visualise the areas where pattern transfer had occurred by illuminating the substrate with light of the wavelength exciting the dye. The total area covered by the protein pattern could then be determined on photographs using standard image evaluation software.

As shown in Figure 3.1, ECM-gel transferred significantly better than laminin and this effect was not notably changed by the addition of polylysine to either solution. Differences in transfer efficiency could arise at two steps: Either as a result of a different adsorption rate of the inking solution to the stamp: The more material adsorbs, the more material is available for patterned transfer. Stamp wetting is a difficult issue as PDMS is a hydrophobic material and thus not the ideal interaction partner for water-soluble proteins. A more hydrophilic stamp on the other hand would impede transfer to the equally hydrophobic substrate which is a similarly bad interaction partner. A compromise was taken by soaking the stamps in water before printing in order to increase hydrophilicity. Alternatively, the efficiency with which the molecules transferred in the printing step could be divergent between different inks. Transfer to the substrate is a similarly critical step as wetting since the hydrophobic substrate is as unattractive for interaction with water soluble compounds as the stamp itself.

Determining which of the two steps determined the difference in transfer efficiency was beyond the scope of this thesis.
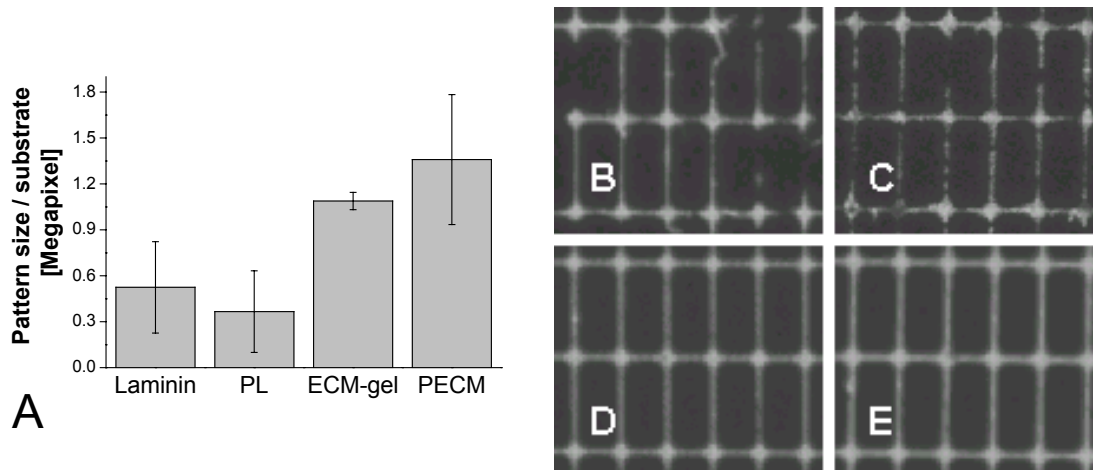
Figure 3.1: Pattern transfer during microcontact printing. Four different inking solutions are compared by visualising the protein pattern through the addition of a fluorescent dye. ECM-gel and PECM show a higher rate of pattern transfer than laminin and PL. A: Transfer quantification B-E: Exemplary pictures of patterns stamped with different inks. B: Laminin, C: PL, D: ECM-gel E: PECM

The enhanced transfer obviously is a significant advantage of the ECM-system, since the patterned area should be as large as possible in order to allow the growth of a large network. Besides, a minimum of adhesive area attracting a minimum number of adherent cells is required to obtain a critical amount of cells on the substrate required for a healthy cell culture. The necessity for a minimum number of adherent cells was additionally fulfilled by a different measure: In addition to the printed area in the middle of the dish, small regions at the edge were coated with the respective inking protein in an unstructured manner. These served as additional adhesion areas for neurons and glia in order to increase the overall cell density and thus cell longevity on each substrate (see also chapter 4).

3.3 Pattern Imaging by SEM and AFM

For a more detailed analysis of the micropatterns realised with the different inking solutions, SEM (scanning electron microscope) and AFM (atomic force microscope) imaging was performed. For SEM images, an electron beam scans the surface allowing the electrons to interact with it. Reflected and emitted electrons are detected with respect to the angle at which they leave the probe, thus yielding information on surface topography. Although this method can be used to probe many different aspects of a surface e.g. related to its chemistry, here it was applied only to investigate surface topography. A 5 nm gold film was deposited onto the surface before scanning, therefore the different surface chemistry of pattern and background should not have an impact on the image. The AFM picture reveals that the printed microstructure has a height of over 100 nm (see below), hence a gold film of 5 nm should not distort topographical features. On an SEM picture, surface edges appear with a high contrast because secondary electrons are emitted on the side of the ridge. Therefore, edges appear brighter than homogeneously coated areas of the same thickness.

AFM imaging works through a different mechanism. In this technique, the surface is probed by a fine tip fixed to a cantilever moving over it and evaluating the force gradient between tip and surface. Again, differential surface properties can play a role in the obtained image, as they exert different forces onto the AFM tip. The tapping mode was applied, which applies very little force to the surface as the tip touches ("taps") it only transiently. This mode was therefore the most suitable for the probing of the soft protein patterns. In contrast to SEM pictures, which do not yield absolute values, AFM pictures can be used to measure surface structures in height and width.

The AFM pictures of the laminin pattern shown in Figure 3.5 reveal structures of about 150 nm in height. Laminin as an extended chain has a length of about 100 nm [Martin, 1987], therefore a simple monomolecular layer does not seem to be present on the surface, even if it

was assumed that the molecules were oriented perpendicular and that the chain was completely extended. An alternative explanation is that a multilayer formed, although other works using laminin fragments indicate that the layers transferred by microcontact printing are monomolecular [Scholl, 2000]. The most likely possibility appears to be that salt deposited in addition to the protein and that this is responsible for the thickness of the pattern. For inking, laminin was dissolved in PBS buffer. The drying step preceding the actual stamping dramatically concentrated the salts in the ink. It is highly probable that significant amounts of salt transferred during microcontact printing. Most likely, the majority of deposited salt dissolved when the cells were seeded onto the pattern, as this occurred in an aqueous environment. SEM and AFM pictures however were taken on the dry surface without an intermittent washing step, so the salt observed in these images may not represent the situation encountered by the cell culture.

Corresponding considerations about the thickness of ECM-gel patterns (which were in the same range, 130 nm) cannot be made as ECM-gel represents a complex mixture of proteins. It is therefore harder to estimate how thick a monomolecular layer would be. As ECM-gel was treated similarly as laminin, it is probable that a fraction of the patterned layer of ECM-gel observed in the images is also due to salt deposition.

An interesting feature about the micropatterns that becomes obvious in both SEM and AFM pictures (and therefore cannot be attributed to the increased edge contrast typical for SEM) is that more material transferred at the edges of grid lines and nodes than in the middle of a structure. It seems plausible that this effect is due to the hydrophobicity of the PDMS stamp: The hydrophilic proteins try to avoid interaction with this material and therefore enrich at the edges.

Comparing the SEM and AFM pictures of laminin / PL and ECM-gel / PECM patterns shown in Figure 3.2-Figure 3.5, it appears that the surface coverage is denser and more homogeneous in the ECM-gel containing samples. Laminin seems to have transferred more in distinct

clusters and it also appears that the total amount of material transferred per surface area is smaller. This effect may have an impact on the ability of this type of pattern to attract cell adhesion.

Comparing laminin with PL and ECM with PECM samples, it does not seem that the addition of polylysine had a notable effect on pattern properties. Thickness and surface coverage of the forming layers emerge alike between polylysine containing and non containing inks.

3.4 Summary and Conclusions

The micropatterns realised with four different inking solutions were compared with respect to the efficiency of pattern transfer during microcontact printing and with respect to the properties of the patterned surface. It can be concluded first, that ECM-gel during microcontact printing transfers more efficiently to the surface in terms of pattern size, which is an obvious advantage of this ink. Second, on the molecular scale ECM-gel patterns are denser and more uniform than laminin patterns. The addition of polylysine has no observable direct effect on the presentation of the proteins on the surface. However, slight differences in protein orientation or conformation can not be ruled out.
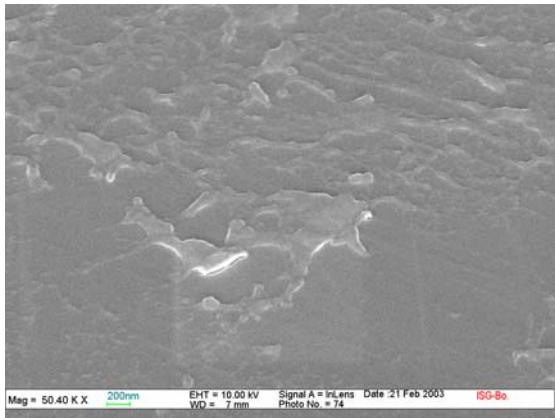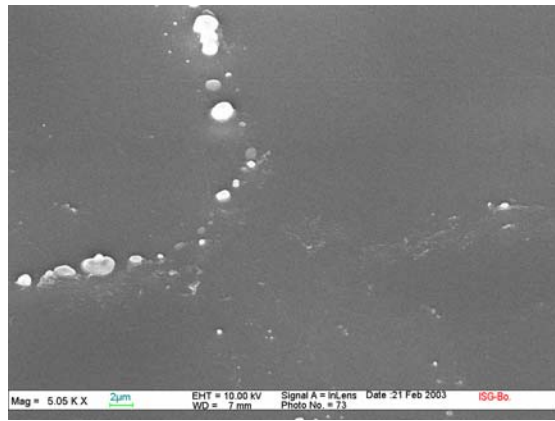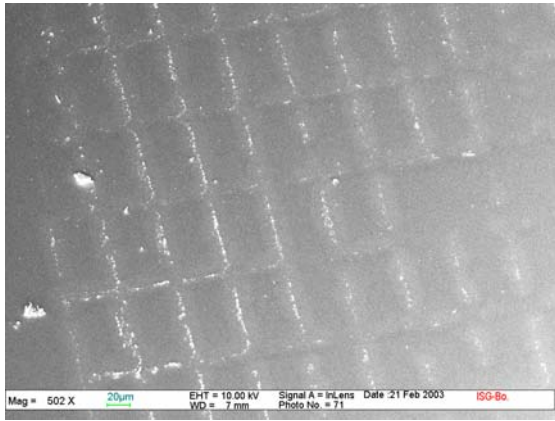
Figure 3.2: SEM pictures of PL substrates at different magnifications. Substrates were printed as normally (pattern B) and investigated under the SEM after evaporation of a 5 nm gold layer.
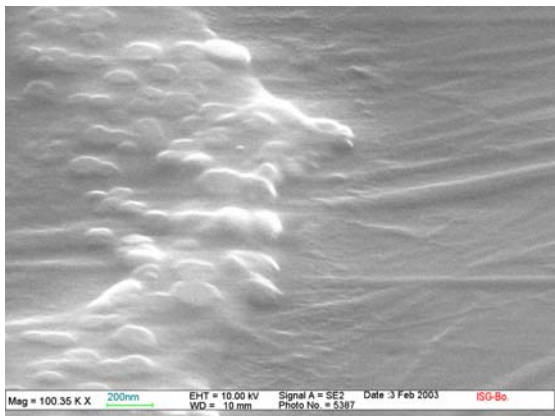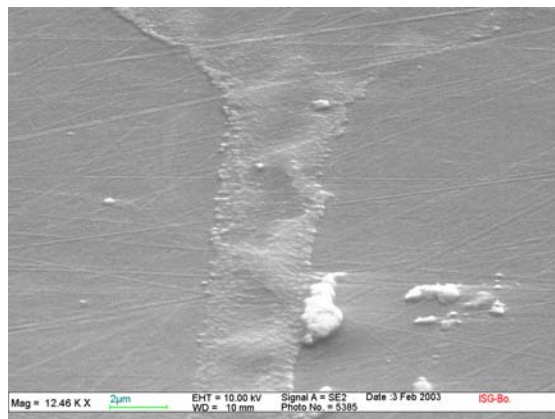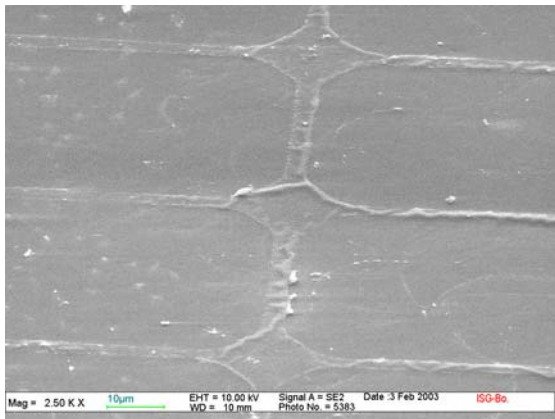
Figure 3.3.: SEM picture of an ECM-gel pattern (pattern A), treated as in Figure 3.2.
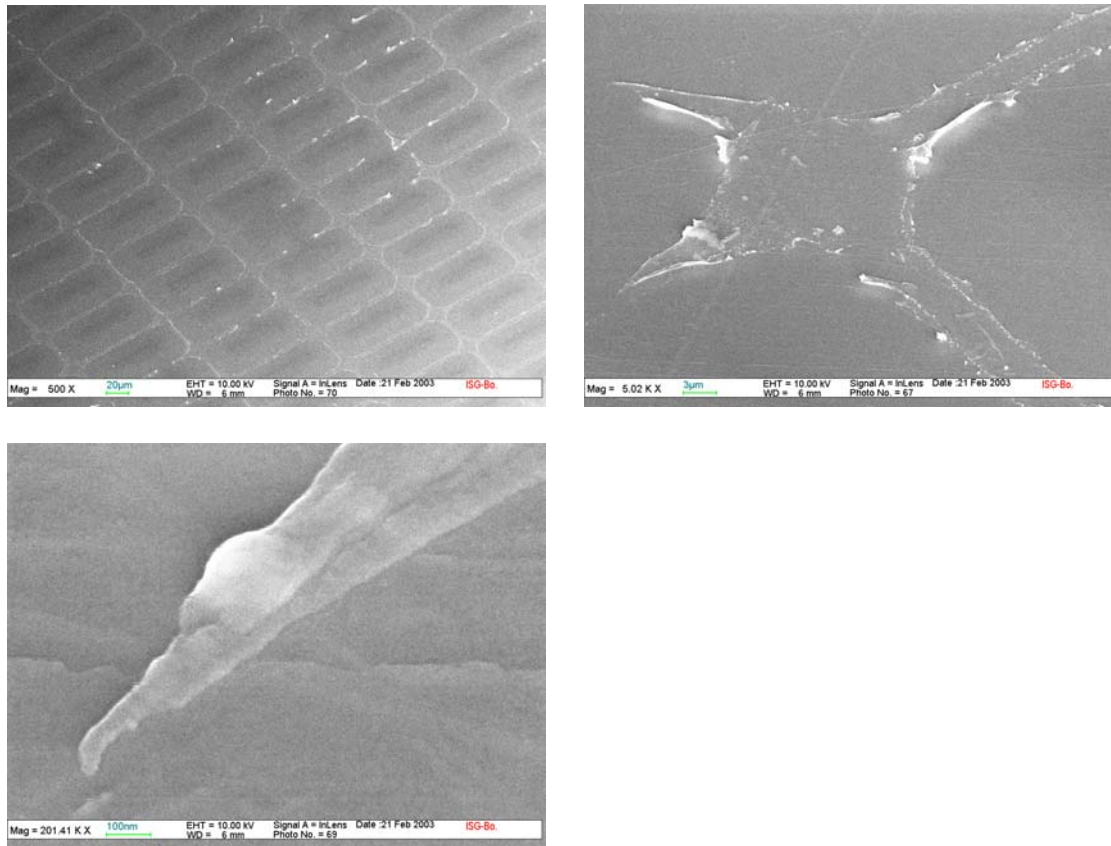
Figure 3.4: SEM pictures of a PECM pattern (pattern B), treated as described under Figure 3.2.

A)

B)

C)

Figure 3.5: AFM pictures of substrates patterned A) with laminin (pattern B), B) PL (Pattern D) or C) ECM-gel (pattern D). The average height of the pattern is fairly similar in all three samples. ECM-gel appears to yield smoother and denser layers than the laminin / PL ink. No obvious differences become apparent between laminin and PL patterns.

91
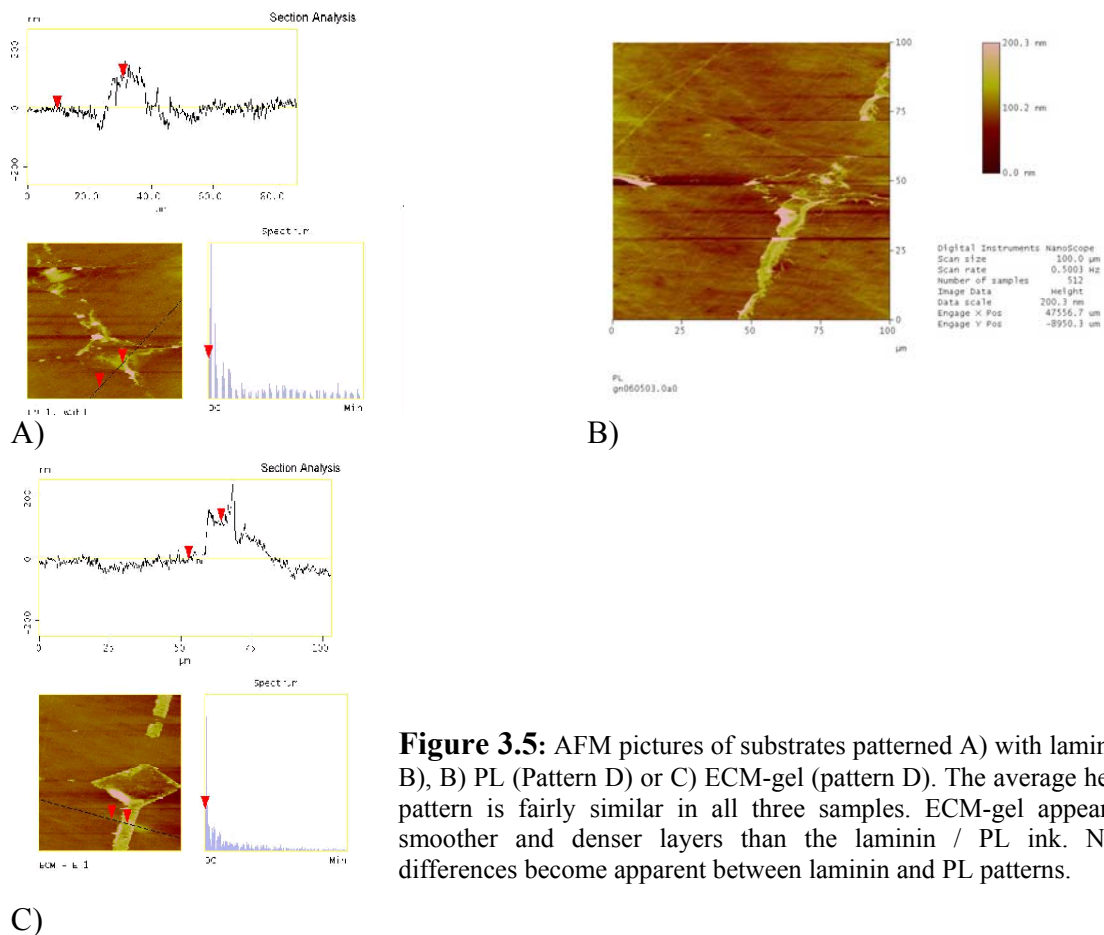
4. Patterned Neuronal Cell Culture

In chapter 1.1 it was described that patterning of neuronal cells is an attractive method for the creation of simplified, well defined neuronal networks. It was further described that the method of chemical patterning uses an antiadhesive background onto which a pattern of cell attracting molecules is applied. Given the choice to adhere to the repellent background or the adhesive pattern, cells seeded onto such substrates will align with the defined adhesion areas and extend their processes according to the chosen geometry. The sharper the contrast between background and pattern chemistry, the better will the cells comply.

In the project presented here, polystyrene is used as a highly hydrophobic and thus cell repellent background onto which patterns of different organic molecules are applied by microcontact printing as described in the preceding chapter. This chapter will now investigate the growth of neurons on these substrates. The first subchapter will deal with the optimisation of the neuronal cell culture protocol in general while the second subchapter will specifically focus on neuronal cell culture on patterned substrates.

4.1 Optimisation of the Cell Culture Protocol

As discussed in chapter 1.6, in the beginning of this project a cell culture protocol using slices from the brain stem was applied. Chapter 1.6 also discusses why this protocol was modified trying to obtain a cell culture that contained a larger amount of chemical synapses. Three major changes were made: Cortical[1] rather than brain stem neurons were cultured and a dissociated rather than a brain slice protocol was applied under the use of a different, serum-free medium. Since the switch from brain slice to dissociated culture represents a fundamental change in the system, a short discussion of the advantages and disadvantages of dissociated versus slice culture will be presented before the results of the two culture conditions are compared.

In a slice culture, a thin slice of brain tissue is placed into a culture dish allowing single cells to migrate onto the substrate. Dissociated protocols in contrast disrupt the tissue mechanically and / or enzymatically, singularising the cells. The cell suspension is then incubated with the substrate, allowing the cells to adhere to the surface out of solution (both techniques are described at length in chapter 2.6). The main advantage initially seen in the brain slice protocol was that the preparation should be less damaging to the cells: The original tissue architecture is not disrupted and an intact cell reservoir is conserved. Since the dissociation process itself can have a cell damaging effect, particularly when enzymatic treatment is involved, the slice protocol was thought to yield physiologically more intact cells. Another advantage seen in the slice culture was that formation of cell clusters does not occur. Cell cluster formation is mostly a consequence of dissociated cells encountering no attractive surface to attach to, which causes them to adhere to each other instead. This fact is of

---

[1] Initially, experiments were performed with both hippocampal and cortical cells. As both cell types yielded similar results and cortical cells were easier to obtain, hippocampal culture was discontinued. All evaluations shown in this study were performed on cortical cells, but in some instances, pictures showing a hippocampal culture are displayed as indicated.

particular interest in the presented project, where a large fraction of the micropatterned surface is deliberately blocked for cell adhesion (see Figure 4.4). For the slice protocol, this doesn't pose a problem because the cells migrating out of the slice are already in contact with the surface and a weak interaction with the substrate suffices to guide them along the pattern lines. As cells will only migrate out of the tissue when they found an adhesive pathway, they will not be bound to stick to each other. The situation is different with a protocol for dissociated cells, where cells encounter the surface out of solution and therefore are much more likely to form clusters. With this protocol, the quality and adhesive properties of the micropattern are much more critical. Addressing this problem, the adhesiveness of the pattern was optimised by investigating different inking solutions as described in chapter 5.

For the presented project, one disadvantage of brain slice over dissociated cell culture lies in the fact that only continuous structures can be used with the slice culture. This is the case because the cells have to migrate over the pattern, a process that is impeded by gaps in the adhesive pathways (pattern geometries containing gaps were used in experiments attempting to control cell polarity which are presented in chapter 7). Additionally, the slice culture demanded that the lines in the grid pattern were wide enough to support the migration of cell bodies rather than only neurite outgrowth.

In order to be able to use pattern geometries containing gaps, it seemed appropriate to switch to a dissociated protocol while cluster formation was kept at a minimum by optimising the adhesive qualities of the micropattern.

Since the major motivation for the application of a new protocol was to improve the cell culture conditions such that the formation of functional networks containing chemical synapses was achieved, several aspects of the culture conditions were compared as presented below. Preliminary studies were performed on unpatterned control substrates to ensure a healthy neuronal culture before the specific situation of patterned growth was taken into account.

4.1.1 Behaviour of Glia Cells

The first focus of investigation was the behaviour of glia cells under the two cell culture conditions. Control of glia proliferation is a central issue in neuronal cell culture (see chapter 2.6). While the brain slice protocol uses a serum-containing (and thus glia proliferation supporting) medium such that antimitotic agents have to be added, the dissociated cell culture protocol applies a serum-free formula that is described not to support glia multiplication. Figure 4.1 A and B depict the typical morphologies of glia cells observed in the two cultures. Figure 4.1 A shows the flat, spread out morphology that has been described for serum-containing cultures which allow glia cells to proliferate. Figure 4.1 B on the other hand shows the "starved" star-shaped morphology associated with serum-free media which do not support proliferation [Suidan, 1997; Dutly, 1991; Beecher, 1994], strengthening the notion that with the new protocol, the amount of glia could be controlled without the addition of antimitotic drugs.

A)   B)
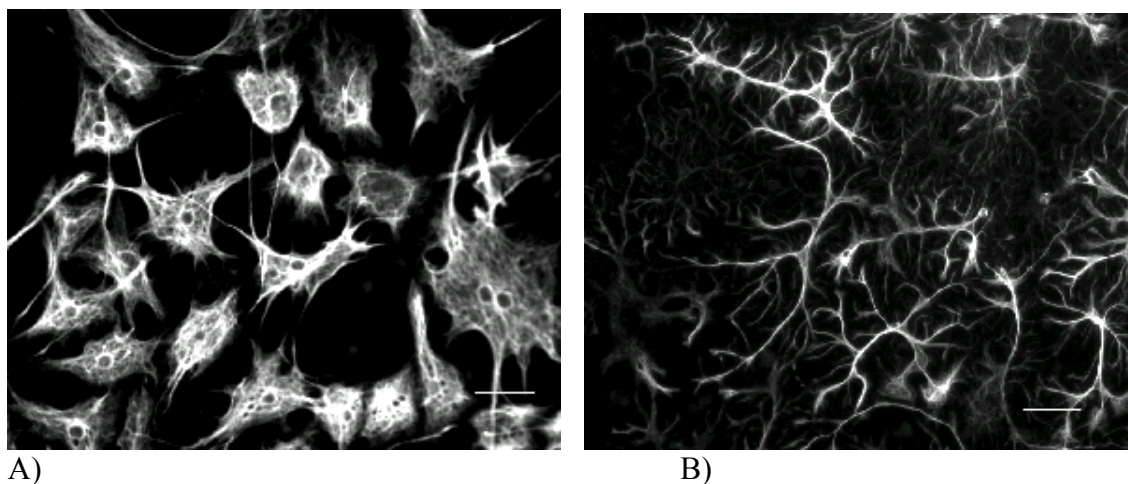
Figure 4.1: Behaviour of glia cells in the two types of cell cultures under investigation. Both were stained with an antibody against the glia-specific cytoskeletal protein GFAP. A) Brain stem slice culture, DIV 12. The cells show the typical spread out morphology described for serum-containing media. B) Dissociated cortical cell culture, DIV 19. The cells are star-shaped, the morphology typically seen in serum-free media which do not allow glia proliferation. Scale bars 100µm.

4.1.2 Electrophysiology

The most important aspect in determining the physiological state of a neuronal cell culture is the electrophysiological behaviour of the neurons. Therefore, electrophysiological measurements of neurons cultivated under the two investigated conditions were performed and compared. As shown exemplarily in Figure 4.2, the cells cultivated with the brain slice protocol are not physiologically intact. Voltage-induced Sodium currents were rarely observed and the cells were unable to fire action potentials (only small non-linear voltage signals were seen). In contrast, cells cultured with the dissociated cell culture protocol had large voltage-induced Sodium and Potassium currents and readily fired one or multiple action potentials upon stimulation.

From these observations, it appears that although the brain slice protocol was thought to be less harmful to the cells, the culture achieved with this protocol was less successful than the dissociated culture. The effect may to a large part be due to the media formulation as the medium used for the brain slice culture had serious drawbacks as discussed in chapter 1.6. The dissociated protocol applies a very gentle (purely mechanical) method of tissue disruption which in combination with the improved medium conditions kept cellular damage at a minimum, enhancing the electrophysiological performance of the cells. More detailed investigation on electrophysiological measurements of the dissociated neurons are reported in chapter 6.
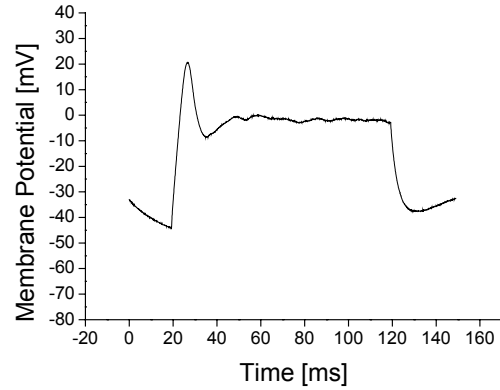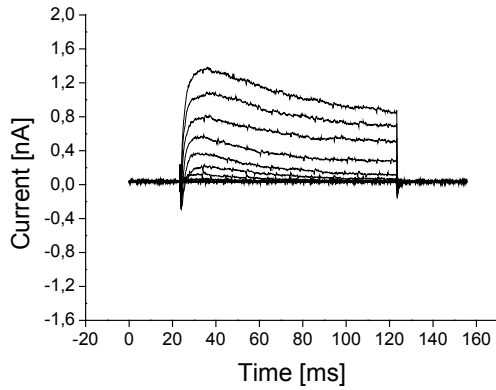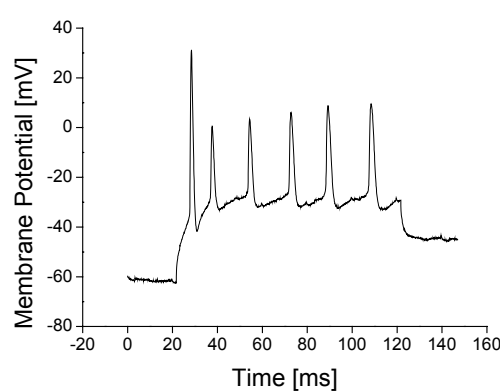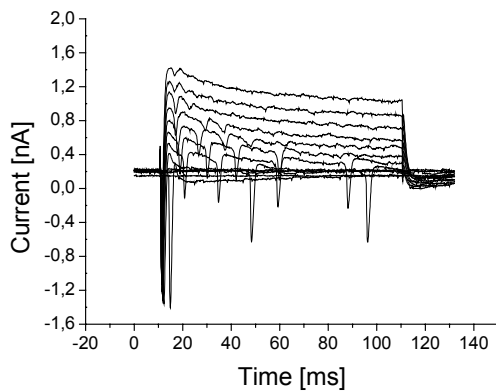
Figure 4.2: Electrophysiological behaviour of neurons cultured with the two investigated protocols. Voltage clamp measurements of the slice culture (A) and the dissociated cell culture (C) are shown. In both cases, a cell was depolarised in a stepwise fashion while the resulting current was recorded. The Sodium current (inward component) is only rudimentary in the slice culture and well developed in the dissociated neuron. Current clamp measurements (B and D, slice and dissociated cell culture respectively) illustrate that neurons cultured with the slice protocol do not fire action potentials (only weak non linear responses to the depolarising stimulus are observed; the spikes are weaker and broader than action potentials) whereas the neurons cultured with the dissociated protocol are able to fire a train of action potentials in response to depolarisation. Both slice and dissociated culture were DIV 13 at the time of recording.

4.1.3 Synapsin Expression

The major aim pursued with the switch to a new cell culture protocol was an increase in the yield of synaptic connections. (A lack of chemical synapses was the major problems observed in previous studies attempting to grow neuronal networks on micropatterned substrates [Lauer, 2001]). Addressing this issue, antibody staining using an antibody against a synapse-specific protein was performed to compare the old and the new culture conditions. Two cell

cultures, one grown from a brain slice with the old medium and one from dissociated cortical neurons using the new medium, were stained with an antibody against synapsin I. The protein should be present in large amounts in existing or developing presynaptic terminals. Additionally, the protein is expected to be found in the cell body where it is being synthesized. The results are shown in Figure 4.3: In neurons cultured with the slice protocol, only a very weak signal in the cell body is detectable, which may not even be specific. No signal in the neurites is visible. In contrast, the same experiment performed with a cell culture maintained under the use of the new protocol shows not only a massive signal in the cell bodies, but also distinct, punctual signals along the neurites, indicating synaptic contacts or vesicles that are transported to developing synapses. Although not every single one of the puncta may represent actual mature synapses, it becomes clear from these investigations that the protein is synthesised by the cells under the new but not the old culture conditions, enabling them to form synapses. From the results presented in this chapter, it appears that the applied changes in the culture conditions were successful in achieving a healthy cell culture able to form synaptic connections. The next question was whether the growth on the pattern had an impact on cellular physiology and synapse formation. These questions are discussed in detail in chapter 6, however, some first observations will be presented in the next subchapter.
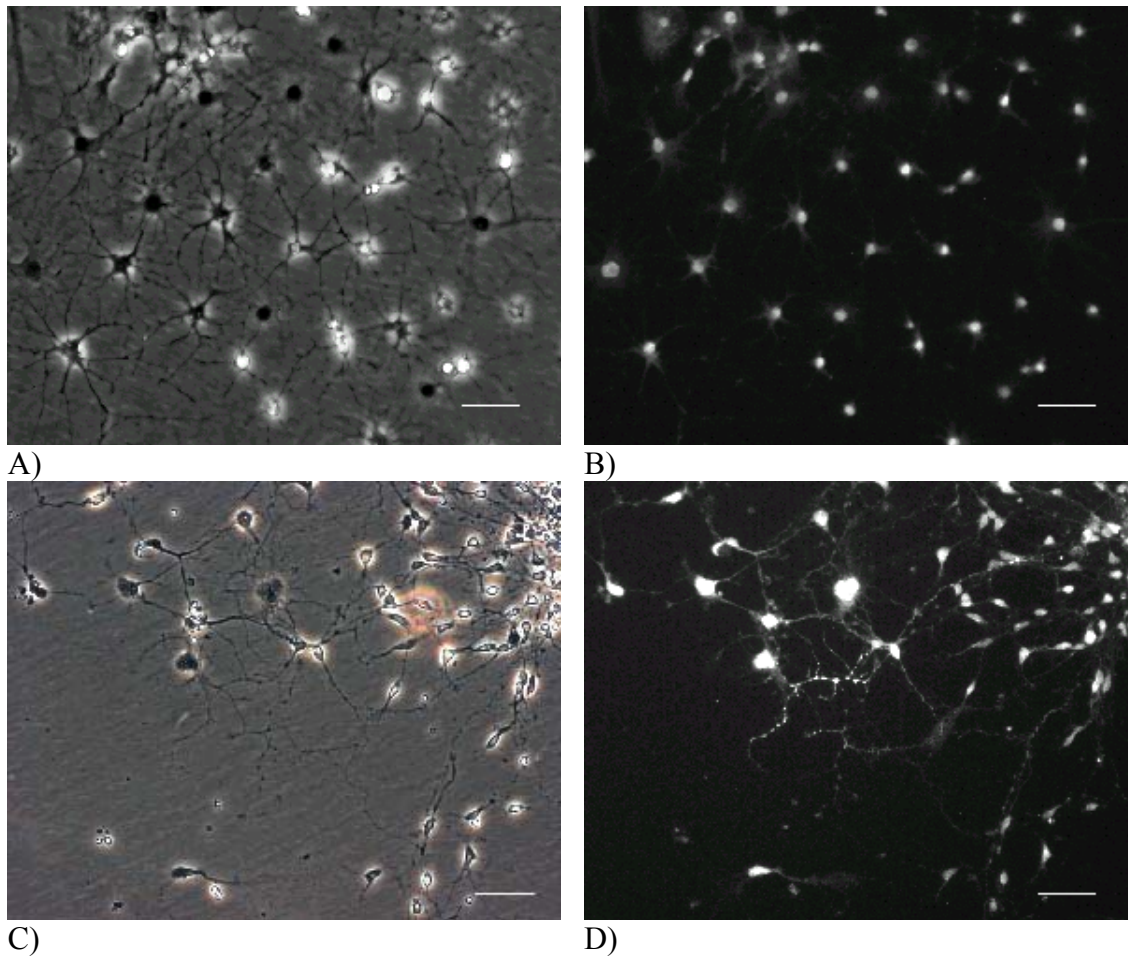
Figure 4.3: Synapsin expression by neurons cultured with the brain slice and the dissociated protocol. A) Brain slice culture, phase contrast image, DIV 12 B) Slice culture stained with αsynapsin I. C) Dissociated cortical culture, phase contrast, DIV 5. D) Dissociated culture stained with αsynapsin I. Scale bars 100μm

4.2 Neuronal Cell Culture on Patterned Substrates

Having established a cell culture protocol containing physiologically intact cells connecting through chemical synapses, the next challenge was culturing the cells correspondingly on the micropatterned substrates. Very low density cell cultures (which naturally occur on the pattern as only a small fraction of the surface is permissible to cellular adhesion, see scheme in Figure 4.4) can be problematic physiologically due to the strong dilution of cytokines and trophic factors secreted by the cells. Addressing this problem, extra adhesion areas in addition to the micropattern were offered at the edge of the substrate. This was done by homogeneously coating small areas with the respective inking solution used for the pattern. By this measure,

99

the overall cell density per substrate could be increased to a density closer to that on control substrates without changing the desired low local density on the pattern (a picture of an unstructured adhesion area is shown in Figure 4.4).

On the structured areas, adhesion of neuronal cells to the pattern was achieved with a high compliance. On the grid patterns, the cells adhered to the node points and extended their processes along the lines defined by the pattern. After several days in culture, network formation along the pattern could be observed (Figure 4.5 A). Initially, line patterns were also applied (shown in Figure 4.5 B). However, line geometries proved to be problematic as cell cluster formation occurred more frequently than on grid patterns, probably because of the extremely limiting geometry. In addition, neurites crossing the pattern and forming connections between separate lines in an uncontrolled manner were seen frequently. Therefore, grid patterns were used predominantly for further investigations.

Taken together, the transfer of the dissociated cell culture protocol to the micropattern which had been developed under the use of a slice culture [Lauer, 2001] was successful. In order to assess whether the growth on a micropatterned substrate has an impact on synapse formation, synapsin staining was also done on a patterned culture. As depicted in Figure 4.6, neurons grown on the pattern exhibit synapsin puncta along their neurites similar to cells grown on controls. From these preliminary observations it appears that synapse formation should be observable in networks cultivated with the new protocol and that growth on a micropattern does not impede this feature.
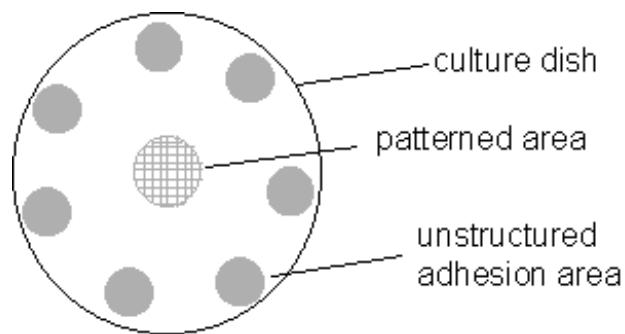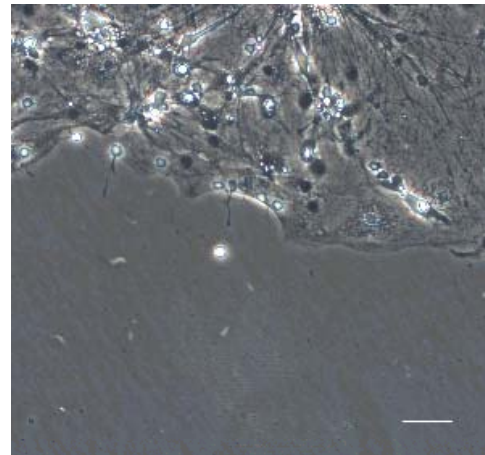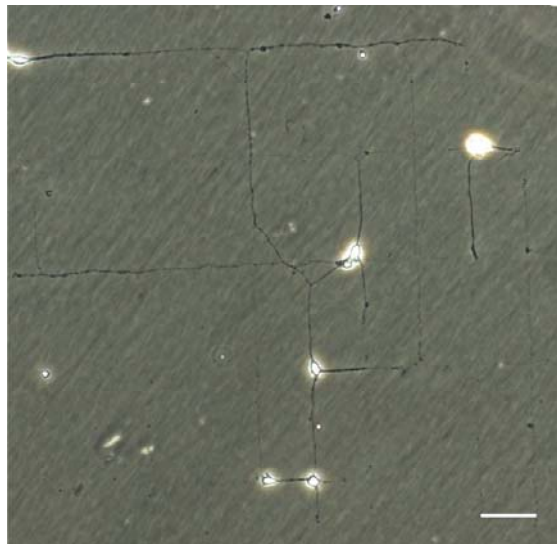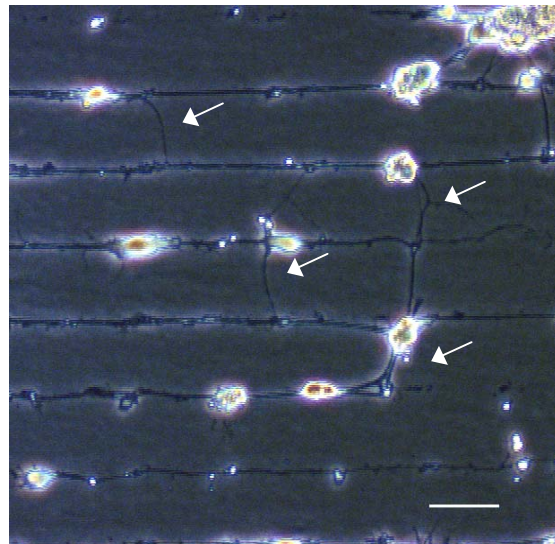
A)   B)

Figure 4.4: A: Scheme of a patterned substrate dish. Adhesive areas are depicted in grey, cell repellent areas in white. Note that most of the surface is blocked for cell adhesion. B) Microscopic picture of glia and neural cells growing on one of the unstructured adhesion areas at the edge of the substrate. Scale bar 100μm.


A)   B)

Figure 4.5: Neurons growing on grid- and line patterns created by microcontact printing. On both patterns, cell adherence complies well with the pattern geometry, but on the line pattern, neurites forming uncontrolled connections to the neighbouring line are often observed (white arrows). A) Dissociated cortical culture on a grid pattern (pattern B) printed with ECM-gel, DIV 7 B) B) Dissociated hippocampal culture on a line pattern (pattern C) printed with a mixture of polylysine and laminin, DIV 12, scale bars 50μm
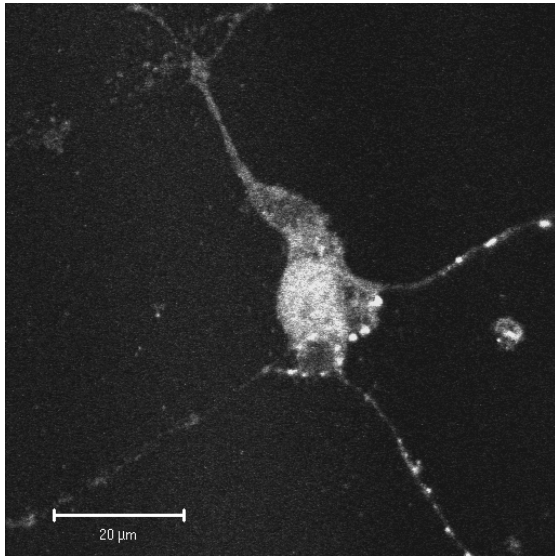
Figure 4.6: Immunohistochemistry picture of a patterned neuron to demonstrate synapsin expression. A cortical neuron grown on a PE micropattern (pattern G) was stained with an antibody against synapsin I (DIV 5). Punctual signals along the neurites are observable, some close to the cell body. These may belong to a neurite extended by a neighbouring cell and represent presynaptic terminals. The picture was taken with a laser scanning microscope, scale bar 20μm.

4.3 Summary and Conclusions

Two different cell culture protocols were compared, one involving a serum-containing medium and brain slices (which has been used in the preceding project [Lauer, 2001]), the other a serum-free formulation and a dissociated cell culture. It could be shown that under the use of the dissociated cell culture protocol the cells were in a better physiological state and that synapsin expression was increased. It could further be demonstrated that cell culture using the dissociated culture protocol was feasible on patterned substrates. Immunohistochemistry experiments indicated that synapsin expression was not impeded by patterned growth.

5. Cell Adhesion to Differently Modified Surfaces

Chapter 3 compared the behaviour of different inking solutions used for microcontact printing with respect to their transfer to the substrate during the patterning process. This chapter will deal with another aspect that is important for their suitability to pattern cells: The efficiency of different surface modifications in recruiting cells to the surface.

As a first step, cellular morphology was examined on substrates that were homogeneously coated with the different inking solutions.

5.1 Morphology on Different Surfaces

The morphology of *in vitro* cultured neuronal cells may vary significantly depending on the surface they are grown on [Stoeckli, 1996]. Several groups linked morphological characteristics directly to the strength of cell-surface interactions. Strong interaction of cells with the underlying substrate is often described to result in a dark appearance in phase contrast pictures and in extended, branching neurites. In contrast, cells adhering weakly to the surface are described to look phase bright, to have a tendency to form lumps and to show fasciculated neurites [Ravenscroft, 1998; Cestelli, 1992; Makohliso, 1993]. Although other groups report that the degree of fasciculation does not depend on the strength of the cell-substrate interaction [Lemmon, 1992], it appeared interesting to compare cellular morphology on surfaces homogeneously coated with the inking solutions that were used in microcontact printing.

As shown in Figure 5.1, neurons on ECM-gel or laminin coated substrates have a phase bright appearance and show extended, bundled neurites. In contrast, cells on substrates

homogeneously coated with polylysine (50 μg / ml) looked dark, flattened out and have a large arbour of branching dendrites, which may indicate a stronger interaction with the substrate. A similar effect is seen on samples coated with a mixture of polylysine and laminin (12.5 μg / ml each). When 1 μg/ml of polylysine was added to the ECM-gel inking solution, cellular morphology was fairly similar to that seen on ECM-gel alone. On the other hand, the addition of 10 μg/ml polylysine resulted in substrates looking similar to the ones coated with polylysine only; the cells were phase dark and spread out and the neurites branched extensively. (In subsequent experiments, only the mixture of ECM-gel with 10 μg/ml polylysine was used and will be referred to as PECM).

In the light of the studies describing cellular morphology to reflect the strength of cell-substrate interaction, it may be concluded preliminarily that the presence of polylysine at the surface increases the strength of cellular adherence to the substrate and that this effect is dose-dependent. Given the polycationic nature of polylysine, it seems likely that such an increase in adhesion strength is mediated through electrostatic interactions tethering the cells to the surface. Positively charged polymers like polylysine or polyornithine have been described before to enhance cell adhesion [Makohliso, 1993; Goldberger, 1999; Cestelli, 1992] and may attract cells through the interaction with negatively charged groups on the cell surface like phosphorylated proteins or sulfated proteoglycans.
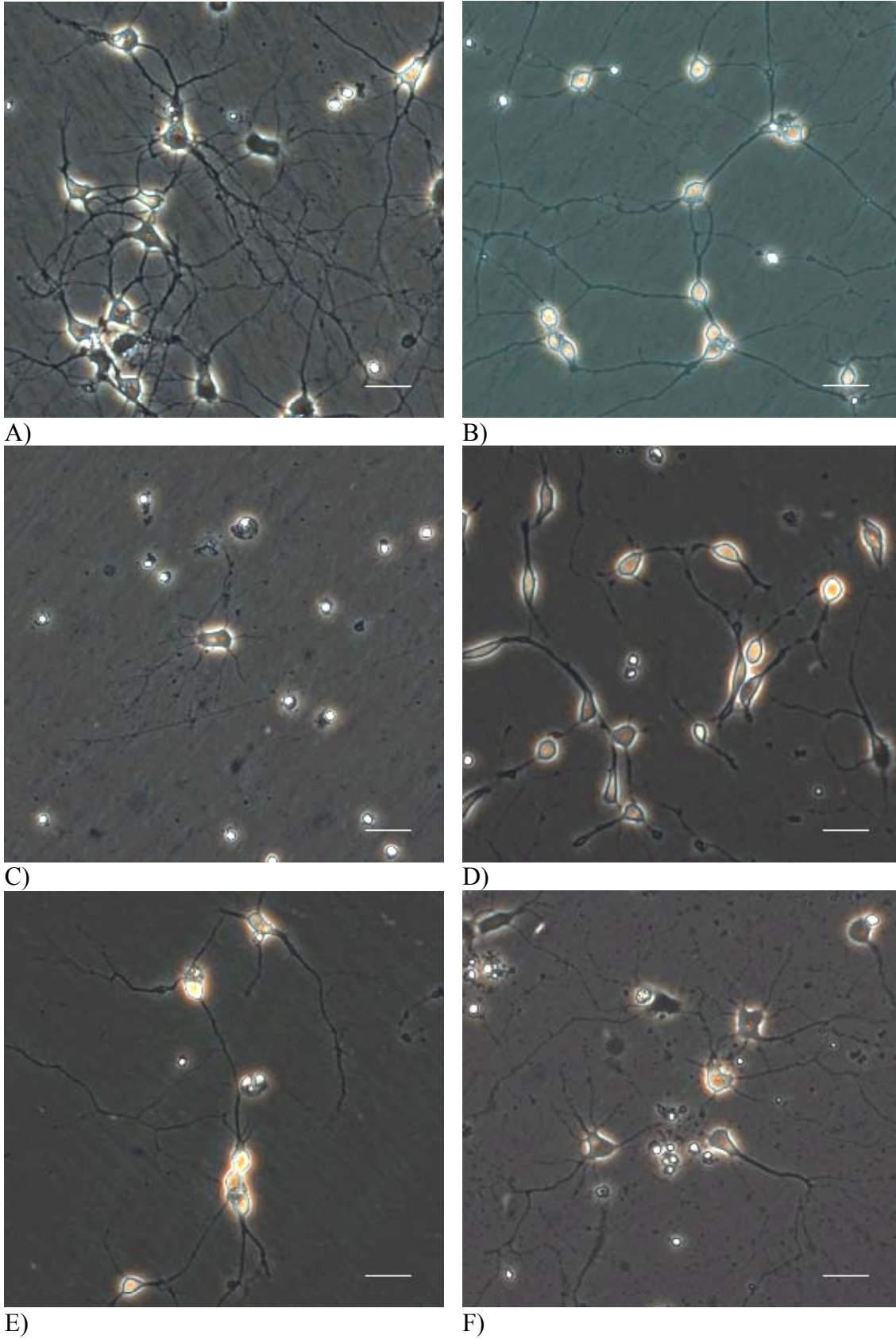
Figure 5.1: Morphology of cortical neurons grown on substrates homogeneously coated with different protein solutions (all pictures were taken at DIV 4). Surfaces were coated with the following solutions: A: Polylysine (50 μg / ml), B: Laminin (25 μg / ml), C: Polylysine and laminin (12.5 μg / ml each), D: ECM-gel (1:100 dilution of the stock) E: ECM-gel (1:100) with 1 μg / ml polylysine, F: ECM-gel (1:100) with 10 μg / ml polylysine

5.2 Cell Attachment to Patterned Surfaces

Cell attachment is an important factor for cell survival *in vivo* and *in vitro*. In cell culture, when cells are plated onto a surface they cannot adhere to they lump together and die.

The previous paragraph indicated that the strength of cellular adhesion to homogeneously coated substrates varies with the type of surface modification used and appears to be increased in samples containing polylysine. It seemed to be an interesting question whether on micropatterned substrates - where the available adhesion area is limited - such a difference in adhesion strength reflects itself in the number of cells that can be recruited to the surface and thus be allowed to survive.

To test this possibility, equal amounts of cells were seeded onto substrates patterned by microcontact printing with different inks. After one week in culture, the numbers of cells growing on the different patterns were compared. Figure 5.2 shows the total number of cells adhering to the substrate per randomly chosen area. Clearly, a larger amount of cells survived on samples printed with PECM than with ECM-gel and similarly more on PL than on laminin samples (although the latter effect was less pronounced).

In chapter 3, pattern transfer during microcontact printing was compared for the different inking solutions. It could be shown that the addition of polylysine has no impact on the amount of protein that transferred during the patterning process or on the quality of the forming protein layer. Therefore, a larger patterned area on polylysine-containing samples cannot be accounted for the observed difference in cell recruiting potential. It therefore appears that the addition of polylysine to the inking solution as such increases the potential to recruit more cells to the pattern. This result is in agreement with the suggested hypothesis, namely that polylysine as a positively charged polymer amplifies cellular adherence to the surface allowing a larger fraction of cells to survive on the patterned substrate. The idea was further tested by directly relating the number of adherent cells per available adhesion area on

individual substrates: Since pattern transfer during microcontact printing varied significantly not only depending on the inking solution as discussed in chapter 3 but also from sample to sample (such that not necessarily all evaluated areas provided a similar amount of adhesive pattern), the number of adherent cells per available adhesion area was determined. This was done by calculating the number of occupied versus empty nodes in the grid pattern. Empty nodes, where material transfer had taken place but no cell body had adhered, were registered when the empty pattern was either visible in the phase contrast image or when the node was overgrown by neurites, indicating the presence of enough material for cellular adherence. As depicted in Figure 5.3, samples printed with polylysine containing inks also recruited more cells per available surface area (PECM more than ECM and PL more than laminin).
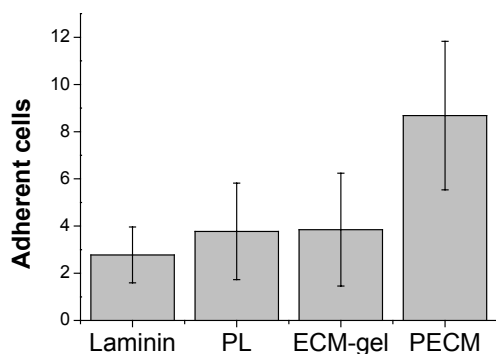
Figure 5.2: The amount of adherent cells per randomly chosen surface area was compared between substrates patterned with different inking solutions. Pictures taken under a 100x magnification at DIV 11-15 were evaluated by counting all single adherent cells. Adherence on PECM substrates is notably higher than on all other surfaces.
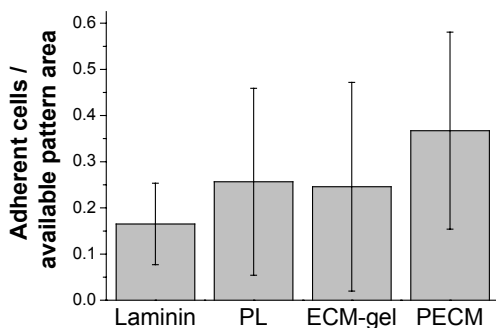
Figure 5.3: The number of adherent cells per available surface area is compared. This was done by normalising the data from Figure 5.2 with respect to the amount of pattern present in each picture, calculating the number of occupied versus empty adhesion sites. Available adhesion sites were counted when a node point of the grid was either visible in the phase contrast picture or when transferred micropattern could be deduced from neurites growing over the node point.

It should be noted that the amount of available pattern may be slightly underestimated by the method described above: Immunohistochemistry experiments allow the visualisation of the pattern as the thin protein layer in the patterned areas always binds a small amount of antibody and the DNA dye DAPI (which is used to stain the nuclei of the cells) unspecifically. Severely overexposing the pictures of stained substrates therefore allows to visualise the pattern. As shown in Figure 5.4, although part of the pattern can be seen in the phase contrast picture, a much larger amount becomes apparent under UV light (which excites the DNA dye DAPI). As for the evaluation in Figure 5.3 live cultures were used, only the phase contrast picture was available for evaluation. It was assumed though that the described effect was similar for all inking solutions and therefore did not distort the results. In any event, the major fraction of registered empty adhesion spots were identified through neurite overgrowth.
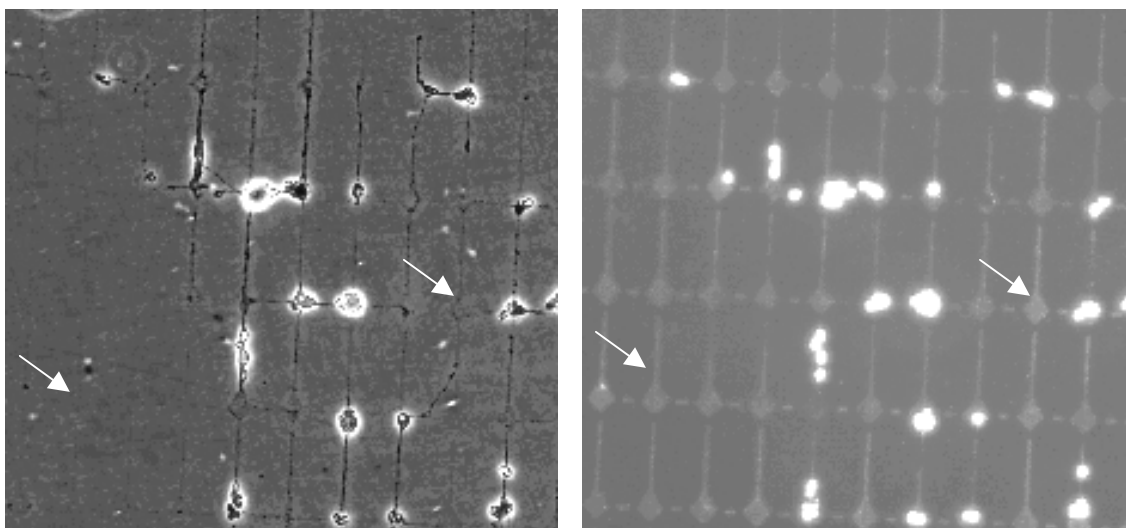
Figure 5.4: Although some of the protein pattern can be seen in phase contrast pictures, estimation of pattern transfer in phase contrast images probably underestimates the actual amount of transferred protein: Overexposed pictures from immunohisochemistry experiments reveal a much larger amount of pattern than the phase contrast image. (Due to a certain amount of unspecific binding of the DNA binding dye DAPI, the pattern becomes visible under UV-light which excites the dye). Left: phase contrast picture, the right arrow indicates a spot where pattern is visible, the left arrow an area where no pattern transfer can be seen. Right: The same area under UV-light (the white dots represent the nuclei of the stained cells, appearing extremely bright because of the overexposition). The arrows point to the same spots as in the left picture, note that pattern is clearly visible at both locations.

The comparison of the number of cells recruited to the pattern by different inking solutions in Figure 5.3 reveals another interesting fact: ECM-gel with respect to laminin (as well as PECM with respect to PL) attracts a larger number of cells per surface area. ECM-gel has been demonstrated in chapter 3 to transfer more efficiently (such that larger patterned areas are realised) to the surface during the patterning process, but Figure 5.3 shows that in addition, this inking solution has a higher potential for cellular adherence per transferred area. This could be due to particular adhesive molecules present in the mixture of matrix proteins present in the ECM-gel that are missing in the pure laminin solution. An alternative possibility would be that the quality of the protein pattern printed with ECM-gel differs, e.g. by forming denser layers on the surface that offer more adhesive units per patterned area.

This seems to be the case as indicated by scanning electron microscope (SEM) and atomic force microscope (AFM) pictures that are discussed in chapter 3. This may at least partially account for the difference in the recruiting potential of the two types of inking solution although a contribution of particular adhesion molecules present in the ECM mixture can not be excluded.

Another relevant information extracted from the AFM / SEM images is that no significant differences between the patterns formed with ECM-gel and PECM or laminin and PL become apparent. It therefore seems unlikely that the addition of polylysine has an immediate effect on the type of protein layer that forms. On the other hand, neither technique yields sufficiently detailed information on how individual molecules are presented and oriented on the surface. Therefore, a qualitative discrepancy in the respective protein layer responsible for the different adhesiveness cannot be ruled out. However, given the large amount of literature reporting the potency of positively charged polymers to attract cells to a surface, it appears more likely that the increase in adherence is due to the positive charge associated with the pattern when a polylysine-containing ink is used. The denser layers formed by ECM-gel / PECM samples may be responsible for the greater success of these substrates to attract cells to

the pattern in comparison to laminin. Remarkably, PL attracted a similar number of cells per surface area as ECM-gel. It appears that the less homogeneous transfer of the PL pattern with respect to ECM-gel was compensated by the positive charge associated with the pattern.

5.3 Summary and Conclusions

The different inking solutions used for microcontact printing were compared with respect to their ability to recruit cells to the pattern. Based on morphological observations on homogeneously coated substrates, it seems that the presence of polylysine on the surface result in a stronger cell-substrate interaction. This effect is most likely due to the positive charge associated with this polymer. In accordance with this observation, polylysine-containing micropatterns recruit more cells per adhesive area than micropatterns realised with the same ink without polylysine. Of the uncharged inks, ECM-gel recruits more cells than laminin. This can either be due to particular adhesive molecules in the protein mixture represented by ECM-gel or to the denser protein layer that this ink forms after patterning as discussed in chapter 3. PECM, the mixture of ECM-gel and polylysine shows by far the highest potential for recruiting cells to the micropattern. It appears possible that the improved performance of PECM samples over all other formulations stems from the fact that under the use of this ink, which allows the formation of dense protein layers on the surface, a large amount of positive charge can be immobilized on the pattern. The outstanding performance of PECM patterns in terms of transfer to the surface as well as in efficiency in recruiting cells to the pattern makes this ink the most attractive of the four tested, since efficiency of transfer and high recruiting potential are crucially important for any application. Particularly when extracellular recording of patterned cells is desired, a high gate occupancy is necessary and therefore, the ink with the highest potential to tether cells to the substrate should be used.

6. Electrophysiological Characterization of Neurons Growing on Patterned Substrates

The aim of the work presented here is the creation of simplified neuronal circuits as a model system. Previous chapters dealt with the geometrical confinement of neuronal networks growing on micropatterned surfaces, such that each neuron should be restricted in its connectivity. As important as a strict confinement of connectivity is the physiological integrity of the cells in such a network if it is to be a suitable model. In part 6.1 of this chapter, physiological parameters of single cells are compared between patterned cells and cells growing on controls. Part 6.3 will investigate aspects of synapse formation on the micropattern.

6.1 Characterisation of Single Cells

To analyse the impact of patterned growth on neuronal physiology, some physiological parameters of cells growing on a micropattern were compared with those of cells cultivated on homogeneously coated controls. All evaluations were done on cultures that were 7-19 days in vitro (DIV); the mean age of the two types of culture was similar in the two groups.

Table 6.1 summarises the results for the investigated parameters: Strikingly, the membrane capacity, which is a measure for the size of the cell (see chapter 2.1.), is smaller on average for patterned cells than for those grown on controls. This effect has been described before *(1)* and is most likely due to the limited adhesion area the patterned cells encounter, which restricts the expansion of the cell body.

	Pattern (av)	Pattern (sd)	Control (av)	Control (sd)
DIV [days]	12,26	1.65	12,29	1.91
Resting Potential [mV]	-76,1	11.05	-75,52	10.78
Membrane Capacity [pF]	24,64	11.54	31,44	15.56
Na $_{max}$ [nA]	-1,32	0.96	-1,87	1.12
K $_{max}$ [nA]	1,25	0.64	1,53	0.84
Na $_{max}$ / Surface area [pA/pF]	-56,06	43.93	-64,94	40.96
K $_{max}$ / Surface area [pA/pF]	57,88	35.05	56,73	39.34

Table 6.1: Comparison of several physiological parameters of neurons grown on patterned and control substrates respectively (av: Average, sd: Standard deviation). The listed resting potentials are the recorded values from which the liquid junction potential was subtracted, see chapter 2.1. Apart from a reduced membrane capacity of cells grown on patterned substrates, no striking differences are observed between the two groups.

Next, the resting potential of the two different groups of cells was regarded. The resting potential critically depends on a difference in ionic composition between the cytoplasm and the extracellular medium. This difference is created and maintained through the activity of membrane proteins that pump ions against their concentration gradient, a highly energy-dependent process. Therefore, the resting membrane potential can be used as an indicator for the physiological state of the cell. As shown in Table 6.1, the resting potential is extremely similar between patterned cells and controls.

Besides the resting potential, an important indicator of the physiological integrity of the cell is its ability to create and conduct electrical signals. This is achieved through the activity of voltage-gated Sodium and Potassium channels in the cell membrane. Therefore, an estimation of the amount of voltage-gated Sodium and Potassium channels expressed by the two groups of cells was done. To this end, voltage clamp experiments were performed, depolarising the neuron in a stepwise fashion with voltage pulses that had amplitudes between 10 and 100 mV (experiments started with the cell clamped at −75 mV, such that maximal depolarisation held the cell at +25 mV for the duration of the pulse; Voltage Clamp experiments are described in detail in chapter 2.1.). Traces of the resulting currents were recorded and the maximal Sodium (early inward component) as well as the maximal Potassium current (sustained outward

component) in the series were noted. Again shown in Table 6.1, maximal Sodium and Potassium currents are reduced for cells grown on patterned surfaces. One plausible explanation for this lies in the smaller average cell size, since a larger membrane surface should be able to accommodate a greater total number of ion channels. Therefore, Sodium and Potassium current per surface area were calculated by normalising the current with respect to the membrane capacity (as done e.g. by Joshi et al [Joshi, 2002]). Both maximal Sodium and Potassium currents per surface area are similar between patterned cells and controls.

In summary, it can be concluded that the only striking difference observed between patterned and unpatterned cells consists in a slight decrease of cell size on the pattern, which is probably due to the limited adhesion area. However, a reduced spreading of the cell body doesn't have to imply an impairment in cellular development, since similar restrictions to cell expansion may occur under physiological conditions. The extracellular matrix is a highly heterogeneous substrate that doesn't necessarily provide an infinite number of adhesion molecules for a given cell. In addition, competition for such molecules with other cell types may limit spreading as well as steric limitations in the three dimensional tissue architecture. No differences in the investigated parameters were observed between cells grown on patterns printed with different inking solutions (not shown). For this reason, cells from different patterned cultures were pooled for this evaluation.

Since neither the resting potential nor the average sodium or potassium current per surface area differ significantly between the two groups, it can be assumed that the cells grow and differentiate normally on the patterned substrates.

6.2 Synapse Investigation by Double Patch Clamp Measurements

In the double or triple mode, patch clamp measurements can serve to detect synaptic coupling between neurons. In such experiments, two or three cells are patched simultaneously. One of the cells is excited externally while the response of the other(s) is recorded without applying stimuli. Therefore, any response from the cells that are not stimulated must result from an interaction with other neurons through synaptic connections. Primarily two types of synapses can be distinguished in these measurements:

The first type is the electrical synapse, also called gap junction, that consists of a pore spanning the adjacent membranes of the coupled cells. With an inner diameter of about 2 nm, these pores are large enough for small ions to pass and therefore allow the direct flow of current between the two cells. Consequently, on the electrophysiological level, the following features are characteristic for gap junctions:

- their bidirectional connectivity, normally distinguishing neither cell as pre or postsynapse (although asymmetrical pore proteins have also been described as discussed in chapter 1)

- a very small (not resolvable by the methods presented here) delay in signal transmittance from cell to cell

- a transmitted signal that is proportional to the height and length of the voltage signal induced in the stimulated cell and not dependent on a presynaptic action potential.

In contrast to the electrical synapse, pre- and postsynaptic cell in the chemical synapse are not directly connected but divided by the synaptic cleft which is about 30 nm in width. This distance is too big for electrical current to pass directly, therefore signal transmission occurs indirectly through the release of neurotransmitter by the presynapse. Neurotransmitter is released only when an action potential arrives at the presynaptic terminal. The neurotransmitter diffuses through the synaptic cleft and binds to specific receptors in the

postsynaptic membrane, thus activating them. Receptor activation causes an opening or closing of ion channels which allow an ion flux that either depolarises or hyperpolarizes the postsynaptic cell. These sequential steps cause a delay in signal transmittance of several milliseconds.

Chemical synapses are identified in patch-clamp experiments through the following characteristics:

- signal transmission occurs asymmetrically from pre- to postsynapse only

- the signal arrives at the postsynapse with a characteristic time delay of several ms

- the transmittance of a signal crucially depends on a presynaptic action potential; subthreshold depolarisations are not transmitted at all.

Both electrical and chemical synapses were found in the presented system. Since chemical synapses were more abundant and since they were also the type more relevant to this work, the following sections will predominantly focus on chemical synapses.

6.2.1 Rate of Synapse Formation on Patterned Substrates

The first issue investigated was the rate at which cells on the patterned substrates formed synapses. It seemed possible that the high confinement of neuronal outgrowth had an impact on the likelihood that two cells coming into physical contact form a synapse. In order to better analyse physical contact formation, microinjection studies were performed to visualise the connective pathways. This method is explained in detail in chapter 2.9; briefly, the cells in a patch clamp measurement are injected with a non toxic dye labelling their cell bodies and neurites. The concomitant use of different dyes allows the distinction of neurites originating from different cells and the visualisation of the areas of physical contact. Figure 6.1 A and B show an example of two cells that appeared to be in contact in the phase contrast picture but were determined by the microinjection image to actually grow past each other while the

seemingly connecting neurite came from another cell. Although lack of physical contact is an obvious reason for not forming a synapse, some other examples have shown cells that don't connect either in spite of an intimate physical linkage. This is illustrated in Figure 6.1 C and D: Three cells in close contact with each other are shown, touching in multiple locations while only two of them form a synapse (white arrow) and no communication is observed with the third cell. Clearly, physical contact is necessary but not sufficient for synapse formation.
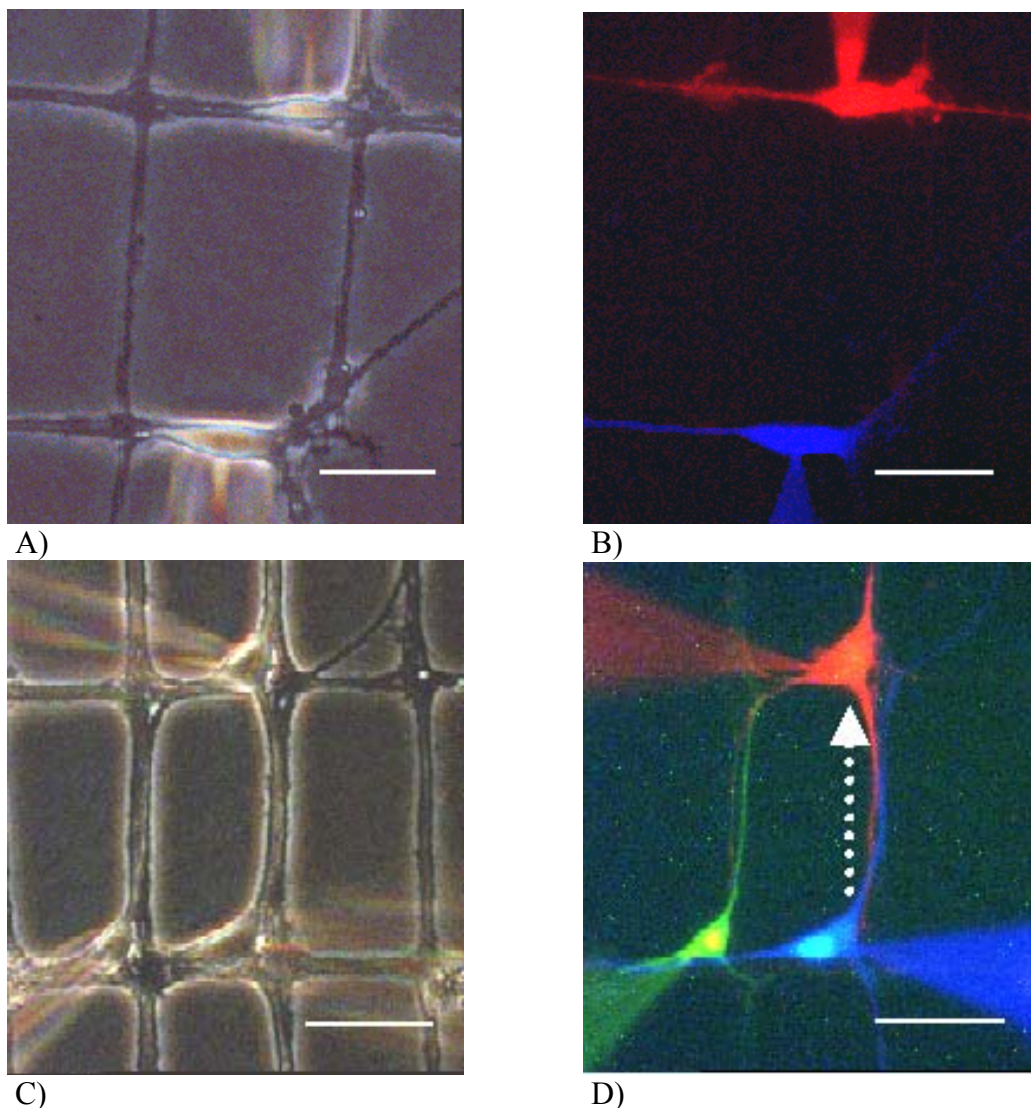
Figure 6.1: Visualisation of cellular connectivity by microinjection studies. Microinjection of polar fluorescent dyes allows the tracing of neurites emerging from a patched cell. Superimposition of pictures under illuminations exciting the different dyes allows to visualise physical connectivity. A, B: Example of two seemingly connected cells shown by the microinjection image to grow past each other. Scale bars 25μm. C, D: Physical contact is necessary but not sufficient for synapse formation: All three cells are in close physical contact while only two are forming a synapse (white arrow). Scale bars 50μm.

As cells grown on patterned surfaces have a significantly reduced number of potential interaction partners, it appeared possible that they would be more prone to form a synapse upon encountering another neuron. To test this idea, the percentage of physically contacting cells that were synaptically coupled was determined. The result was surprisingly similar in the two groups, namely 49% each (82 coupled pairs out of 168 on patterned substrates and 27 out of 55 on controls). Although this was unexpected after the considerations mentioned above, it seems reasonable regarding the *in vivo* situation: Synapse formation in the brain doesn't occur randomly between any two cells happening to come into contact. Instead, connectivity is highly organized between different tissues of the CNS, e.g. between the different layers of the mammalian cortex, such that signal transmission is routed by the functional architecture of the network [Nicholls, 2001; Kandel, 2000]. During the development of such structures, axons are guided by matrix components and diffusible factors to their appropriate target. There are many indications for a highly specific recognition between axon and target cell as well as for repulsion to prevent contact between "non matching" cells [Yoshikawa, 2003; Kandel, 2000]. Specificity of cellular interaction between cells from different brain areas has been shown to be conserved even if the original tissue structure is disrupted, indicating highly defined recognition mechanisms distinguishing cells by their origin rather than by their actual physical location. Proposed recognition mechanisms are the differential expression of receptors and their ligands [Yoshikawa, 2003; Mellitzer, 1999] or area-specific splice variants of particular adhesion molecules [Chamak, 1989]. In the applied cell culture protocol, cells from different cortical areas were dissociated and plated onto the substrates as a mixture. Assuming that the contacting but non synapse forming cells were prevented from connecting by their respective origin in the intact tissue (or other cell-specific determinants), it seems that the recognition process between the different cell types was unimpaired by the growth on patterned substrates. Additional evidence for specific cell-cell recognition events in the

patterned networks will be presented in chapter 8. There results can be taken as a further indication of an undisturbed, physiological behaviour of the cells on the pattern.

An additional topic that was looked into was the formation of reciprocal synapses. 18.5% of all synaptically coupled pairs on control substrates were coupled reciprocally and 14.6% on patterned substrates. The similarity of these numbers infers that the lines used in the grid pattern were wide enough to allow the coexistent outgrowth of two neurites (this is also seen in Figure 6.1 D). The applied line width had been optimised in the preceding project [Lauer, 2001], applying a cell culture protocol using brain slices. In that project, the geometry had to be adjusted to allow the migration of cells out of the slice onto the pattern. Consequently, one requirement was a line thickness sufficient for the temporary accommodation of a migrating cell body. Since this is not necessary in a dissociated cell culture, a new geometry with thinner lines could be designed, attempting to limit the adhesive area on the line sufficiently to restrict neurite outgrowth to just one per lane. It would be interesting to test whether the formation of reciprocal contacts could be reduced on such structures.

Figure 6.2 shows synapsin expression in patterned neuronal networks by antibody staining. Expression of the protein is demonstrated and the formation of connectivity at an early time point after adherence (DIV 5) can be visualised.

A)   B)
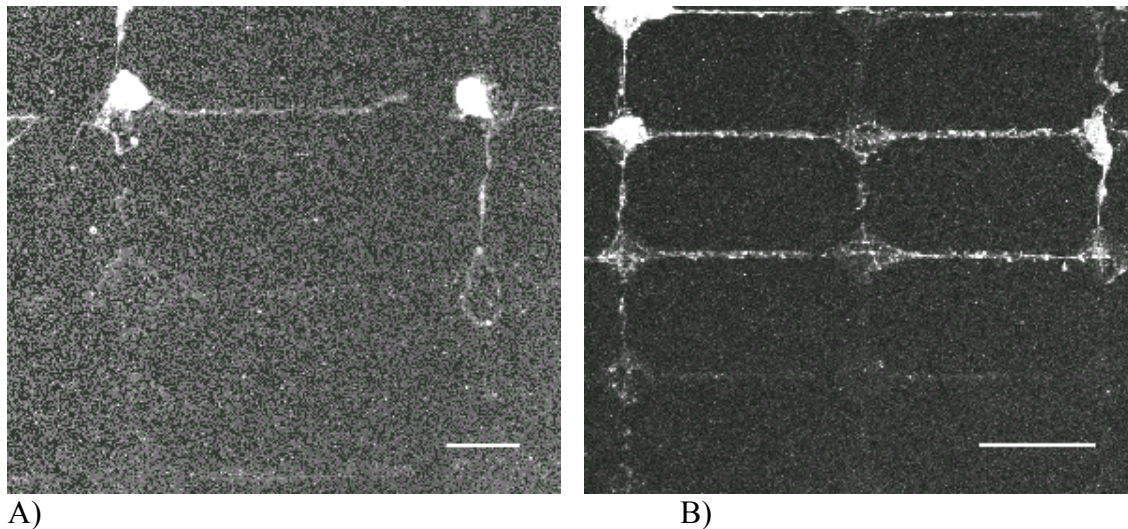
Figure 6.2: Network- and synapse formation on micropatterned substrates illustrated by immunohistochemistry pictures using an antibody against the synapse specific protein synapsin I. Two images of a cortical neuronal culture on grid pattern G, DIV 5 are shown. Note how the left neuron in A) is just about to innervate the right neuron. Both images show characteristic puncta along the neurites indicating the transport of synaptic vesicles to developing presynaptic terminals. Scale bars 20µm (A) and 50µm (B). Pictures are taken with a laser scanning microscope.

6.2.2 Evaluation of Synaptic Efficacy

Part 6.1 of this chapter compared the general physiological state of cells growing on micropatterned substrates with cells on controls. The second issue, addressed in part 6.2.1, was whether the rate of synapse formation was altered by patterned growth. This part will now explore whether the synapses that actually formed on the micropattern exhibit any difference in functionality from synapses on control substrates.

Within an externally applied stimulus train, some stimuli evoking an action potential in the presynapse fail to induce a postsynaptic response. This phenomenon is called synaptic failure and has been described many times in the literature [Selkoe, 2002; Taschenberger, 2000; Pouzat, 1998; Redman, 1990]. The rate at which it occurs can be used to determine the efficacy of a synapse, which may change upon maturation, modulation by certain stimuli or vary depending on the physiological state of the cells [Maccaferri, 1998]. Pfrieger et al. and Vlkolinsky et al. for example used the rate of synaptic failure to compare the reliability of synaptic transmission under different physiological conditions [Pfrieger, 1997; Vlkolinsky,

1999]. In this context, it appeared reasonable to determine the rate of synaptic failure on patterned and on unpatterned substrates as a measure for synaptic quality. As an additional parameter, the average height of the postsynaptic potential (as an indicator for the strength of the transduced signal) was assessed. Figure 6.3 shows that both the rate of synaptic failure and the average EPSP height are similar on patterned and on unpatterned substrates, indicating that the growth on a micropatterned substrate had no negative impact on the synapses that formed.
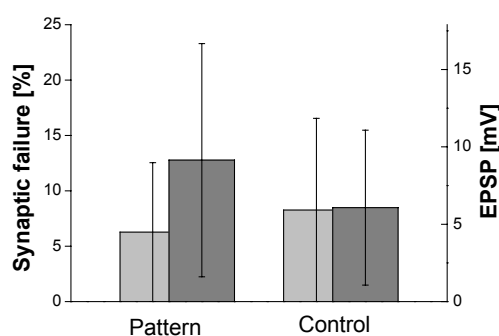
Figure 6.3: Synaptic efficacy on patterned and on control substrates. Both the rate of synaptic failure (light grey bars) and the average EPSP height (dark grey bars) are similar in the two groups.

6.2.2.1 Synaptic Efficacy on Different Surface Modifications

Chapters 3 and 5 started to compare the suitability of different inks used for microcontact printing. While chapter 3 investigated the transfer to the substrate during the patterning process, chapter 5 compared the efficiency with which different surface modifications were able to recruit cells to the pattern. It was shown that the addition of polylysine to the inking solution increased the ability of the micropattern to tether cells to the substrate. It seemed interesting to explore whether the type of solution used for microcontact printing had an impact not only on the adhesion of the cells but also on the synapses they form. Figure 6.4 depicts synaptic failure and average EPSP height of cells grown on micropatterns printed with the four inks under investigation. Synaptic failure on PECM substrates is by far lower than on the other three surface modifications which show similar values, while the average EPSP height is in the same range for all groups.
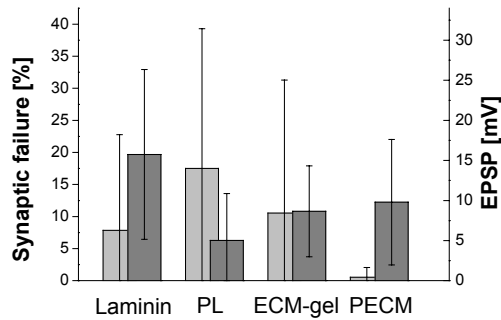
Figure 6.4: Synaptic failure (light grey bars) and average EPSP height (dark grey bars) on patterned substrates printed under the use of different inking solutions. The rate of synaptic failure is by far lowest on PECM patterns.

The similarity of the results obtained with laminin, PL and ECM-gel is somewhat surprising. It would have seemed plausible that ECM-gel, as a complex substrate rather than one single protein, would improve the formation and maturation of synapses. Such an effect could e.g. be mediated through signalling pathways triggered by the engagement of specific cell-matrix receptors, particularly since several types of adhesion molecules have been implicated in the formation and maturation of synapses [Ranscht, 2000; Chavis, 2001; Brusés, 2000] . However, no such effect was observed. Amazing was also that the rate of synaptic failure was so notably reduced on PECM substrates. As polylysine didn't cause an increase in synaptic efficacy when mixed with laminin, it seems unlikely that it is directly responsible for the increase seen in PECM over ECM-gel. Possibly the greater number of adhering cells which causes a greater local density of neurons and maybe also glia cells may be responsible for the effect, since the presence of glia cells in the culture is known to reduce synaptic failure [Pfrieger, 1997]. Alternatively, polylysine could have an indirect effect on proteins present in the ECM micropattern that is beneficial to cellular development, e.g. on protein conformation or orientation on the surface. Another potential reason could lie in the fact that the extracellular matrix is known to bind neurotrophic molecules such as fibroblast growth factor (FGF) [Cestelli, 1992]. It seems possible that the positive charge associated with polylysine improves the attraction of such factors from the medium or again their presentation on the surface, improving cellular development and synapse maturation.

6.2.3 Synapse Types

Chemical synapses can roughly be divided into two major groups: Excitatory ones, that depolarise the postsynaptic cell, bringing it closer to the firing threshold and inhibitory ones that hyperpolarize the cell and thus reduce the likelihood of it firing an action potential.

The distinction between excitatory and inhibitory synapses in patch clamp measurements is not as obvious as it may seem at first due to an artefact arising with the method: As explained in chapter 2.1., the intracellular concentration of Chloride is unphysiologically high during a patch clamp measurement, such that the reversal potential for Chloride is shifted to a value higher than the resting potential of the cell. Therefore, the opening of Chloride channels causes a depolarisation rather than a hyperpolarisation in the postsynaptic cell, similarly as it occurs in an excitatory synapse. However, there are several methods to distinguish excitatory and inhibitory synapses in spite of this artefact, which again are described in more detail in Chapter 2.1.

One simple, non invasive way lies in the analysis of the shape of the postsynaptic current. The shape of this current reflects the gating kinetics of the postsynaptic receptors and is characteristic for each synapse type. A distinguishing feature of the current shape is the decay constant τ (describing the time from maximal postsynaptic current to half of the resting value). A slightly more tedious but similarly non invasive method is the determination of the reversal potential, which gives an indication about the ion species involved in the postsynaptic response and thus allows inference on the synapse type. The most straightforward method is the use of chemical inhibitors specific for a particular receptor type. This method has the disadvantages of being time-intensive and interfering strongly with the cell's physiology, it therefore was not used routinely.

6.2.3.1 Establishment of the Methods for Synapse Characterisation

The analysis of the synapse type by determination of the reversal potential and the decay constant τ of the postsynaptic current was to be established in this work. The literature reports the reversal potential for excitatory synapses to lie around 0 mV and that for inhibitory synapses around -45 mV. Described values for the decay constant τ vary from 0.4 to 7.1 ms for excitatory and from 14 to 45 ms for inhibitory synapses [Muller, 1997; Taschenberger, 2000; Joshi, 2002; Liu, 2000; Varela, 1999; Wyart, 2002].

The distribution of the reversal potentials observed experimentally is depicted in Figure 6.5 A. Very clearly, two populations of data points can be distinguished, one showing a reversal potential around -45 mV , the other around 0 mV, which fits well with the values expected for inhibitory and excitatory synapses respectively. The values encountered for the decay constant τ are depicted in Figure 6.5 B. Again, two populations can be distinguished, although not as distinctly. One group clusters around 5-6 ms (which is about the value described for excitatory synapses) while the other shows decay constants of 14 ms and more; these values are rather scattered and reach up to 46 ms (which is about the range described for inhibitory synapses). Thus, Figure 6.5 A and B each show two groups of values that fit with those described in the literature as typical for excitatory and inhibitory synapses respectively.

In order to test whether the conclusions that can be drawn from the two sets of data correlate, a two dimensional plot was created displaying those synapses for which both types of information were available (Figure 6.5 C). The data points clearly fall into two groups: One has a reversal potential clustering around 0 mV (average 1.8 mV ± 6.5), values for τ ranging from 2.0 ms to 5.9 ms (average 3.8 ms ± 1.5). The other group was found to reverse around -45 mV (average -43.2 mV ± 4.8) and to have decay constants of 16 to 45 ms (average 23.5 mV ± 7.7) except for one data point found at 9.5 ms. Thus, with the exception of the

mentioned data point, the values for the reversal potential and for τ correlate well in assigning

each data point unambiguously to the same type of synapse.

A)

B)

C)
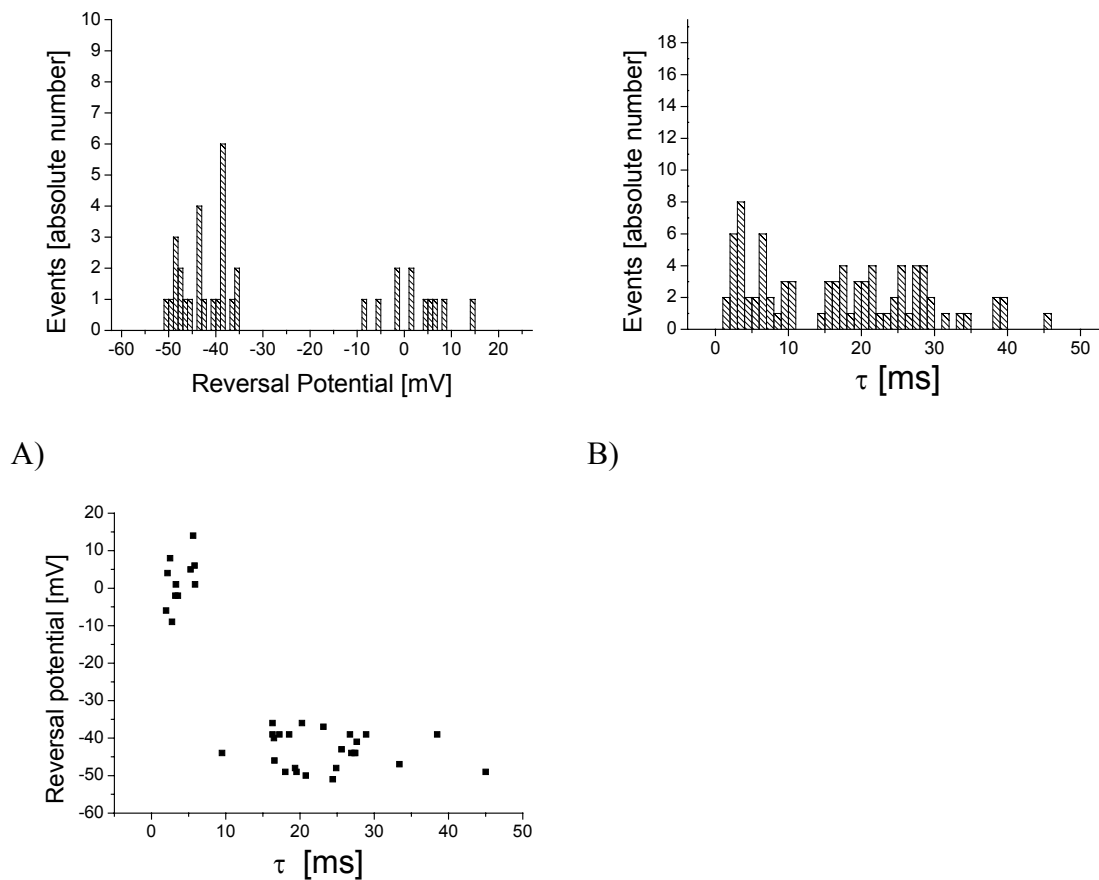
**Figure 6.5:** Distribution of the values observed for the reversal potential (A) and for the decay constant τ (B). Synapses measured on patterned and control substrates were pooled. A) shows two distinct groups of reversal potentials clustering around the values expected for excitatory and inhibitory synapses respectively. The decay constants displayed in B) also fall into two groups although these are not as well defined. Those synapses for which both values are available are depicted in a two dimensional plot (C). The two parameters correlate well in assigning each synapse to either of two groups: One is defined by reversal potentials of -51 to -35 mV and decay constants of 16 to 45 ms. The other group has reversal potentials of -9 to 14 mV and decay constants between 2 and 6 ms.

The reversal potential was not available for all measured synapses mostly because it was

difficult to determine for weaker synapses due to the inferior signal to noise ratio. Because of

the good correlation between the reversal potential and the decay constant, it seemed justified

in these instances to deduce the synapse type from τ only. Taking into account the values

displayed in Figure 6.5 and in accordance with the literature, synapses with a decay constant

of 7 ms and below were regarded excitatory, those displaying values above 14 ms inhibitory.

Synapses with values between 7 and 14 ms were excluded from the evaluation to avoid ambiguities.

Since chemical inhibition is the best established method for the characterization of synapse types, it was performed exemplarily a number of times to test whether the results coincided with the findings obtained by the two methods described above.

Figure 6.6 depicts the time course of chemical inhibition in two examples. Each example shows two synchronously patched synapses responding to bicuculline which is an antagonist to GABA-ergic synapses. In Figure 6.6 A, two synapses that were both determined to be inhibitory by the reversal potential (-39 mV and -48 mV respectively) and by the shape of the postsynaptic current (τ 18.5 ms and 19.5 ms) are blocked by bicuculline in a similar fashion and a similar time course. Contrary, Figure 6.6 B shows an example of two synapses one of which was determined to be inhibitory (reversal potential -46 mV, τ 16.6 ms) while the other one was determined to be excitatory (reversal potential –2 mV, τ 5.9 ms). In this example, blocking of the inhibitory synapse can be observed while the excitatory one is unimpaired, demonstrating the specificity of the used chemicals and the coincident result for the three independent methods for the determination of the synapse type. Synapses identified as excitatory could be blocked with CNQX, an antagonist for non-NMDA glutamatergic synapses (not shown). Consistently with the expectation, one neuron forming two synapses always formed either two inhibitory or two excitatory ones.
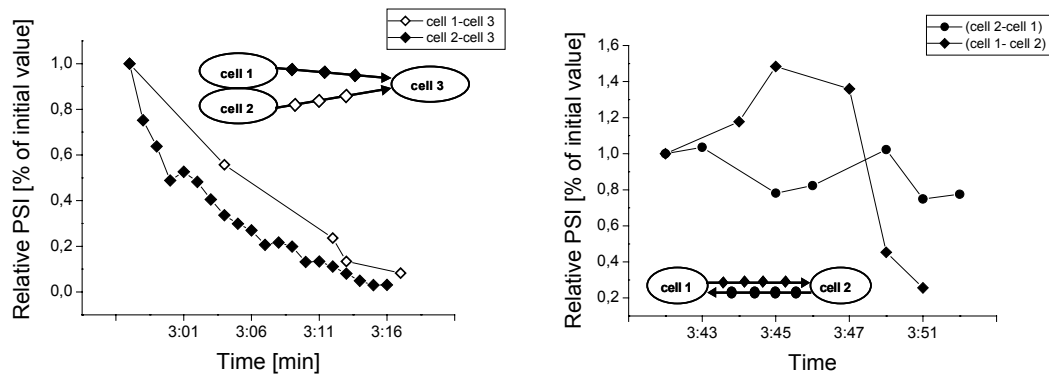
Figure 6.6: Chemical inhibition of GABA-ergic synapses with bicuculline. A) Two synchronously patched inhibitory synapses are blocked at a similar time course by the addition of bicuculline. B) An inhibitory synapse (◆) is blocked by bicuculline while a concomitantly patched excitatory synapse (●) is unaffected.

6.2.3.2 Excitatory and Inhibitory Synapses on Patterned and Control Substrates

The encountered amounts of synapses of the respective types are summarised in Table 6.2. In both patterned and unpatterned cultures, inhibitory synapses are seen more frequently than excitatory ones. This can either be due to a larger number of inhibitory neurons in the system, to these neurons forming synapses more frequently or both.

	Total number of characterised synapses	Excitatory Synapses	fraction of total	Inhibitory Synapses	fraction of total
Patterned Substrates	69	**21**	30%	**48**	70%
Controls	13	**5**	38%	**8**	62%
Total	82	**26**	32%	**56**	68%

Table 6.2: Occurrence of excitatory and inhibitory synapses on patterned and on control substrates. In both groups, inhibitory synapses are more abundant than excitatory ones.

A prevalence of inhibitory over excitatory synapses in a dissociated neuronal culture was also reported by Ma et al. and Liu et al. [Liu, 2000; Ma, 1998]; both groups used hippocampal neurons. Wyart et al. report about 25% of cultured hippocampal neurons (both on patterned and homogeneous substrates) to stain positive for GABA, assuming the rest of the population

126

to be glutamatergic. Although this group says to have discriminated between excitatory and inhibitory synapses, they do not give the relative amounts of the encountered synapse types, so no direct comparison can be made to the presented data set. However, the much larger number of excitatory neurons seems to contradict the results presented here.

A very interesting work in this context is a study published by Müller et al. [Muller, 1997]: This group cultured hypothalamic neurons (on unpatterned substrates) and examined the types of synapses that formed as well as aspects of the randomly forming networks. Similarly to Wyart et al., they found a larger number of neurons in the culture system to be excitatory in accordance with previous results of the same group [Wahle, 1993] (only one third of the neurons were shown to be inhibitory by antibody staining). Interestingly though, the majority of the encountered synapses was inhibitory, suggesting that inhibitory neurons on average form more synapses than excitatory ones. If such a behaviour was seen not only in the specific brain area investigated by the group but was a principle underlying neuronal network formation in general, these results could explain the apparent contradiction between the results in this work and the ones reported by Wyart et al.. Müller et al. indeed suggest that the larger number of inhibitory synapses is a general feature of neuronal networks, as a predominance of inhibitory connections is necessary to prevent uncontrolled spreading of excitatory events throughout the networks (this notion is also supported by other groups [Varela, 1999]). Uncontrolled activity bursts, which also occur in disorders like epilepsy, are observed when the inhibitory synapses in a network are blocked by a chemical antagonist [Keefer, 2001; Plenz, 1996; Golshani, 1999] further pointing out their importance in constraining rythmic network activity. The necessity of inhibitory connections to dominate in a system as well as the vital role of inhibition in shaping network activity has also been recognised by theoretical studies [Bush, 1996; van Vreeswijk, 1994; Kopell, 1994]. The presented results thus appear to fit well with the findings in the literature. The discussion on

connectivity of excitatory and inhibitory neurons and the implications on network activity will be continued in chapter 8, where further aspects of network formation are investigated.

As the ratio of excitatory to inhibitory neurons does not differ much between patterned and unpatterned substrates in the presented study, it does not appear as if the growth on a patterned substrate as such enriches one type of neuronal connection over the other.
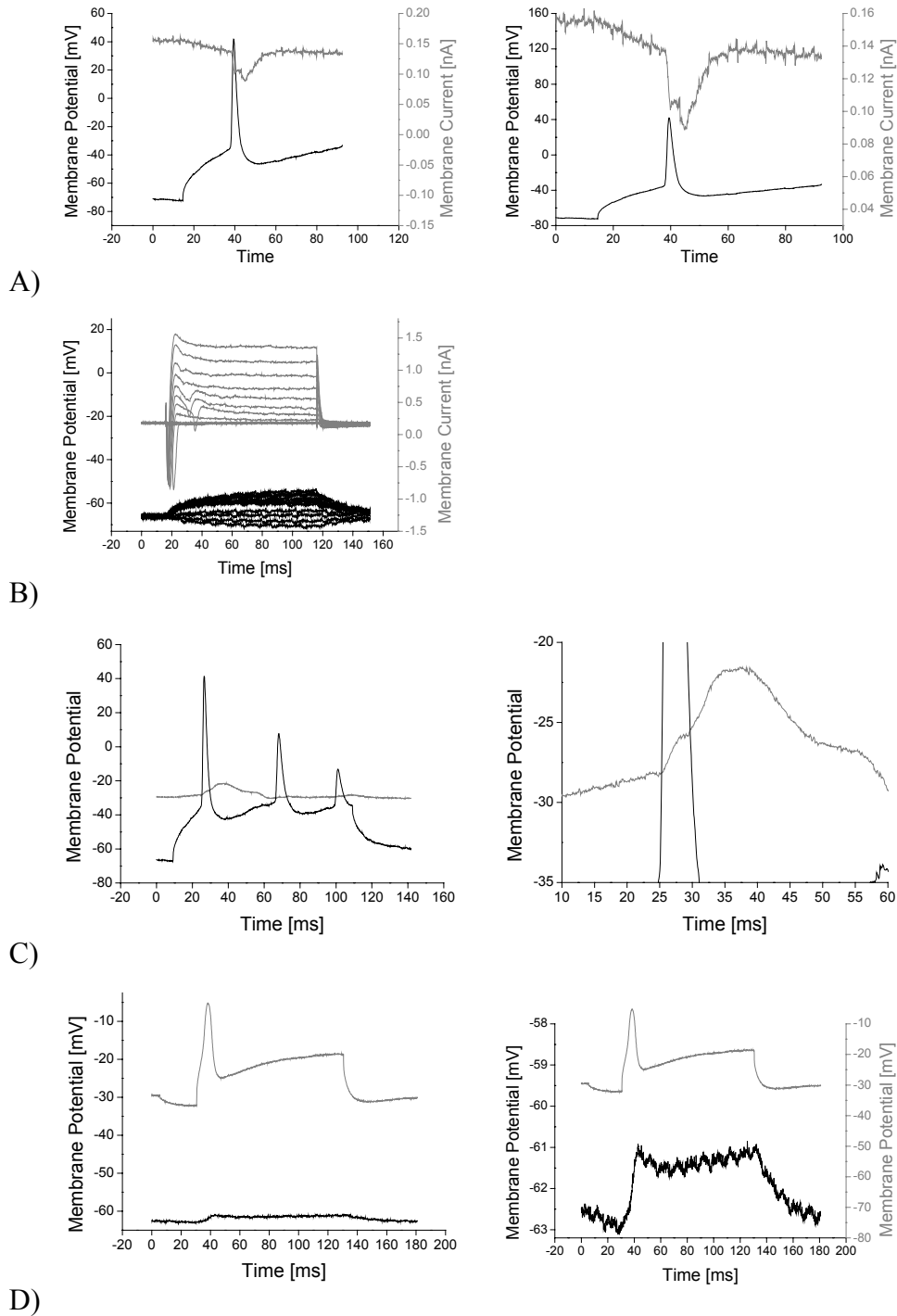
6.2.4 Gap Junctions

Contrary to the results obtained with micropatterned neuronal networks before [Lauer, 2001], gap junctions were only found rarely in the presented project. A total of 3 gap junctions was found on patterned substrates as opposed to a total of 93 chemical synapses. Gap junctions were found to coexist with chemical synapses, such that the two postsynaptic signals overlaid. The coexistence of gap junctions and chemical synapses has been described since the early 1960s [Rovainen, 1967] and has recently been shown to be important in the coordination of cortical activity [Galarreta, 1999]. Figure 6.7. shows an example of a chemical and an electrical synapse coexisting: Almost coincident with the action potential in the presynaptic cell, a response in the postsynapse can be observed. This response is detected as an inward current if the postsynapse is held in the VC mode (Figure 6.7.A) or as a depolarisation if the cell is recorded in the CC mode (Figure 6.7C). With a delay of some ms however, a characteristic second peak occurs. This second peak - in contrast to the first one - is transmitted unidirectionally, meaning that a stimulation of the postsynapse causes no corresponding delayed signal in the presynaptic cell. This unidirectional transmittance matches the expectations for a chemical synapse. In contrast, the non delayed part of the signal is transmitted bidirectionally (as seen in Figure 6.7 B and D), which is typical for a gap junction. Of particular interest is Figure 6.7 D: When both cells are held in the CC mode and the postsynapse fires an action potential, the shape of this event is reflected accurately in the

voltage signal of the presynaptic cell: The spike of the AP is seen as well as the plateau of the applied stimulus, illustrating that signal transmission through the gap junction is strictly proportional and not dependent on an action potential.

It would also be expected that only the part of the signal attributed to a chemical synapse can be blocked by the addition of chemical inhibitors. This can be seen in Figure 6.8: Again, an overlay of a chemical synapse and a gap junction is shown, with the characteristic two peaked signal in the postsynapse. The chemical synapse was determined to be excitatory and could therefore be blocked by the addition of CNQX. The signals recorded after the block are shown in Figure 6.8 C and D: In the direction from pre- to postsynapse (Figure 6.8 C), only the first, non delayed peak remains, while the late component is completely suppressed. Contrary, signals travelling from post- to presynapse (Figure 6.8 D) are unimpaired. Taken together, these results confirm the assignment of the two components of the signal to two independent but concomitantly present synapse types.

Figure 6.7: Overlay of a chemical synapse with a gap junction. A,B: The presynaptic cell (black trace) is kept in the current clamp mode, the postsynapse (grey trace) in the voltage clamp mode. A) depicts the postsynaptic current induced by a presynaptic action potential. Note how both the subthreshold depolarisation and the action potential are transmitted to the postsynapse without time delay through the gap junction. The additional peak occurring after the action potential with a short delay can be attributed to the chemical synapse. B) shows a voltage clamp measurement on the postsynaptic cell in which membrane currents are induced through a stepwise depolarisation. The evoked currents lead to a voltage signal in the presynaptic cell transmitted through the gap junction. C,D: Both cells are held in the current clamp mode. C) The postsynaptic potential consists of two distinct signals similarly as the postsynaptic current in A). D) A postsynaptic action potential is transmitted to the presynapse through the gap junction. The transmitted signal is not dependent on an action potential, such that both the peak and the plateau are transmitted.

130
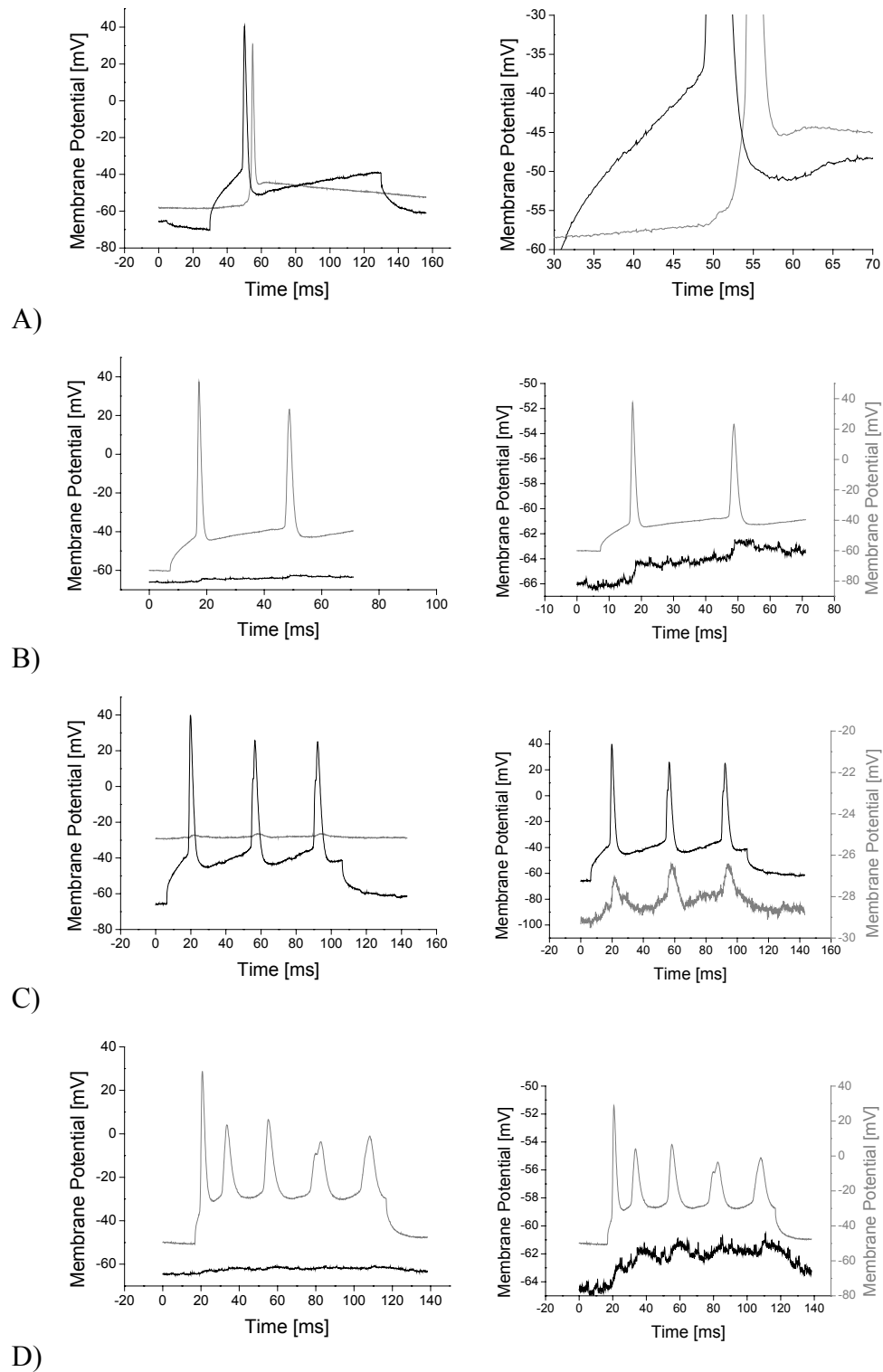
Figure 6.8: Block of the (excitatory) chemical synapse with CNQX while the coexisting gap junction is not affected. A,B: Before chemical inhibition. A) Action potentials in the presynapse are transferred as biphasic signals to the postsynapse as in Figure 6.7. B) Non delayed signals are transmitted from post- to presynapse through the gap junction. C,D: After inhibition. C) Only the non delayed part of the signal transmitted from pre- to postsynapse remains. D) Signalling from post to presynapse through the gap junction is unaffected.

6.3 Summary and Conclusions

Cells grown on micropatterned substrates were characterised electrophysiologically and compared to cells grown on controls. Patterned cells appeared to develop normally with respect to their resting potential and voltage-inducible Sodium and Potassium currents per surface area. The only striking difference that could be observed consisted in a reduced cell size. This is probably due to the limited adhesion area the cells experience on the node points of the grid pattern and not a sign of physiological problems as indicated by the normal resting potential.

The synapses encountered on patterned substrates showed average EPSP heights and rates of synaptic failure similar to synapses on controls. Interestingly, the rate of synaptic failure varied between cells grown on micropatterns realised with different inking solutions in that the rate of synaptic failure was strongly decreased on PECM patterns. PECM was also the inking solution that attracted most cells per surface area to the surface as described in chapter 5. One possible explanation for the improved performance of networks grown on this type of pattern therefore may be the larger local cell density. Alternatively, a stronger interaction with the substrate – which has been proposed for polylysine containing patterns – may have triggered intracellular signals that were beneficial for synaptic maturation. It also seems possible that trophic factors from the medium bound to the pattern through electrostatic interactions and were therefore available in larger quantities than on other surfaces.

On both patterned and unpatterned cultures, a larger number of inhibitory than excitatory synapses was measured; a prevalence of inhibitory connections in neuronal networks has also been described many times in the literature and is thought to be crucial in preventing the uncontrolled spreading of activity.

In addition to chemical synapses, gap junctions could be found on patterned substrates and on controls, sometimes both types of synapses overlaid. The presence of gap junctions as well as their overlaying with chemical synapses plays an important role in network behaviour and synchronisation [Galarreta, 1999].

7. Polarity Inducing Structures

The presented work aims at the creation of simplified neuronal circuits of defined geometry. As described in previous chapters, this was accomplished by growing neurons on grid-micropatterns, restricting the amount of potential interaction partners to the neighbours on the pattern. However, this approach does not define the orientation of synapse formation and thus the pathway along which in- and output occur, still leaving a certain amount of randomness in the forming networks. Control over the polarity of the patterned neurons (by defining the pathway along which axonal as opposed to dendritic outgrowth occurs) would add control over signal transduction in the network: As neuronal signalling is strictly asymmetrical, input being received via the dendrites and output being passed on down the axon, orientation of axo-dendritic polarisation in a network would also orient the pathway along which signal transduction takes place.

The issue of controlling neuronal polarity on a synthetic substrate has been addressed by Stenger et al. [Stenger, 1998]: This group grew embryonic rat hippocampal neurons on substrates containing a micropattern of cell attracting amine-groups (trimethoxysilyl-propyldiethylenetriamine (DETA)) against a background of cell repellent fluorinated silane (tridecafluoro-1,1,2,2-tetrahydroctyl-1-dimethylchlorosilane (13F)). Similarly to the presented work, grid patterns were used, allowing attachment of the soma to one adhesion spot and neurite outgrowth into four directions along the grid lines. Contrary to the work presented here however, Stenger et al. did not offer equally attractive paths in all four directions. Instead, a "permissive" pathway consisting of a solid DETA line was presented in one direction while in the other three DETA lines interspersed with "speed bumps", consistent of non permissive 13F dots, were offered.

It has been proposed before that the decision of a neuron which of its processes to differentiate into an axon and which into dendrites depends - at least *in vitro* - critically on the length of these processes at an early time after attachment [Dotti, 1987]. It has further been proposed that just after adhesion to the substrate, the cell extends undifferentiated neurites into all directions and that the first neurite to exceed a critical length becomes the axon while the others by default differentiate into dendrites. Stenger et al. reasoned that an attachment promoting pathway such as a solid DETA-line would allow growth cone elongation at a faster rate than a line that is interrupted by non-permissive F13 spots. Consequently, axonal outgrowth was expected to occur predominantly along the solid DETA line while dendrites should extend in the direction of interrupted lines.

The group describes a high preference of the patterned neurons to extend a single process along the uninterrupted DETA-line. This process expressed axonal marker proteins as shown by antibody staining, while shorter processes containing dendritic markers were extended along the three alternative pathways.

If the observed effect was solely due to the differential adhesiveness of the four pathways, it would be expected to be reproducible in the system presented here, namely with substrates patterned by microcontact printing. Although a very different surface chemistry is applied, the principle, a pattern of permissive molecules on a cell repellent background, is similar to the work performed by Stenger et al..

7.1 Design of Interrupted Micropatterns

In order to create grid structures containing pathways of different adhesiveness, new micropatterns were designed: The established grid geometries were applied but with one solid and three interrupted lines starting from each node, interruptions ranging from 1 to 5 µm in size; the line width was 2-4 µm (shown schematically in Figure 7.1 ; a detailed description of

the different applied structures can be found in the appendix). These parameters are similar to the ones applied by Stenger et al., who used 5-10 μm interruptions and a pathwidth of 5 μm. As polystyrene has in previous chapters been shown to repel cell adhesion strongly, printed lines with interruptions of bare polystyrene would be expected to slow down neurite outgrowth similarly as the 13F spots in the mentioned work while the printed PECM pattern should provide a cell attracting path. If a more adhesive surface indeed induced neurites to elongate at a faster rate and if facilitated outgrowth was the mechanism responsible for axonal differentiation along the solid DETA line in the quoted work, a similar orientation of cellular polarity would be expected on the described substrates.

Since the presented system not only allowed the attachment of single cells but supported cellular survival for weeks and also the formation of functional circuits, it appeared attractive to analyse neuronal polarity on the functional level - by measuring the orientation of the synapses that ultimately formed - rather than by antibody staining.

The transfer of the cell culture protocol to patterns with interrupted lines proved not to be a problem, and networks could be cultured on the new patterns as well as on continuous structures. However, electrophysiological analysis of the encountered synapses shows no preferential orientation along the anticipated axis. As shown in Table 7.1, only 35% of all encountered synapses were oriented the expected way indicating that the axon had actually grown along the "permissive" path. This is hardly more than the 25% that would have been expected if the direction of axonal outgrowth was at random. Patterns with different gap sizes have been used, 5 μm interruptions as applied by Stenger as well as 2 μm and 1 μm gaps. Correctly oriented synapses were found more frequently on patterns with smaller interruptions, making it seem unlikely that a further increase in gap size would result in a higher yield of correctly oriented cells.

size of gap	correctly oriented synapses [number]	incorrectly oriented synapses [number]	correctly oriented synapses [% of total]
1 μm	10	16	38.5
2 μm	3	5	37.5
5 μm	4	11	26.6
sum	17	32	35

Table 7.1: Orientation of synapses on polarity inducing micropatterns according to Stenger et al.. Grid patterns with interruptions of different sizes were printed onto polystyrene culture dishes as described in chapter 2.3. (all samples included in this evaluation were done with PECM as the inking solution); synapses were identified by patch clamp measurements. The exact geometries of the different patterns that were applied can be found in the appendix. Interruptions of 1 μm were present in pattern D, interruptions of 2 μm in patterns E and F and interruptions of 5 μm in patterns G-I. In this table, the results for patterns with the same interruption size are pooled. Counted as "correctly oriented" were those synapses in which the presynaptic cell had extended its axon along the solid line rather than along one of the interrupted ones (schematically depicted in Figure 7.1)

Correct orientation   Wrong orientations
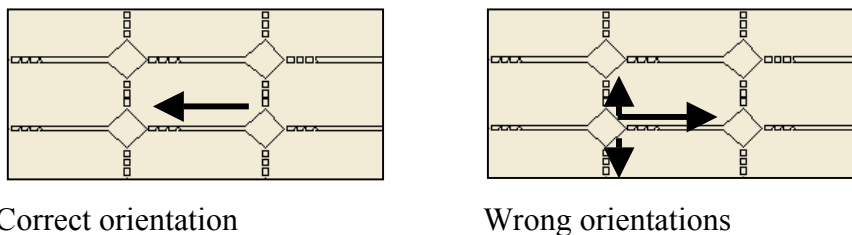
Figure 7.1: Schematic depiction of the intended orientation of neuronal polarity. As axons were thought to extend preferably along the solid and dendrites along the interrupted lines, synaptic signalling was expected to occur along the direction defined by the arrow.

7.2 Analysis of Cellular Behaviour on Interrupted Microstructures

Since a reproduction of the quoted work was not possible, the question arises which differences in the patterned surfaces used by Stenger and in this work could be accounted for that. An argument could be raised that faults in the surface preparation by microcontact printing may be responsible, leading to a too adhesive surface along the "impeding" paths and thus not providing enough contrast to the permissive line. This could be due to contaminations of the gaps with protein unintentionally transferring during printing.

However, no such contamination became obvious when the pattern was visualised by mixing the inking solution with sulforhodamine as it was done in chapter 3 for the quantification of pattern transfer; typical pictures are presented in Figure 7.2 Additionally, AFM-measurements of patterns with interrupted lines were made to probe the surface in detail (also shown in

Figure 7.2). Both imaging methods show high resolution micropatterns consisting of continuous lines in one direction and lines with well defined interruptions into all other directions. The AFM measurement shows a steep slope at the edge of the imprint, indicating that material transfer had taken place strictly from the embossed regions of the stamp. It therefore can be assumed that pattern transfer had occurred as intended and that the pattern should provide the expected differential adhesive properties.


A)

B)

C)

D)
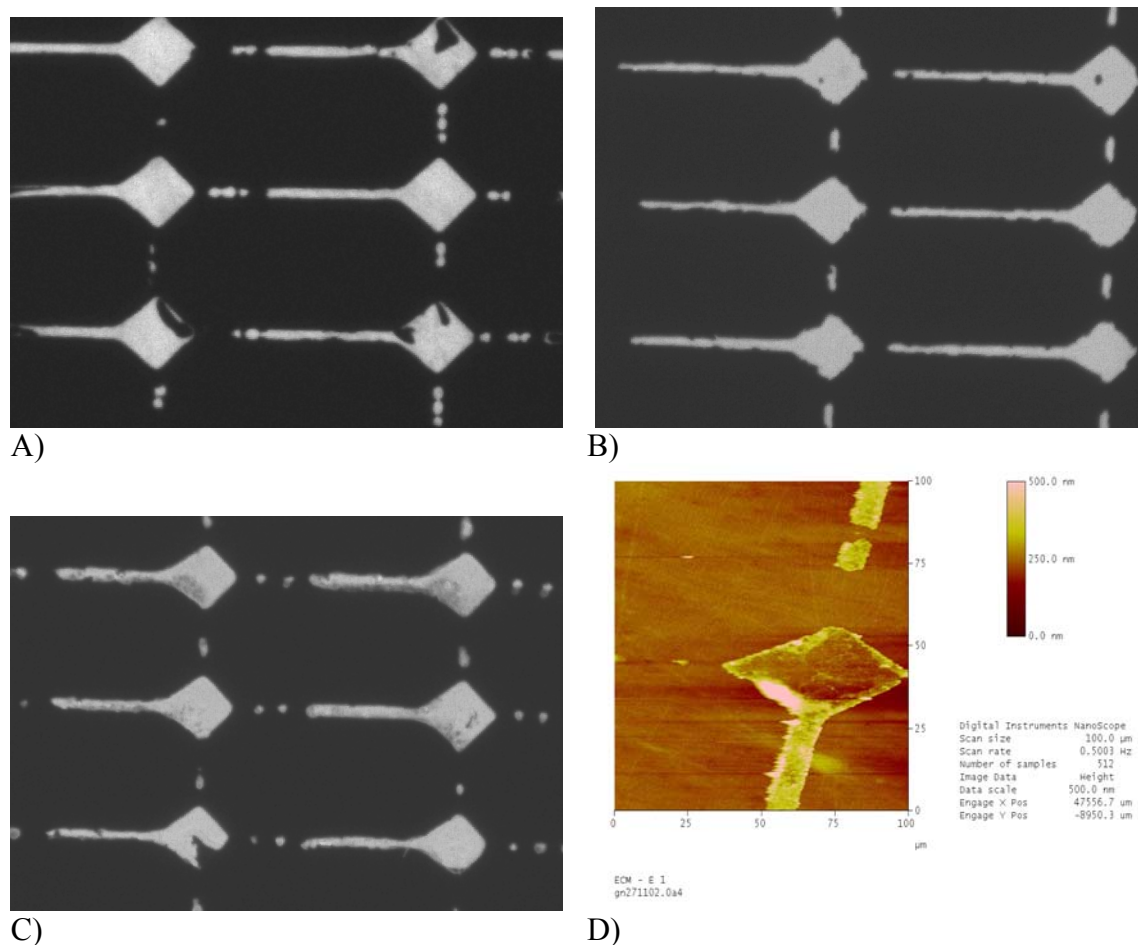
Figure 7.2: Imaging of the structures containing interrupted lines. A-C) The inking solution was mixed with a fluorescent dye and viewed under light of the excitatory wavelength. A: Pattern E, B: Pattern G; C: Pattern H. B) AFM-image of pattern D. No contaminating protein is seen in the gaps of the designed patterns in either type of picture.

In addition to these direct investigations on the patterned surface itself, surface properties were tested with regard to their interactions with neuronal cells. Although the cell repellent properties of polystyrene have already been shown by the strong compliance of the cells to the

pattern, the issue whether the cells were able to adhere to the small spots of bare polystyrene on the interrupted lines was looked into. It appeared possible that the cells were able to "bridge" these small gaps e.g. by secreting ECM-molecules themselves.

The following method was applied to test the relative adhesive properties of permissive and non permissive paths: Relatively young cultures (DIV 4) were stained with the neuron-specific antibody α neurofilament-M (NF-M). During the washing steps in the protocol, the cells were subjected to mechanical stress by using a vacuum pump applying a rather strong force to remove the buffer. This treatment had been shown before to pull the cells off their adhesion spots. When pictures of the stained cells were taken later, only a slight displacement of the cells from the somal adhesion site could be seen. Importantly though, shown in Figure 7.3, although the neurites were not displaced from the permissive, solid line, they were partially washed off the interrupted lines. More specifically, they still adhered to the anchoring sites provided by the dots of the protein pattern while loops of displaced neurite spanned the distance between these dots, showing that the neurite was washed off the non coated areas. This picture shows very clearly that adhesion had occurred on the stamped but NOT on the unstamped parts of the interrupted lines. Taken together, these results indicate that the creation of a micropattern containing a permissive, adhesion promoting line in one direction and discontinuous lines with non adhesive interceptions has been successful. Apparently, offering a substrate with these properties is not enough to orient neuronal polarity.
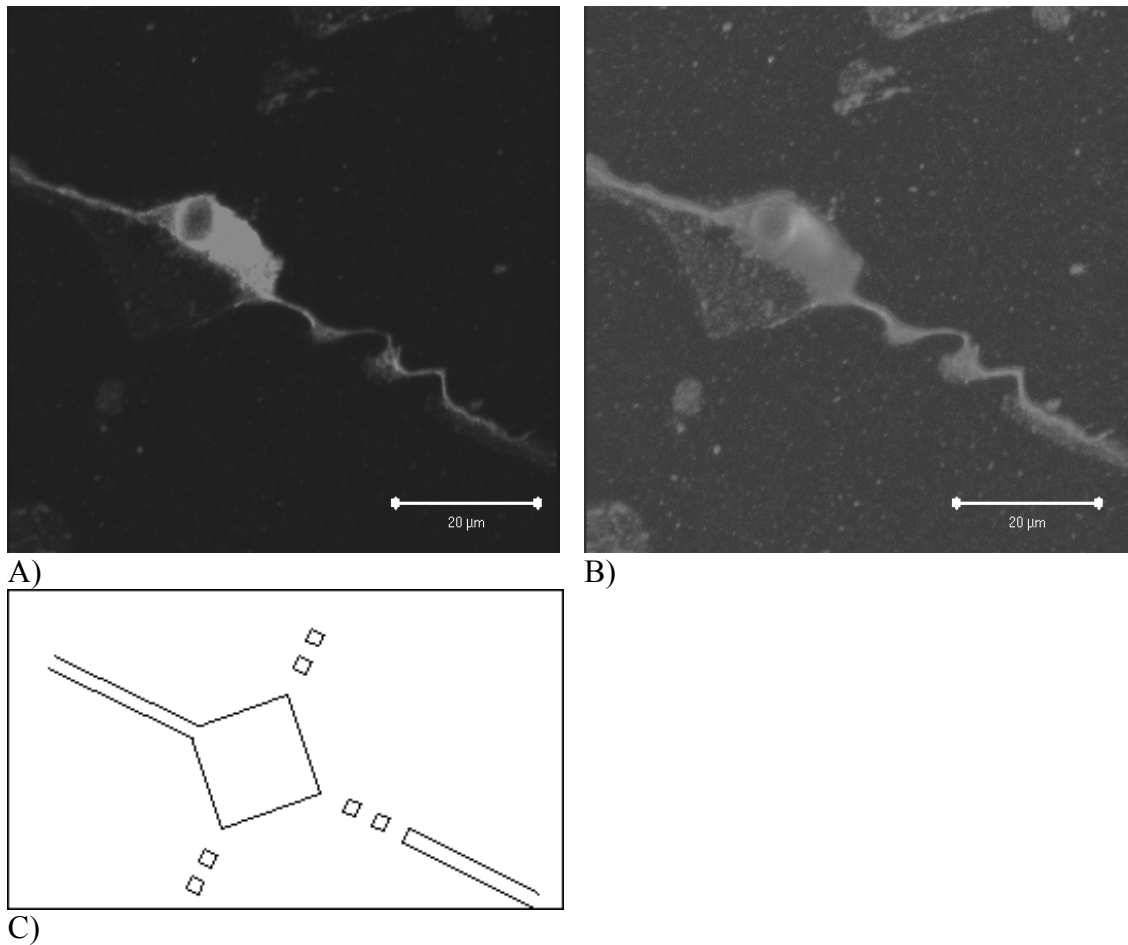
Figure 7.3: A) cortical neuron DIV 4 stained with anti-neurofilament M (the indentation in the middle shows the location of the nucleus). Note how the neurite pointing upward to the left along the solid line is not displaced from its adhesive pathway while the neurite pointing down to the right forms loops of displaced neurite leading from one adhesive spot to the next. B) Same picture as A, but overexposed to visualise the underlying micropattern. This picture clearly shows that the neurite adhered to the areas where protein transfer had taken place and was washed off the non coated interruptions of bare polystyrene. This indicates that neurite adhesion had only taken place on the surface areas which were protein coated. C) Schematic depiction of the underlying microstructure.

In this context, it can be asked whether the small non adhesive areas on the interrupted lines actually do slow down neurite extension as assumed. Figure 7.4 shows again a neuron in a very young culture (DIV4) extending two processes. The major process is clearly directed along the interrupted line, while a shorter process follows the permissive path. It therefore doesn't appear that adhesiveness alone controls the speed of neurite elongation.

139
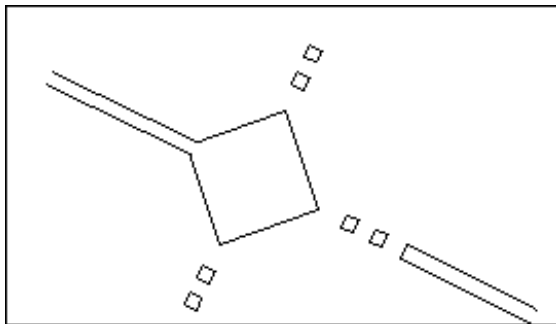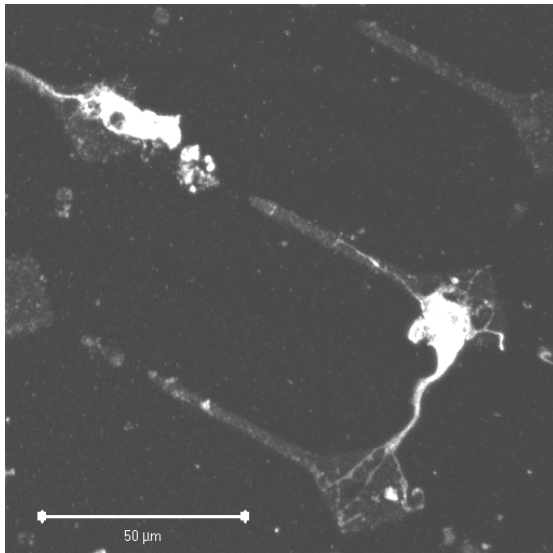
Figure 7.4: cortical neuron DIV 4, stained with αneurofilament-M. The neuron extends two processes onto the grid lines, the major one (presumably the axon) directed along an interrupted line. Note how the axon splits upon encountering a larger adhesive surface on a somal adhesion site.

This result is in accordance with studies by Isbister et al [Isbister, 1999] and Lemmon et al. [Lemmon, 1992], who investigated the impact of substrate adhesiveness on the extension rate of axons. Little correlation was found between adhesiveness and rate of growth cone elongation. Both groups concluded that although cell substrate interactions play a critical role in axon guidance and also in the control of filipodia extension rates, these effects do not appear to be principally mediated via the relative adhesiveness of different surface areas.

(Similarly, Calof et al. report that although the migratory behaviour of neurons is strongly influenced by the type of underlying substratum, no correlation, neither positive nor negative, between rate and speed of migration and the strength of cell-substratum adhesion could be found.) These observations indicate that although regulation of axonal outgrowth and probably also the establishment of neuronal polarity most likely are - at least partially -

140

regulated by interactions with the underlying matrix molecules, the actual mechanisms delivering these effects are much more complex than simply differences in the relative adhesive strength of different pathways.

7.3 Summary and Conclusions

It was attempted to control neuronal polarity by offering pathways of differential adhesiveness in the different directions defined by the micropattern. The approach was taken following the work by Stenger et al. [Stenger, 1998], who had reasoned that adhesive pathways favoured axonal outgrowth while pathways with interspersed non-adhesive regions would favour dendritic outgrowth. The group used adhesive DETA lines with interspersed regions of 13F. If the mechanism through which neuronal orientation was induced was different adhesiveness, the effect should have been reproducible in a micropattern of PECM and polystyrene accordingly, however, this was not the case. It could be shown that pathways of different adhesiveness do not suffice to induce neuronal orientation. Based on these findings, it is an intriguing question which molecular clues presented by the DETA / 13F surface used by the Stenger group was critical for the control of neuronal polarity. One explanation might be that the fluorinated groups as such provide a barrier to neuronal outgrowth (or present a signal inducing dendritic differentiation) not so much through their non adhesive properties but maybe through another, more specific mechanism. Alternatively, the process applied for surface preparation (laser ablation of the permissive amine groups in the non adhesive areas and subsequent rederivatization of the liberated hydroxyl groups with 13F) may have created a gradient of presented amine groups rather than a sharp edge between the contrasting areas. It seems possible that such a gradient could present a signal influencing the rate of neurite extension and that such a gradient was not provided by the abrupt change in surface properties on the substrates created by microcontact printing. An alternative

explanation could lie in the fact that Stenger et al. used a cell culture system with hippocampal rather than cortical neurons. It is theoretically possible that the two cell types reacted differently to the adhesive clues provided by the micropattern. However, the literature does not report any dramatic differences in the expression of adhesion molecules by hippocampal and cortical neurons or axon extension mechanisms particular to either of the two cell types.

It would be interesting to find out through which mechanism neuronal polarity was oriented on the DETA / 13F pattern and whether this mechanism can be combined with the system presented here. A robust cell culture that is stable long enough for synaptically coupled networks to form would be very attractive to combine with a system that allows control over the orientation of the forming connections.

8. Network Formation

Triple patch-clamp measurements (in which three neurons are patched simultaneously) as opposed to double patch clamp measurements have the advantage that actual network activity can be observed rather than just the communication between two cells. The triple patch-clamp approach was therefore applied in this thesis to investigate principles of neuronal network formation on micropatterned substrates. In addition, network activity and modulations were recorded and analysed.

8.1 Synaptically Connected Triplets of Neurons

Figure 8-1 shows an example of a synchronously patched cell triplet: Three cells on neighbouring positions of a grid pattern were held in the current clamp mode and action potentials were evoked in one cell at a time by a depolarising current pulse. The three cells were found to be connected through two successive synapses: A signal evoked in the first cell (c1) was transduced through the first synapse to the second cell (c2), resulting in an excitatory postsynaptic potential (EPSP), while no effect on the third cell (c3) was observed (Figure 8-1 C). An action potential evoked in c2 induced an EPSP in c3 through the second synapse, but not in c1 (Figure 8-1 D), whereas an action potential in c3 had no effect on the other cells (Figure 8-1 E). This indicates a unidirectional connection from c1 via c2 to c3 through two synapses in succession. In another recording shown in Figure 8-1 F, stimulation of c1 resulted in an EPSP in c2 that was large enough to trigger an action potential, which in turn induced an EPSP in c3. In this recording, the signal travelled via two synapses through all three cells of the constellation.
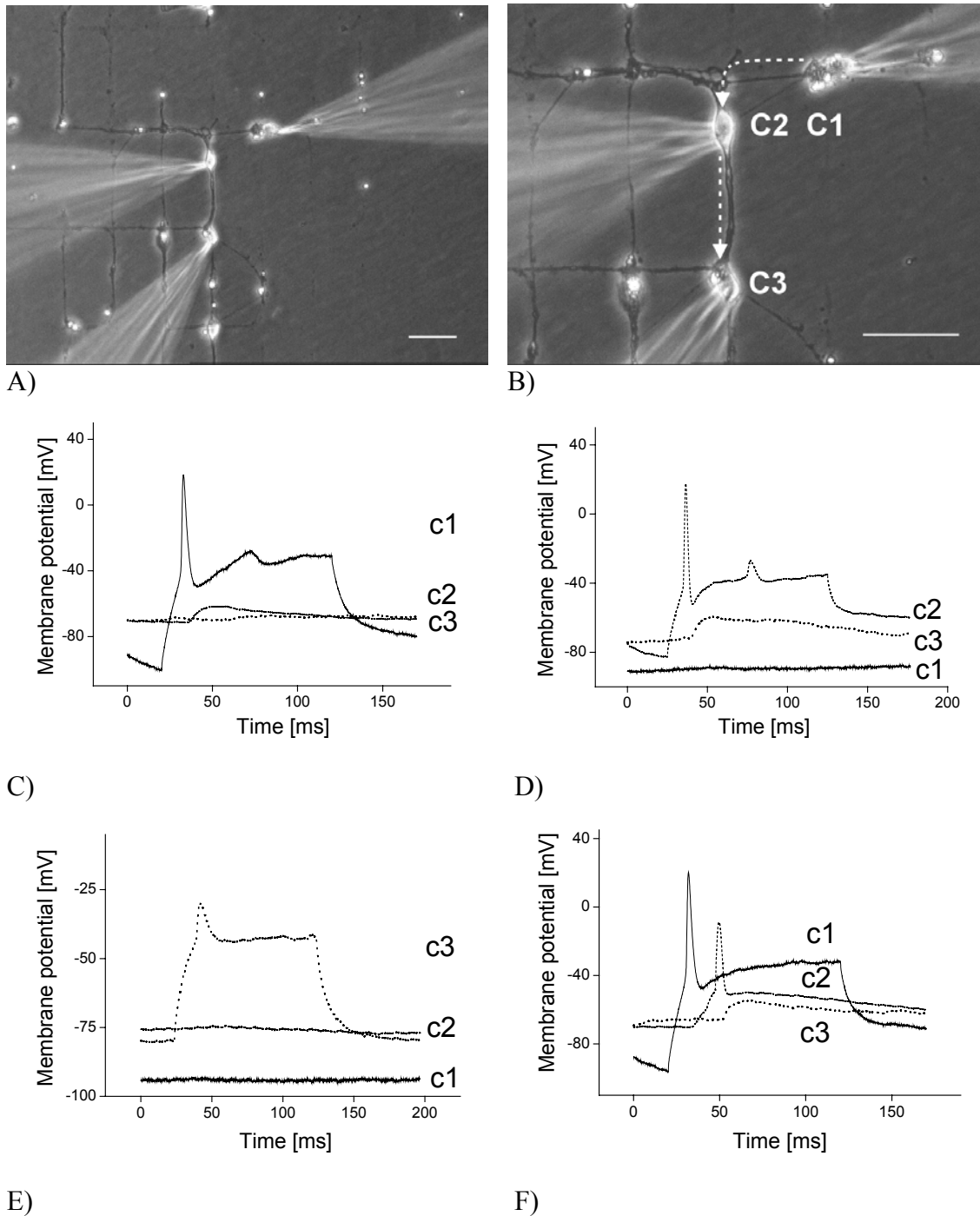
Figure 8-1: Constellation of three cells connected through two successive synapses. A,B: Phase contrast pictures at magnifications of 100x and 200x respectively. Arrows in B) indicate the two synapses. Scale bars 50 μm. C) An AP evoked in c1 induces a postsynaptic potential in c2 but not in c3. D) An AP in c2 induces a postynaptic potential in c3 but not in c1. E) An AP in c1 has no impact on either c1 or c2. F: When an AP in c1 induces postsynaptic potential large enough to trigger an AP in c2, the signal travels through all three cells of the network. C1 solid line, c2 dashed line c3 dotted line.

This example shows that the formation of functional networks following the predefined geometry of a micropatterned substrate was achieved. As in previous chapters, it appeared interesting to investigate whether features of network formation differed between patterned

144

and control substrates. More specifically, it was asked whether – as suggested in chapter 6.2. – specific recognition mechanisms between different types of cells existed, favouring one type of connectivity over another and whether these were influenced by the growth on a patterned substrate. This aspect will be addressed in the next subchapter.

8.2 Principles Underlying Network Formation on Patterned Substrates

Different aspects of network formation *in vitro* have been investigated by other groups. A particularly interesting study was performed by Müller et al. [Muller, 1997]. The group examined network architecture and network properties of cultured hypothalamic neurons, focussing on the impact of network structure on synchronised activity patterns. Although the group used hypothalamic rather than cortical neurons, it seemed attractive to compare their results to the data presented here. Features found similarly in both systems may be important to network formation in general. In chapter 8.2.1 and chapter 8.2.2, two central findings of the quoted study will be presented and compared to the results of this thesis. The first concerns branching of excitatory and inhibitory neurons, the second addresses the formation of feedback loops.

8.2.1 Branching of Excitatory and Inhibitory Neurons

The first finding reported by Müller et al. was that although excitatory neurons outnumbered inhibitory ones in the culture, the total number of inhibitory synapses was greater, as inhibitory neurons on average formed more contacts. Both facts were deduced from the observations described below.

First, the group measured a representative amount of synapses and determined the ratio of excitatory to inhibitory connections. Next, to evaluate the number of synaptic contacts formed per cell, the group introduced the term "branching", meaning that the axon split and innervated more than one postsynaptic cell. The rate of branching was determined by quantifying the occurrence of synchronized excitatory postsynaptic currents (EPSCs) or inhibitory postsynaptic currents (IPSCs) in simultaneously patched neurons. When in at least 3 instances PSCs occurred within 3 ms of one another in both cells, a common presynaptic neuron was postulated and a branching event was counted. In the next step, the branching rate of inhibitory versus excitatory neurons was related to the ratio of inhibitory to excitatory synapses in the system. It turned out that although the total amount of inhibitory synapses found was greater than the total number or excitatory ones, more excitatory neurons must be present since they have a far lower branching rate and therefore were deduced to form fewer contacts. This conclusion matched histochemical observations; it had been shown by antibody staining that excitatory neurons were more abundant than inhibitory ones [Wahle, 1993].

It was appealing to use the same approach in the work presented here. Deduction of the relative amounts of excitatory and inhibitory neurons was feasible as the relative numbers of excitatory and inhibitory synapses as well as the branching rates of the two types of neuron could be extracted from the available data.

As a first step, the branching rate of excitatory and inhibitory neurons was to be determined, which could not be done analogously to Müller et al: Due to the nature of the conducted experiments, which aimed at keeping the amount of interaction partners per cell at a minimum, synchronized synaptic input to two patched cells was rare. It was observed occasionally though, particularly in older cultures when overgrowth of the non permissive areas of the surface started and compliance to the pattern was reduced (Figure 8-2). As the cells were held in the current clamp mode throughout most of the measurement, postsynaptic potentials rather than postsynaptic currents were recorded, impeding the identification of the

synaptic input as excitatory or inhibitory. The few events of synchronous synaptic input could therefore not be used for evaluation. (While it is possible to deduce the synapse type from the postsynaptic current (see chapter 2.1.2.2.2.1), postsynaptic potentials don't display a sufficiently characteristic shape for this end).

A)   B)
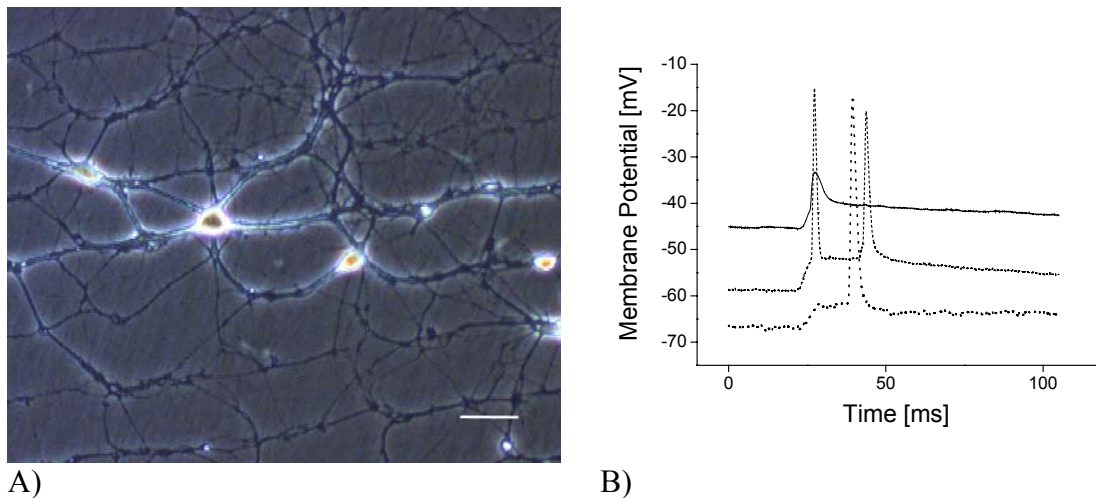
Figure 8-2: In older cultures, cells tend to overgrow the pattern and connect over non permissive areas, resulting in multiple synaptic input from unknown cells. A) Phase contrast picture of hippocampal neurons on laminin Pattern B, DIV 18. Scale bar 50 µm B) Synchronous synaptic input to three recorded cells from an unknown fourth neuron. No external stimulus was applied. Cortical culture DIV 14 on PE pattern D.

The rate of branching was therefore determined by a different method: Patched triplets of neurons with at least one synapse (such that the presynapse could be identified as excitatory or inhibitory) were evaluated. As illustrated in Figure 8-3., cells in these triplet constellations that had one postsynaptic interaction partner were termed "non branching" whereas those that formed synapses with both of the other patched cells were termed "branching". The rate of branching for excitatory and inhibitory neurons was quantified. As shown in Table 8-1., 43% of all inhibitory neurons in triplet constellations exhibited branching while only 20% of all excitatory neurons did, suggesting that inhibitory neurons in this system form approximately twice as many synapses as excitatory ones.

Branching	total	branching	non branching	% branching
excitatory neurons	5	1	4	20
inhibitory neurons	21	9	12	43%

Table 8-1: Branching rate of excitatory and inhibitory neurons. Total numbers indicate the number of excitatory and inhibitory neurons identified in triplet constellations

A)   B)

Figure 8-3: Scheme illustrating the criteria used for the determination of the branching rate. A: Non branching neuron B: Branching neuron

From the branching rates and the ratio of excitatory to inhibitory synapses, the relative numbers of excitatory and inhibitory neurons can be deduced using the approach described in chapter 2.10. The ratio of inhibitory to excitatory neurons after this calculation is 1.6, (Müller et al. report approximately the opposite ratio in the hypothalamic culture, 0.7).

While the deduced ratios of excitatory to inhibitory neurons differ, the findings concerning the branching rate fit well with those reported by Müller et al. who also found inhibitory neurons to branch at a higher frequency than excitatory ones. It is especially interesting to note that the different branching behaviour of excitatory and inhibitory neurons was not only similar between neurons from different brain areas, but also seemed to be unaltered by the growth on a micropattern. The possibility to branch on the grid pattern is highly restricted to the node points, which is depicted in a different context in Figure 7.4 (chapter 7). It would not have been unexpected if the characteristic branching behaviour of the two cell types had been levelled by the geometrical restrictions: These might have reduced the opportunities to form branches to a level below even that displayed by the less branching cell type on homogenous substrates. It would have seemed plausible that both cell types branched at any possible occasion, resulting in a similar rate. This did not appear to be the case and the differential behaviour of excitatory and inhibitory neurons could be reproduced even under the highly restraining geometry applied by growth on a micropattern.

8.2.2 Feedback Circuits

Another interesting result presented by Müller et al. lied in the analysis of circular connectivity, in the form of feedback loops. Focussing on the most simple type of loop, cell pairs connected reciprocally through two synapses were investigated.

The occurrence of the three possible constellations was monitored: Reciprocal excitatory, reciprocal inhibitory and mixed pairs of one excitatory and one inhibitory synapse. Pairs of two inhibitory neurons reciprocally innervating each other were found at the frequency predicted by theoretical considerations, while reciprocal excitatory synapses were never encountered. Strikingly, mixed constellations of excitatory and inhibitory neurons connected reciprocally were found three times more frequently than predicted. It was concluded that the formation of synaptic contacts does not occur randomly but that specific cell-cell recognition mechanisms exist which favour reciprocal connectivity between excitatory and inhibitory cells. It was found remarkable that cellular recognition was still occurring in the dissociated culture where the tissue architecture conferring spatial information was completely disrupted.

It was examined whether a similar effect could be observed in the system presented here. As shown in Table 8-2, on patterned substrates, 73% of all reciprocal connections consisted of mixed pairs of excitatory and inhibitory synapses. This is almost twice the rate that would have been predicted if synapse formation occurred randomly (predictions based on a statistical model are described at length in chapter 2.10.). The deviation of the experimentally acquired results from the predicted values is statistically significant (significance level $\alpha = 0.05$, see chapter 2.10.)). Reciprocal excitatory synapses were observed at the predicted rate, while reciprocal inhibitory ones were found less frequently than expected. The same trend is seen on control substrates, but due to the smaller number of available data, these values do not reach significance.

	pattern number	fraction	control number	fraction
total number of reciprocal synapses	**11**	**100%**	**4**	**100%**
excitatory - excitatory	**1** (0.9)	**9 %** (8%)	**0** (0.6)	**0 %** (16%)
inhibitory - inhibitory	**2** (5.6)	**18 %** (51%)	**1** (1.5)	**25 %** (37%)
excitatory - inhibitory	**8** (4.4)	**73 %** (40%)	**3** (1.9)	**75 %** (47%)

Table 8-2: Occurrence of different constellations of reciprocal synapses on patterned and on control substrates (bold numbers). The values for the respective constellation expected if synapse formation occurred randomly are depicted in brackets; the calculations leading to the predicted values can be found in chapter 2.10.. The formation of mixed constellations is strongly enriched over reciprocal inhibitory ones.

In summary, the preferred formation of reciprocal synapses between excitatory and inhibitory cells reported by Müller et al. could be reproduced not only using cells from a different brain area but also under the special circumstances applied by the micropattern. It appears that a preference for this type of connectivity is a feature occurring in both hypothalamic and cortical networks and may occur in other brain areas as well. Additionally it was shown that cellular recognition mechanisms still occur in a dissociated culture, enabling neurons to selectively form synapses with a subset of their potential interaction partners.

The importance of inhibition in general and reciprocal inhibitory synapses in particular in controlling and shaping network activity is well established experimentally and in computer models [Bush, 1996; Roberts, 1995; Sil'kis, 1996; Manor, 1999; Whittington, 1995]. Similarly, reciprocal excitatory synapses as a positive feedback mechanism and their importance for pattern recognition by the brain and network plasticity have been recognized [Douglas, 1995; Sil'kis, 1995]. However, reciprocal connections between excitatory and inhibitory neurons have been studied relatively little. It can be speculated about the role this type of feedback circuit plays e.g. in the generation or stabilisation of network oscillations or other types of activity patterns. Implementing a preference for such a feedback mechanism in

neuronal networks in computer models would be a highly interesting approach to shed light on the functional significance of this phenomenon.

8.3 Network Plasticity

Throughout the 20th century, the ability of the brain to learn from experiences and store memories has been attributed to activity dependent modifications of synaptic connections. Experimental support for such a process came in 1973 through the work of Bliss and Lomo, who were able to show that repetitive activation of excitatory synapses in the hippocampus lead to an increase of synaptic strength that could last for hours or days [Bliss, 1973]. This phenomenon, which was termed long-term-potentiation (LTP), has been investigated intensely as it is widely believed to be a key feature in the cellular basis of learning and memory formation [Malenka, 1999; Fitzsimonds, 1997; Ganguly, 2000; Kirkwood, 1993; Nicoll, 1995; Sanes, 1999]. In addition, many forms of short-term modulations in synaptic strength are known, such as synaptic facilitation and depression [Varela, 1999]. Background information on long- and short time modifications can be found in chapter 1. It was intriguing to investigate whether the synapses in the patterned neuronal networks that are described here exhibit activity dependent changes analogous to those described in the literature. As a first aspect, described in the next paragraph, short term modulations were assayed while long term changes will be discussed in chapter 8.3.2.

8.3.1 Short Term Plasticity

Frequency dependent synaptic depression has been described for both excitatory and inhibitory synapses in the neocortex [Markram, 1996; Metherate, 1994]. Interestingly, Varela et al. report that inhibitory synapses are depressed to a much smaller extent than excitatory ones after repetitive activation [Varela, 1999]. The group stimulated neurons with trains of stimuli at different frequencies and evaluated the relative height of the subsequent EPSPs in the train. They found that above a frequency of 0.1 Hz, the EPSP height decayed exponentially within the train and that this effect was more pronounced in excitatory synapses (no effect was observed at 0.1 Hz, the next frequency investigated was 0.5 Hz).

The experiments conducted in this thesis routinely assayed synapses by applying trains of 10 stimuli at a frequency of 0.8 Hz to the presynaptic neuron. In some experiments, an alternative stimulation protocol was applied in which the cells were excited by 10 stimuli at 0.4 Hz. Figure 8-4 shows the average height of the successive EPSPs within a stimulus train delivered at the two different frequencies. One excitatory and one inhibitory synapse are shown. Clearly, stimulation at 0.8 Hz causes short-term synaptic depression. This effect is much stronger in the excitatory synapse. The rate of depression can be fit with a single exponential as described by Varela et al.. Contrary, no similar decay of EPSP height is seen at a stimulation frequency of 0.4 Hz, in consistency with the work described above. It is also noticeable that the values of the excitatory synapse vary much more than those of the inhibitory one.

Thus, short-term plasticity matching the effects described in the literature could be demonstrated in the patterned neurons.
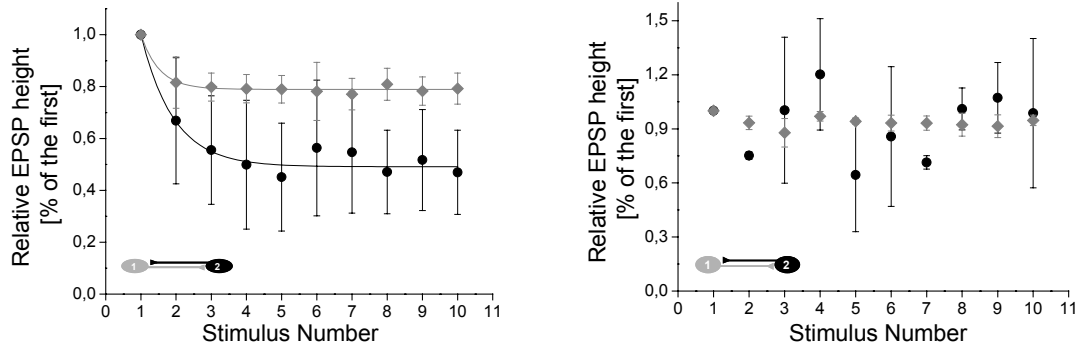
Figure 8-4: Stimulation of two synapses with trains of 10 stimuli delivered at different frequencies. A cell pair reciprocally connected through one excitatory and one inhibitory synapse was used for the experiment. Cell one and cell two were stimulated alternatingly with trains of stimuli; the relative EPSP height following each of the 10 presynaptic APs was plotted. 11 stimulus trains delivered at 0.8 Hz were averaged for each synapse in A, 3 trains at 0.4 Hz in B. Cortical culture, DIV 12 on PECM pattern D ●: Excitatory synapse ◆: Inhibitory synapse. Short-term synaptic depression is induced through stimulus trains with a frequency of 0.8 Hz but not 0.4 Hz. Depression is more pronounced in the excitatory synapses.

8.3.2 Long Term Plasticity

In order to determine whether long-term changes in synaptic plasticity were observable in the patterned networks, LTP induction was attempted. Different forms of LTP have been described (see chapter 1), which are triggered by different stimuli and transduced through different mechanisms. Therefore, a variety of protocols able to induce LTP exist in the literature.

In the intact brain or in brain slices, the repetitive activation of particular pathways at a high frequency by inserted electrodes has been described as an induction mechanism. In these protocols, the strength of the stimulus is crucial, as it needs to activate several afferent fibres from the same pathway. Only through the concomitant activation of several fibres is the requirement for LTP induction met, namely the synchronous activity of pre- and postsynaptic neurons [Maccaferri, 1998; Madison, 1991], see chapter 1. LTP induction on the single cell basis in a patch clamp configuration on the other hand requires a more specific induction. Synchronous activity of pre- and postsynaptic neuron can e.g. be mimicked by inducing presynaptic spiking while the postsynaptic cell is voltage clamped at a depolarising potential

[Otsu, 1995; Kirkwood, 1995]. Particularly interesting studies were performed by Bi et al. and Makram et al. who showed that stimulation of pre- and postsynapse in rapid succession can induce either LTP or LTD depending on the relative timing of the stimuli [Bi, 1998; Makram, 1997].

The experiments conducted in this thesis utilised a protocol similar to that described by Bi et al.: The presynaptic cell was stimulated sufficiently to induce an action potential. An analogous stimulus was applied to the postsynapse with a time delay of 10 ms such that the postsynaptic potential coincided with the externally applied stimulus. This protocol had been termed "positive correlated spiking". Trains of 60 positively correlated stimuli were applied at 1 Hz followed by a series of recorded test pulses to ensure cellular intactness. 2-4 series of stimulation and test pulses were applied. Before and after this protocol, series of pulses at the standard frequency were applied to the presynaptic neuron to determine synaptic strength (the protocol is schematically depicted in Figure 8-5). Contrary, "negative correlated spiking" were stimulus trains in which the postsynaptic neuron was stimulated 10 ms before the presynaptic one such that the EPSP arrived at the postsynaptic cell just after spiking during its refractory phase. Thus, the protocol for LTD induction was the exact mirror image of the LTP protocol. Consequently, applying the stimulation protocol to two reciprocally connected cells should induce LTP in one synapse and LTD in the other. As Bi et al. report spiking with a time delay of 5 to 20 ms as optimal for LTP / LTD induction (Makram et al. report 10 ms to be ideal), the chosen delay time appeared to be suitable.
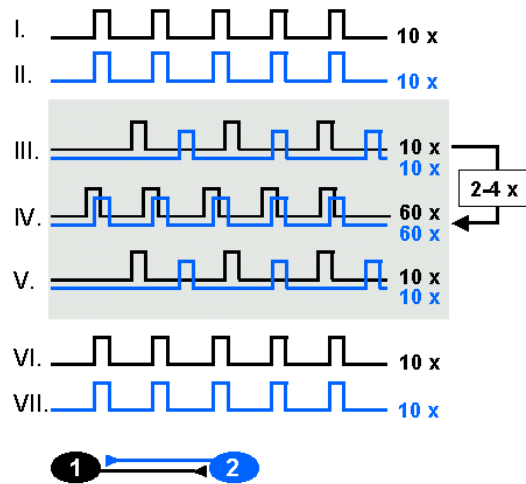
Figure 8-5: Scheme of the different modes for the evaluation and stimulation of synapses. I, II: Before specific LTP / LTD protocols were applied, both cells were stimulated separately with trains of 10 stimuli delivered at a frequency of 0.8 Hz (each stimulus was designed in strength and duration to elicit an action potential). For most evaluations, the average EPSP evoked by one stimulus train was taken as a measure for synaptic strength at the corresponding time point (except in part 8.3.1 where the relative EPSP height of successive stimuli within one train was compared). III-IV: LTP /LTD protocol. The protocol started with 10 test stimuli (III.) delivered alternatingly to the two cells at a frequency of 0.4 Hz. Pulses to cell one and to cell two were delayed by 1.225 s, such that the two stimuli did not interfere with each other. These test pulses were recorded to ensure cellular intactness (the stimulation pulses (step IV) were not recorded). IV: The stimulation sequence consisted of 60 paired pulses to cell 1 and cell 2 delivered with a time delay of 10 ms at a frequency of 1 Hz. Preceding stimulation of the presynaptic neuron was expected to result in LTP, while preceding stimulation of the postsynaptic neuron was expected to cause LTD. In the depicted example, the synapse from cell 1 to cell 2 would experience potentiation, that of cell 2 to cell 1 depression. After one stimulus train, steps III to IV were repeated to a total of 2-4 cycles. V: At the end of each LTP / LTD protocol, another test sequence was recorded. VI, VII: Synapses were assayed after attempted LTP / LTD induction again by separate stimulation at 0.8 Hz.

The average EPSP height after the LTP / LTD protocol relative to the average value before stimulation is shown in Figure 8-6. Results obtained on both patterned substrates and controls are shown. It can clearly be seen that no effect similar to that described by Bi or Makram can be observed in either group: The EPSP amplitudes observed after stimulation scatter closely around their initial value with no trend to an increase after the LTP protocol or a decrease after the LTD protocol. No deviations from the initial value in the range described by Bi (who reports a change in synaptic strength around 50%) or by Makram (who reports 20-40%) can be observed.
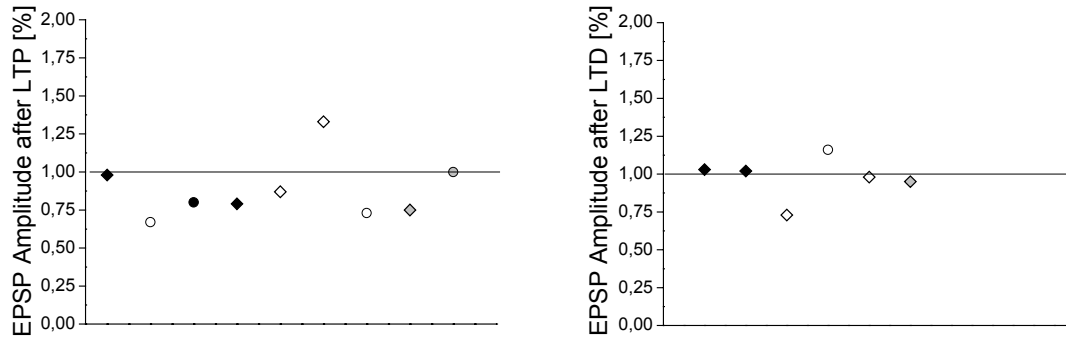
Figure 8-6: Average EPSP height of several synapses after stimulation with the LTP (A) or LTD (B) protocol. For each synapse, the EPSPs evoked through 5 trains of 10 stimuli each before and 5 x 10 stimuli after correlated stimulation were averaged. The displayed value is the average EPSP height after the protocol relative to the initial value. ● = excitatory synapse ◆ = inhibitory synapse. Open symbols stand for measurements on patterned substrates, filled ones for measurements performed on controls. Grey symbols depict measurements performed with a low-EGTA intracellular patch solution (as explained in the text; all measurements were performed on patterned substrates).

To investigate the impact of the LTP / LTD protocol in more detail, the development of the EPSP height before, during and after the stimulation protocol was plotted as a function of time. A decline of synaptic strength after each LTP or LTD stimulus train became apparent, irrespective of which of the programs was applied. The synapses typically recover as soon as stimulation is performed with the standard protocol again. A typical time-course is shown in Figure 8-7, depicting the behaviour of a reciprocal synapse. The applied protocol should have induced LTP in the excitatory synapse and LTD in the inhibitory one. Neither of the synapses shows a significant long-term effect, but both display short-term depression as indicated by the reduced EPSP in the test pulses between the LTP / LTD stimulus trains. The synapse that was supposed to undergo LTD recovered notably after the end of the LTD-protocol, indicating that the observed depression is short-term and not long-term in nature.

The transient depression may be explained by the repetitive stimulation at 1 Hz (the frequency of the LTP / LTD protocol). Prolonged synaptic stimulation has been shown before to cause depression, probably through depletion of releasable synaptic vesicles. It occurs in dependency of the number and the frequency of the applied stimuli as reported by Galarreta et

156

al. [Galarreta, 1998]. Although this group investigated stimulation at frequencies higher than 1 Hz (5 Hz and more), it seems likely that the effect observed here is related.

In summary, the impact of the LTP / LTD protocol on synaptic strength is only a short-term effect and can be explained in consistency with the literature by repetitive activation at the applied frequency alone. The long-term changes expected to result from the particular protocol which applied correlated stimulation of pre and postsynapse, are lacking.
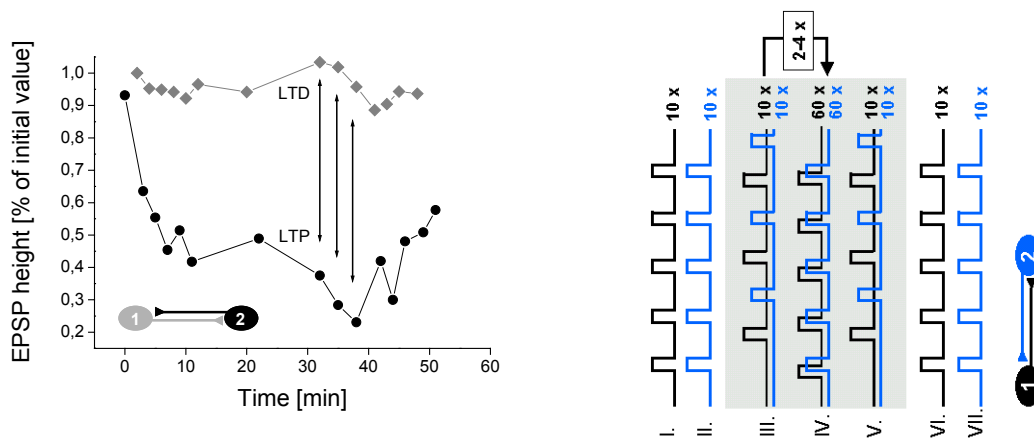
Figure 8-7: Development of synaptic strength of two synapses reciprocally connecting an inhibitory and an excitatory neuron. The three data points marked by arrows illustrate synaptic strength during the recorded test pulses before and after the LTP / LTD protocol (corresponding to III. and V. in the scheme). ● represents the excitatory synapse, ◆ the inhibitory one. Note that both synapses show transient depression after the LTP / LTD protocol but recover equally.

The question arises why LTP / LTD induction failed. One possibility seemed to be that the EGTA content (5mM) of the intracellular patch solution was too high: EGTA as a Calcium chelator might complex too much of the intracellular Calcium to allow LTP induction (which is a process that depends on intracellular Calcium signalling, see chapter 1). On the other hand, the concentration used by groups who deliberately wanted to remove Calcium from the cytoplasm was higher by two magnitudes (500 mM [Brocher, 1992]). It appears unlikely that the concentrations applied here sufficed to chelate intracellular Calcium altogether and thus completely block LTP induction. Additionally, a complete removal should have impeded transmitter release, which also depends on Calcium entry to the presynaptic terminal. As no impairment of synaptic strength during the course even of very long measurements (> 1.5

hours) could be observed, it can be assumed that the amount of EGTA diffusing into the neurites was not large enough to chelate a significant fraction of cytoplasmic Calcium there. Nevertheless, some experiments were performed with a different intracellular solution that contained minimal amounts of EGTA (0.2 mM); the results of this set of experiments are depicted in grey in Figure 8-6. LTP / LTD was not observed upon this change either; it can therefore be excluded that Calcium chelation was the factor preventing LTP induction.

Another explanation could lie in the types of cells that were used for the experiments. Most investigations on LTP have been performed in the hippocampus, where different, cell type specific forms are observed (see chapter 1). Although LTP has also been described in the cortex [Otsu, 1995; Markram, 1996] and has been reported to be inducible through the same mechanisms as in the hippocampus [Kirkwood, 1993], much less about the underlying mechanisms are known in this brain area [Kirkwood, 1995]. It seems possible that some cortical areas respond differently to certain stimuli, such that the applied protocols were not suitable for LTP induction in the cortical cells used in this thesis. In addition, it is established that not all synapses are equally susceptible to LTP induction: LTP / LTD expression depends heavily on initial synaptic strength [Bi, 1998] as well as the postsynaptic cell type [Maccaferri, 1998; McMahon, 1997]. LTP was shown in certain cortical areas to be inducible only when bicuculline was applied concomitantly to block inhibitory input [Kirkwood, 1995]. Bi et al. report a complete failure to induce LTP in synapses of glutamatergic onto GABA-ergic neurons, while the same stimulation protocol elicited a strong response in two coupled glutamatergic neurons [Bi, 1998]. It is possible that the synaptic constellations that were stimulated in the presented experiments were unresponsive for similar reasons.

8.3.2.1 Depression of Excitatory Synapses by Inhibitory Synaptic Input

As described in part 8.1 of this chapter, the triple patch clamp approach allowed the analysis of small circuits of up to three cells. A particularly extensively interconnected constellation is depicted in Figure 8-8: Three cells had formed six synapses, such that every cell was connected with every other cell reciprocally. Four of these synapses were strong enough to regularly elicit postsynaptic APs (indicated by thick arrows in Figure 8-8 B), while the other two are much weaker (indicated by thin arrows). The strength of the synaptic connections between these three neurons allowed a signal to travel through all three cells in the constellation until it reaches the cell again in which it was evoked. This is shown in Figure 8-9 in three examples. As the stimulated cell is still depolarised by the externally applied pulse when the stimulus returned to it, only a small peak can be induced rather than a second AP. Had it been possible to stimulate the neurons with sufficiently short pulses, longer oscillations might have been observable.

Cell number 1 in the network was determined to be excitatory, while cells number 2 and number 3 were inhibitory. The inhibitory connections induced postsynaptic depolarisation as the excitatory ones, which can be attributed to the elevated intracellular concentration of Chloride arising from the patching process (as described in chapter 2.1.). However, GABA has been described to act as an excitatory transmitter in embryonic neurons which display an equilibrium potential for Chloride different from that typically seen in adult animals [O'Donovan, 1999]. As embryonic cells are used in this system, the depolarising actions of GABA-ergic synapses may not even present an artefact.

The cells had no direct neighbours on the pattern and synaptic input from outside of the patched triplet was never observed, indicating an isolated network.
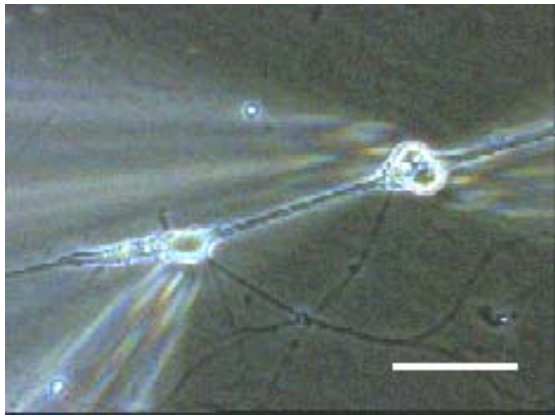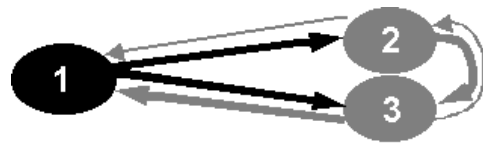
A)   B)

Figure 8-8: A constellation of three extensively interconnected neurons. A: Phase contrast picture, scale bar 50 μm. B: Diagram of the synaptic connections. Excitatory cells are depicted in black, inhibitory cells in grey. Thick arrows: Strong synapses capable of eliciting a postsynaptic action potential, thin arrows: Weak synapses that have not been observed to induce postsynaptic action potentials
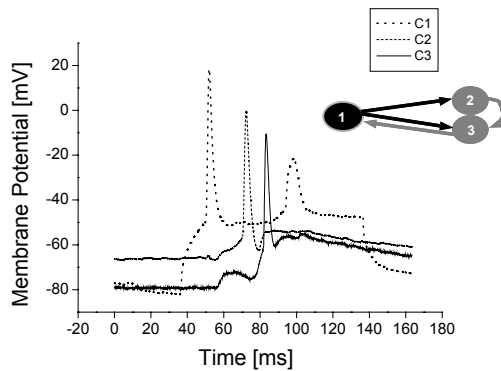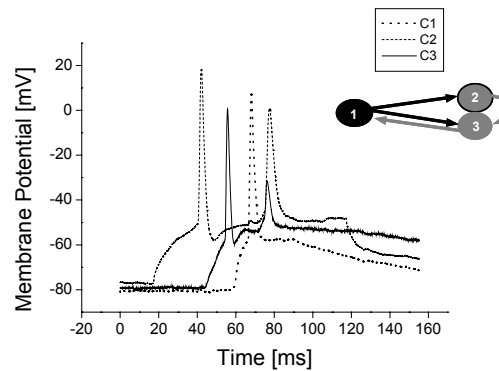
A)   B)
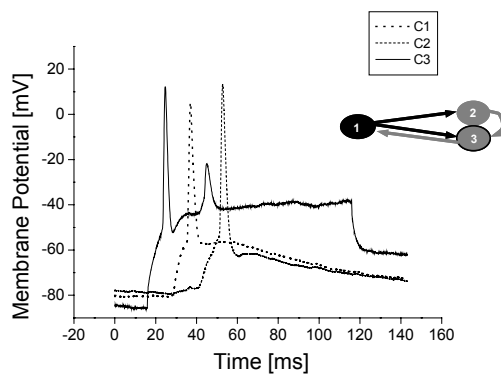
C)

Figure 8-9: Recordings obtained through stimulation of one neuron in the triplet. A: A signal initiated in cell 1 is transduced to cell 2 and 3, inducing an AP in cell 2 only. The AP in cell 2 induces a postsynaptic potential in cell 3, evoking another AP. The AP in cell 3 is transmitted back to cell 1. B: Stimulation of cell 2 results in an AP in cell 3, which is transmitted to cell 1, from where it is transmitted back to cell 2 and to cell 3. C: An AP in cell 3 is transmitted to cell 1, from there to cell 2 and back to cell 3. Note that the cell in which the initial stimulus was induced is still depolarised externally when the signal returns to it, thus impeding the induction of a full second AP (for the induction of a second AP, interim repolarisation would have been necessary).

The constellation could be recorded over a period of more than 100 minutes. During this time, all of the three cells were stimulated successively with trains of 10 depolarising stimuli as described in 0 and in chapter 2.1; the average postsynaptic potential evoked by one stimulus train is plotted as a function of time in Figure 8-10. It is important to bear in mind that the information on synaptic strength at different time points could only be extracted by repeatedly stimulating the three neurons, in other words, observation of a synapse always included stimulating and thus exerting an influence on it. Contrary to the *in vivo* situation in the intact brain, the cells did not fire spontaneously and in accordance with the input they received from other cells. Instead, stimuli were applied externally, inducing the cells regularly to signal to their postsynaptic interaction partners. Network modulations may therefore result from the repetitive stimulation of the three cells that was necessary to analyse them.

Two features are striking about the temporal development of the six synapses in Figure 8-10: First, the strength of different synapses made by one neuron can develop in complete independence of each other, which is consistent with the literature [Malenka, 1999; Bi, 2001]. This is most obvious for cell number three (Figure 8-10 C). Second, the strengths of the two excitatory synapses in the network decay steadily over the course of the measurement until they reach values around 25% of that seen initially. In contrast, the four inhibitory synapses do not display such a steady decay although their strength also varies widely. The question arises why both excitatory synapses are depressed although the integrity of cell number one did not appear to be impaired as indicated by the unchanged firing rate upon depolarising stimuli.
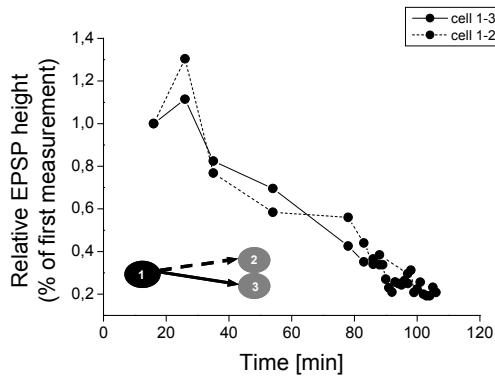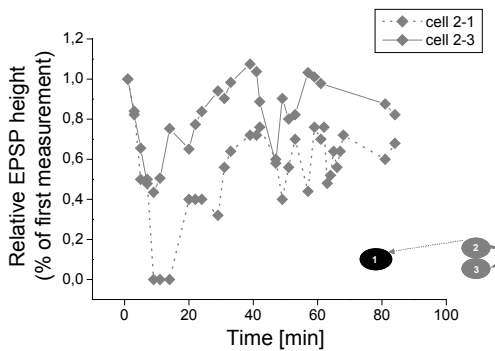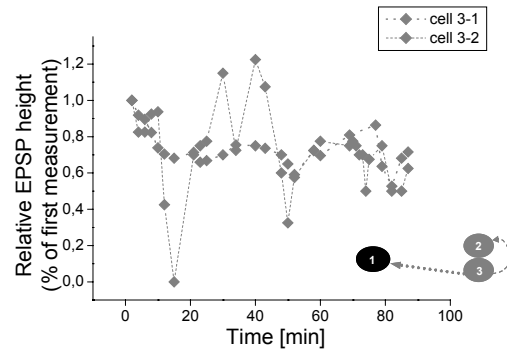
Figure 8-10: Development of synaptic strength over time in the triplet constellation shown in Figure 8-8. The EPSP height for every synapse relative to its initial value is plotted as a function of time.

Excitatory synapses have been shown in part 8.3.1 to be more susceptible to activity-induced depression than inhibitory ones. One possible explanation could therefore be that the two excitatory synapses are depressed by prolonged stimulation. On the other hand, the changes discussed in section 0 are all very short in duration and recovery was always observed within several minutes. Depression through repetitive stimulation is also not indicated with regard to other examples: Single excitatory synapses (in constellations where no neuron conferring inhibitory input was patched and thus stimulated during the experiment) do not exhibit such a decay in strength as illustrated in Figure 8-11 A. Figure 8-11 B displays a reciprocal constellation of an excitatory and an inhibitory neuron. In this constellation, where regular inhibitory input from one other cell to the excitatory neuron was induced experimentally, no depression of the excitatory synapse was observed either.
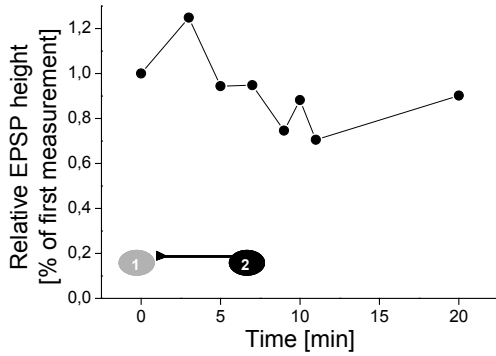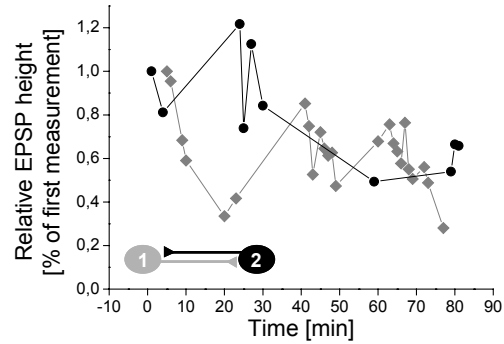
Figure 8-11: Development of the synaptic strength of two excitatory synapses. A) Single excitatory synapse encountered in a constellation in which no inhibitory synapse on the excitatory neuron was patched and thus stimulated during the experiment. (Cortical culture on PECM pattern D, DIV 14). B) Reciprocal synapse in which the excitatory neuron receives inhibitory input from the second cell which is stimulated throughout the measurement (Cortical culture on ECM pattern B, DIV 13). No decay in synaptic strength similar to that seen in Figure 8-10 is observed in either A) or B). ● excitatory synapse, ◆ inhibitory synapse

The different behaviour of the excitatory synapses described in Figure 8-8 may be accounted for by the inhibitory input from two cells. A particularly intriguing explanation would be that the correlation of this input was responsible for the effect: Cell number 2 directly transmitted an inhibitory signal to cell number 1 when it was stimulated. In addition, it stimulated cell number 3 to fire an AP, which then transmitted a second inhibitory signal to cell number 1 with a short time delay (see Figure 8-9). It can be hypothesised that through this repeated and correlated inhibitory input onto cell number 1, which was regularly induced experimentally through the series of pulses applied to cell 2, synaptic output of cell 1 was attenuated.

This result has to remain preliminary as no second constellation with the same properties was available to reproduce the effect. However, it appears that a type of synaptic plasticity in the form of depression mediated by correlated inhibitory synaptic input was observed in this small isolated network.

8.4 Summary and Conclusions

Several aspects of network formation and behaviour were investigated in this chapter. First, the formation of synapses by excitatory and inhibitory neurons on the micropattern was analysed and put into the context of a study by Müller et al. [Muller, 1997]. This group described different rates of synapse formation for excitatory and inhibitory neurons and a preferred formation of reciprocal connections between mixed pairs of excitatory and inhibitory cells. The data shown in part 8.2.1 and part 8.2.2 of this work are consistent with these results, illustrating that recognition mechanisms between different cell types still seem to occur on the pattern similarly as on homogeneous surfaces. In addition, characteristic differences in the branching behaviour of excitatory and inhibitory neurons could be reproduced in spite of the high geometrical restrictions of the micropattern. This strengthens the notion that the system presented here is a suitable model for neuronal networks: Basic features of neuronal connectivity are reproduced in a simplified, highly defined system.

The next focus of investigation were modulations in network activity. Both long-term and short-term changes were analysed. Frequency-dependent short term synaptic depression could be observed in patterned neuronal networks, indicating that the patterned cells exhibited synaptic plasticity. The responses were cell type specific (as shown by the different behaviour of excitatory and inhibitory synapses) and consistent with the results obtained by other groups [Varela, 1999]. It is indicated that excitatory synapses are much more variable in their synaptic strength and more susceptible to activity related depression. This feature may be important for network activity by preventing uncontrolled activity bursts. The induction of long-term changes could not be demonstrated; as it failed both on patterned substrates and on controls, it does not appear that the problem is related to patterned growth. The reason for this failure remains to be determined.

In one triplet constellation, a novel form of activity-dependent changes may have been observed: One excitatory cell received correlated synaptic input from two inhibitory neurons. The excitatory synapses formed by that cell experienced a strong depression during the course of the measurement. This depression may be attributed to the inhibitory signalling the cell received through the (experimentally induced) synaptic input delivered by the inhibitory neurons. Unfortunately, no additional triplet presenting a corresponding constellation was measured, such that the effect could not be reproduced in another set of cells. It will be interesting to perform further experiments on similarly connected triplets to determine which factors were essential in the induction of the observed effect. It could be investigated whether the synchronous spiking of two presynaptic inhibitory cells results in the depression of the synaptic output of a cell and whether this occurs similarly when an inhibitory neuron is the target.

9. Summary and Outlook

In this thesis, it could be shown for the first time that it is possible to grow neurons on a micropattern under geometrically highly restricting conditions without interfering negatively with cellular physiology or synapse formation.

Cells were grown on micropatterned substrates realised by printing organic molecules onto polystyrene culture dishes. Both the patterning process and the cell culture were optimised.

Cell function was not only found to be unimpaired by patterned growth on the level of single cells, but connectivity through chemical synapses could also be demonstrated. The synapses encountered on the pattern were functionally normal by all parameters tested. Moreover, both the overall rate of synapse formation and the cell-specific rates described for excitatory and inhibitory neurons appear to be undisturbed by the growth on the micropattern. This was unexpected, since the patterned surface exerts strong restrictions on cellular adhesion and outgrowth. In the resulting networks, every cell encounters a number of potential interaction partners that is by magnitudes lower than the number it would encounter *in vivo*. It would not have been surprising if such strong geometrical restrictions had had an impact on the rate of synapse formation between neighbouring cells. However, this did not seem to be the case, neither was the specific behaviour of excitatory and inhibitory cells altered. It can therefore be concluded that intrinsic features of cellular behaviour and network formation could be reproduced under the simplifying conditions of the micropattern.

In addition, cell-specific recognition mechanism leading to the preferential formation of reciprocal synapses between excitatory and inhibitory neurons could be demonstrated to occur in the patterned networks as well as on controls. This phenomenon has been described by others in unpatterned cultures [Muller, 1997], although the functional significance and the impact on network behaviour remain to be elucidated.

The physiological integrity of the cells on micropatterned substrates and the reproduction of central features of neuronal connectivity and cell-cell recognition mechanisms indicate that the system presented here is suitable as a model for neuronal network formation and behaviour. Although it has been shown before that dissociated neuronal cultures are pharmacologically similar to cells in living tissues, such that they can be used for fundamental research or drug screening, this has not yet been shown for patterned cultures. Patterned cultures allow electrophysiological investigations of small, well defined neuronal circuits while the complexity of the network is greatly reduced relative to circuits forming on homogeneous surfaces. It can therefore be assumed that the model system described in this thesis will be valuable as a tool for investigations of single synapses.

Although a certain extent of control over the architecture of the forming network could be accomplished by the growth on a micropattern, many challenges lie ahead. An interesting topic to address next is how to achieve control over neuronal polarity. The subject was focussed on in chapter 7 of this thesis, and it was shown that the approach described there – namely offering the neuron pathways of different adhesiveness as suggested by others [Stenger, 1998] – was not suitable for this end. An interesting alternative approach would be to define axonal and dendritic axes in a pattern by printing different physiological molecules in different orientations, as many proteins have been described to direct neuronal polarisation. An additional extent of control could be gained if it were possible to direct the adhesion of excitatory and inhibitory neurons separately, such that their relative location in the network could be manipulated. It would then be possible to direct the formation of particular constellations of excitatory and inhibitory connections.

One of the most fascinating topics that can be explored in a simplified neuronal network are activity-dependent changes in synaptic strength. These can be studied ideally on micropatterned substrates, as the cells receive little or no uncontrolled synaptic input from outside the investigated constellation. This subject has been addressed in chapter 8. Synaptic
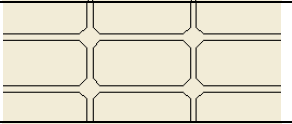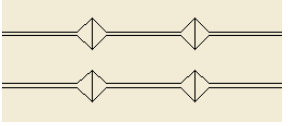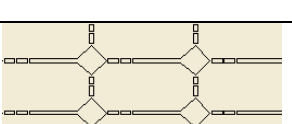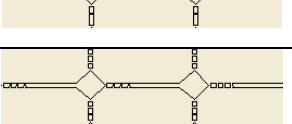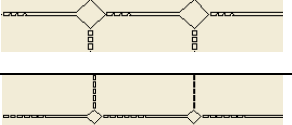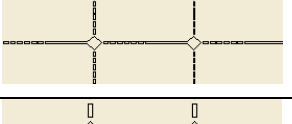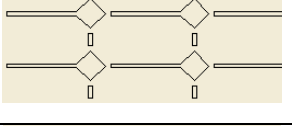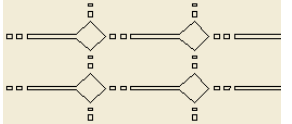
plasticity could be observed to a certain extent; short-term changes such as frequency dependent synaptic depression were found to occur in a cell-specific manner in accordance with the literature [Varela, 1999]. Long-term changes on the other hand could not be induced either in patterned or in control cultures, it therefore appears that a methodical problem is responsible for this failure. Solving this problem e.g. by trying out different types of stimulation protocols will open the way for a wide variety of experiments on the subject of synaptic plasticity.

Furthermore, examining network behaviour over longer periods of time could yield valuable insights into principles underlying network activity. Although patch-clamp measurements are advantageous over extracellular recordings in many ways, as they provide a better signal to noise ratio and allow a much larger degree of manipulation, they have the disadvantage of eventually killing the patched cell. Recordings therefore only span a relatively short period of time. The approach of cellular patterning would be attractive to combine with extracellular recording devices: While such recordings up to now only yield information on a fraction of the cells in a network, a micropattern directing neuronal adhesion exclusively to the sensitive spots of a recording device would allow the long-term observation of a whole network. The approach of immobilising single neuronal cells on an extracellular recording device has already been taken using snail neurons which were shown to connect through electrical synapses [Zeck, 2001]. However, no corresponding studies have been performed with mammalian cells forming chemical synapses which can exhibit plastic changes. The presented work represents a step into the direction of such systems that will allow to monitor synaptic plasticity over longer periods of time on the level of single cells.

10. Appendix

10.1 Applied Microstructures

The following table summarises the different types of microstructures that were applied in this thesis. As standard grid patterns, patterns A and B were used while pattern C was the line pattern applied. Patterns E-I were designed for the induction of neuronal polarity as described in chapter 7.

Name	Structure	Dimensions	Scheme
A	Grid 1	Lines: 4 µm Nodes: 12 µm Meshes: 100 x 50 µm	
B	Grid 2	Lines: 6 µm Nodes: 14 µm Meshes: 100 x 50 µm	
C	Lines with node points	Lines: 4 µm Nodes: 22 µm Line distance: 50 µm Node distance: 100 µm	
D	Grid with interruptions 1	Lines: 4 µm Nodes: 22 µm Interruptions: 1 µm Meshes: 100 x 50 µm	
E	Grid with interruptions 2	Lines: 4 µm Nodes: 22 µm Interruptions: 2 µm Meshes: 100 x 50 µm	
F	Grid with interruptions 3	Lines: 2 µm Nodes: 10 µm Interruptions: 2 µm Meshes: 100 x 50 µm	
G	Grid with interruptions 4	Lines: 4 µm Nodes: 22 µm Interruptions: 5 µm Meshes: 100 x 50 µm	
H	Grid with interruptions 5	Lines: 4 µm Nodes: 22 µm Interruptions: 5 µm Meshes: 100 x 50 µm	
I	Grid with interruptions 6	Lines: 2 µm Nodes: 10 µm Interruptions: 5 µm Meshes: 100 x 50 µm	

10.2 Abbreviations

13 F	Tridecafluoro-1,1,2,2-tetrahydroctyl-1-dimethylchlorosilane
AMPA	α-amino-3-hydroxy-5-methyl-4-isoxalone proprionic acid
AP	Action potential
APV	2-amino-5-phosphonovaleric acid
ATP	Adenosine-triphosphate
CAD	Computer Aided Design
CC	Current Clamp
CNS	Central nervous system
CNQX	6-Cyano-7-nitroquinoxaline-2,3-dione
DAPI	4,6-Diamidino-2-Phenylindole
DETA	Trimethoxysilyl-propyldiethylenetriamine
DIV	Days in vitro
ECM	Extracellular matrix
FET	Field effect transistor
FGF	Fibroblast growth factor
FITC	Fluorescein
GABA	γ-Aminobutyric acid
MEA	Multi-electrode-array
NMDA	N-methyl-D-aspartate
PECM	Mixture of polylysine (10 μg / ml) and ECM-gel (1:100 of stock)
PL	Mixture of polylysine and laminin, 12.5 μg / ml each
PNS	Peripheral nerve system
UV	Ultraviolet
VC	Voltage Clamp

11. Literature

Adler, R., Jerdan, J, Hewitt, AT. Responses of cultured neural retinal cells to substratum-bound laminin and other extracellular matrix molecules. *Developmental Biology* **1985**, 112, (1) 100-114.

Alger, B., Teyler, TJ Long-term and short-term plasticity in the CA1, CA3, and dentate regions of the rat hippocampal slice *Brain Research* **1976**, 110, (3) 463-480.

Banker, G., Goslin, K *Culturing Nerve Cells*; MIT press: Cambridge MA, 1991.

Bear, M., Kirkwood, A Neocortical long-term potentiation *Current Opinion in Neurobiology* **1993**, 3, (2) 197-202.

Beecher, K., Andersen, TT, Fenton, JW Thrombin receptor peptides induce shape change in neonatal murine astrocytes in culture. *Journal of Neuroscience Research* **1994**, 37, (1) 108-115.

Bernstein, J. Untersuchungen zur Thermodynamik der bioelektrischen Ströme. Erster Theil *Pflugers Archiv* **1902**, 92, 521-562.

Bi, G., Poo, MM. Synaptic modifications in cultured hippocampal neurons: dependence on spike timing, synaptic strength, and postsynaptic cell type. *Journal of Neuroscience* **1998**, 18, (24) 10464-10472.

Bi, G.; Poo, M. Distributed synaptic modification in neural networks induced by patterned stimulation *Nature* **1999**, 401, (6755) 792-796.

Bi, G., Poo, MM. Synaptic modification by correlated activity: Hebb's postulate revisited *Annual Review of Neuroscience* **2001**, 24, 139-166.

Bienenstock, E., Cooper, LN, Munro, PW Theory for the development of neuron selectivity: orientation specificity and binocular interaction in visual cortex *Journal of Neuroscience* **1982**, 2, (1) 32-48.

Bliss, T., Lomo, T Long-lasting potentiation of synaptic transmission in the dentate of the anesthesized rabbit following stimulation of the perforant path *Journal of Physiology* **1973**, 232, 331-356.

Bon, C., Garthwaite, J On the role of nitric oxide in hippocampal long-term potentiation *Journal of Neuroscience* **2003**, 23, (5) 1941-1948.

Branch, D. W.; Corey, J. M.; Weyhenmeyer, J. A.; Brewer, G. J.; Wheeler, B. C. Microstamp patterns of biomolecules for high-resolution neuronal networks *Medical & Biological Engineering & Computing* **1998**, 36, (1) 135-141.

Branch, D. W.; Wheeler, B. C.; Brewer, G. J.; Leckband, D. E. Long-term maintenance of patterns of hippocampal pyramidal cells on substrates of polyethylene glycol and microstamped polylysine *IEEE Transactions on Biomedical Engineering* **2000**, 47, (3) 290-300.

Branch, D. W.; Wheeler, B. C.; Brewer, G. J.; Leckband, D. E. Long-term stability of grafted polyethylene glycol surfaces for use with microstamped substrates in neuronal cell culture *Biomaterials* **2001**, 22, (10) 1035-1047.

Brewer, G. J.; Torricelli, J. R.; Evege, E. K.; Price, P. J. Optimized survival of hippocampal neurons in B27-supplemented Neurobasal, a new serum-free medium combination *Journal of Neuroscience Research* **1993**, 35, (5) 567-576.

Britland, S., Morgan, H, Wojiak-Stodart, B, Riehle, M, Curtis, A, Wilkinson, C Synergistic and hierarchical adhesive and topographic guidance of BHK cells *Experimental Cell Research* **1996**, 228, (2) 313-325.

Brocher, S., Artola, A, Singer, W Intracellular injection of Ca2+ chelators blocks

induction of long-term depression in rat visual cortex *Proceedings of the National Academy of Sciences of the United States of America* **1992**, 89, 123-127.

Brusés, J. Cadherin-mediated adhesion at the interneuronal synapse *Current Opinion in Cell Biology* **2000**, 12, 593-597.

Burden Gulley, S., Payne, HR, Lemmon, V Growth cones are actively influenced by substrate-bound adhesion molecules *Journal of Neuroscience* **1995**, 15, (6) 4370-4381.

Bush, P., Sejnowski, T Inhibition synchronizes sparsely connected cortical neurons within and between columns in realistic network models *Journal of Computational Neuroscience* **1996**, 3, (2) 91-110.

Calof, A., Lander, AD Relationship between neuronal migration and cell-substratum adhesion: laminin and merosin promote olfactory neuronal migration but are anti-adhesive *Journal of Cell Biology* **1991**, 115, (3) 779-794.

Carter, S. Principles of Cell Motility- Direction of Cell Movement and Cancer Invasion *Nature* **1965**, 208, 1183-1185.

Cestelli, A., Savettieri, G, Salemi, G, Di Liegro, I Neuronal cell cultures: a tool for investigations in developmental neurobiology *Neurochemical Research* **1992**, 17, (12) 1163-1180.

Chamak, B., Prochiantz, A Influence of extracellular matrix proteins on the expression of neuronal polarity *Development* **1989**, 106, (3) 483-491.

Chang, J., Brewer, GJ, Wheeler, BC Modulation of neural network activity by patterning *Biosens Bioelectron* **2001**, 7-8, (16) 527-533.

Chang, J. C., Brewer, Gregory J., Wheeler, Bruce C. Modulation of neural network activity by patterning *biosensors and bioelectronics* **2001**, 7-8, (16) 527-533.

Chavis, P., Westbrook, G Integrins mediate functional pre- and postsynaptic maturation at a hippocampal synapse *Nature* **2001**, 411, 317-321.

Chen, C., Mrksich, M, Huang,S, Whitesides, GM, Inber, DE Micropatterned Surfaces for Control of Cell Shape, Position, and Function *Biotechnology Progress* **1998**, 14, (3) 356-363.

Cole, K., Curtis, HJ Electrical impedance of *Nitella* during activity *Journal of General Physiology* **1938**, 22, 37-64.

Cole, K., Curtis, HJ Electrical impedance of the squid giant axon during activity *Journal of general physiology* **1939**, 22, 649-670.

Corey, J. M.; Wheeler, B. C.; Brewer, G. J. Compliance of hippocampal neurons to patterned substrate networks *Journal of Neuroscience Research* **1991**, 30, (2) 300-307.

Corey, J. M.; Wheeler, B. C.; Brewer, G. J. Micrometer resolution silane-based patterning of hippocampal neurons: critical variables in photoresist and laser ablation processes for substrate fabrication *IEEE Transactions on Biomedical Engineering* **1996**, 43, (9) 944-955.

Curtis, A., Wilkinson, CD Topographical control of cells *Biomaterials* **1997**, 18, (24) 1573-1583.

Curtis, A., Wilkinson, CD Reactions of cells to topography *Journal of Biomaterials Science, Polymer Edition* **1998**, 9, (12) 1313-1329.

Curtis, A.; Riehle, M. Tissue engineering: the biophysical background *Physics in Medicine & Biology* **2001**, 46, (4) R47-65.

Curtis, A. Breaking the neural code *nature* **2002**, (416) 274-275.

Dallwig, R., Deitmer, JW, Backus, KH On the mechanism of GABA-induced currents in cultured rat cortical neurons *Pflügers Archives - European Journal of Physiology* **1999**, 437, 298-297.

delCastillo, J., Katz, B Statistical factors involved in neuromuscular facilitation and depression *Journal of Physiology* **1954**, 124, 574_585.

Denyer, M., Britland, ST, Curtis, ASG, Wilkinson, CDW Patterning living neural networks on microfabricated microelectronic electrophysiological recording devices *cellular engineering* **1997**, 2, (4) 122-131.

Dotti, C., Banker, GA Experimentally induced alteration in the polarity of developing neurons *Nature* **1987**, 330, (6145) 254-256.

Douglas, R., Martin, KA Neuronal networks. Vibrations in the memory *Nature* **1995**, 373, (6515) 563-564.

Douglas, R., Koch, C, Mahowald, M, Martin, KA, Suarez, HH Recurrent excitation in neocortical circuits *Science* **1995**, 269, (5226) 981-985.

Dutly, F., Schwab, ME Neurons and astrocytes influence the development of purified O-2A progenitor cells *Glia* **1991**, 4, (6) 559-571.

Eckert, R., Adams, B, Kistler, J, Donaldson, P Quantitative determination of gap junctional permeability in the lens cortex *Journal of Membrane Biology* **1999**, 169, (2) 91-102.

Elgersma, Y., Fedorov, NB, Ikonen, S, Choi, ES, Elgersma, M, Carvalho, OM, Giese, KP, Silva, AJ. Inhibitory autophosphorylation of CaMKII controls PSD association, plasticity, and learning *Neuron* **2002**, 36, (3) 493-505.

Fitzsimonds, R. M.; Song, H. J.; Poo, M. M. Propagation of activity-dependent synaptic depression in simple neural networks. [see comments] *Nature* **1997**, 388, (6641) 439-448.

Furshpan, E., Potter, DD Transmission at the giant motorsynapse of the crayfish *Journal of Physiology* **1959**, 145, 289-325.

Galarreta, M., Hestrin, S Frequency-dependent synaptic depression and the balance of excitation and inhibition in the neocortex *Nature Neuroscience* **1998**, 1, (7) 587-594.

Galarreta, M., Hestrin, S A network of fast-spiking cells in the neocortex connected by electrical synapses *Nature* **1999**, 402, (6757) 72-75.

Ganguly, K.; Kiss, L.; Poo, M. Enhancement of presynaptic neuronal excitability by correlated presynaptic and postsynaptic spiking *Nature Neuroscience* **2000**, 3, (10) 1018-1026.

Gauer, D. Diploma, Ruhr-Universität, Bochum, 1997.

Gibson, J., Beierlein, M, Connors, BW Two networks of electrically coupled inhibitory neurons in neocortex *Nature* **1999**, 402, (6757) 75-79.

Goldberger, A., Flaherty, P *Use of ECM Proteins to Optimize Neuronal Cell Function in Vitro*; John Wiley & Sons Ltd.: Bedford, 1999.

Golshani, P., Jones, EG Synchronized Paroxysmal Activity in the Developing Thalamocortical Network Mediated by Corticothalamic Projections and "Silent" Synapses *Journal of Neuroscience* **1999**, 19, (8) 2865-2875.

Gross, G. A new fixed-array multi-electrode system designed for long-term monitoring of extracellular single unit neuronal activity in vitro *Neuroscience Letters* **1977**, 6, 101-105.

Hammarback JA, P. S., Furcht LT, Letourneau PC. Guidance of neurite outgrowth by pathways of substratum-adsorbed laminin. *Journal of Neuroscience* **1985**, 13, (1-2) 213-220.

Harris, E., Cotman, CW Long-term potentiation of guinea pig mossy fiber responses is not blocked by N-methyl D-aspartate antagonists *Neuroscience Letters* **1986**, 70, (1) 132-137.

Harrison, R. Observations on the living developing nerve fiber *Anatomical Record* **1907**, 1, 116-118.

Hebb, D. *The organization of Behavior*; Wiley: New York, 1949.

Hermann, L. Zur Theorie der Erregungsleitung und der elektrischen Erregung *Pflugers Archiv* **1872**, 75, 574-590.

Hermann, L. Beiträge zur Physiologie und Physik des Nerven *Pflugers Archiv* **1905**, 109, 95-144.

Hille, B. *Ion Channels and Excitable Membranes*, 3 ed.; Sinauer Associates: Sunderland, Massachusetts, 2001.

Hodgkin, A., Katz, B The effect of sodium ions on the electrical activity of the giant axon of the squid *Journal of Physiology* **1949**, 108, 37-77.

Hodgkin, A., Huxley, AF, Katz, B Ionic currents underlying activity in the giant axon of the squid *Arch Sci Physiol* **1949**, 3, 129-150.

Hodgkin, A., Huxley, AF, Katz, B Measurements of current-voltage relations in the membrane of the giant axon of *Loligo Journal of Physiology* **1952**, 116, 424-448.

Honore, T., Davies, SN, Drejer, J, Fletcher, EJ, Jacobsen, P, Lodge, D, Nielsen, FE Quinoxalinediones: Potent competitive non-NMDA glutamate receptor antagonists *Science* **1988**, 241, 701.

Ingebrandt, S., Yeung, CK, Staab, W, Zetterer, T, Offenhausser, A Backside contacted field effect transistor array for extracellular signal recording *Biosensors and Bioelectronics* **2003**, 18, (4) 429-435.

Isbister, C., O'Connor, TP Filopodial adhesion does not predict growth cone steering events in vivo *Journal of Neuroscience* **1999**, 19, (7) 2589-2600.

Jimbo, Y., Robinson, HP, Kawana, A Simultaneous measurement of intracellular calcium and electrical activity from patterned neural networks in culture *IEEE Transactions on Biomedical Engineering* **1993**, 40, (8) 804-810.

Joshi, I., Wang, LY Developmental profiles of glutamate receptors and synaptic transmission at a single synapse in the mouse auditory brainstem *Journal of Physiology* **2002**, 540, (Pt 3) 861-873.

Kandel, E., Schwartz, JH, Jessel, TM *Principles of Neural Science*, 4 ed.; McGraw-Hill, 2000.

Kast, B. The best supporting actors *Nature* **2001**, 412, (6848) 674-676.

Katz, B., Miledi, R The role of calcium in neuromuscular facilitation *Journal of Physiology* **1968**, 195, (2) 481-492.

Keefer, E., Gramowski, A, Gross, GW NMDA receptor-dependent periodic oscillations in cultured spinal cord networks *Journal of Neurophysiology* **2001**, 86, (6) 3030-3042.

Kirkwood, A., Dudek, SM, Gold, JT, Aizenman, CD, Bear, MF Common forms of synaptic plasticity in the hippocampus and neocortex in vitro *Science* **1993**, 260, (5113) 1518-1521.

Kirkwood, A., Bear, MF Hebbian synapses in visual cortex *Journal of Neuroscience* **1994**, 14, (3 Pt 2) 1634-1645.

Kirkwood, A., Bear, MF Elementary forms of synaptic plasticity in the visual cortex *Biological Research* **1995**, 28, (1) 73-80.

Kirkwood, A., Rioult, MC, Bear, MF Experience-dependent modification of synaptic plasticity in visual cortex *Nature* **1996**, 381, (6582) 526-528.

Kleinfeld, D., Kahler, KH, Hockberger, PE Controlled outgrowth of dissociated neurons on patterned substrates *Journal of Neuroscience* **1988**, 8, (11) 4098-4120.

Komatsu, Y., Nakajima, S, Toyama, K, Fetz, EE. Intracortical connectivity revealed by spike-triggered averaging in slice preparations of cat visual cortex *Brain Research* **1988**, 442, (2) 359-362.

Kopell, N., LeMasson, G Rhythmogenesis, amplitude modulation and multiplexing in a cortical architecture *Proceedings of the National Academy of Sciences of the United States of America* **1994**, 91, 10586-10590.

Kullmann, D., Siegelbaum, SA The site of expression of NMDA receptor-dependent LTP: new fuel for an old fire *Neuron* **1995**, 15, (5) 997-1002.

Kumar, A., Whitesides, GM Features of Gold Having Micrometer to Centimeter Dimensions Can Be Formed through a Combination of Stamping with an Elastomeric Stamp and an Alkanethiol Ink Followed by Chemical Etching *Applied Physics Letters* **1993**, 63, 2002-2003.

Lauer, L.; Klein, C.; Offenhausser, A. Spot compliant neuronal networks by structure optimized micro-contact printing *Biomaterials* **2001**, 22, (13) 1925-1932.

Lauer, L.; Ingebrandt, S.; Scholl, M.; Offenhausser, A. Aligned microcontact printing of biomolecules on microelectronic device surfaces *IEEE Transactions on Biomedical Engineering* **2001**, 48, (7) 838-842.

Lauer, L., Johannes Gutenberg-Universität, Mainz, 2001.

Lauer, L.; Vogt, A.; Yeung, C.; Knoll, W.; Offenhausser, A. Electrophysiological recordings of patterned rat brain stem slice neurons *Biomaterials* **2002**, 23, (15) 3123-3130.

Lein PJ, H. D. Laminin and a basement membrane extract have different effects on axonal and dendritic outgrowth from embryonic rat sympathetic neurons in vitro. *Developmental Biology* **1989**, 136, (2) 330-345.

Lemmon, V., Burden, SM, Payne, HR, Elmslie, GJ, Hlavin, ML Neurite growth on different substrates: permissive versus instructive influences and the role of adhesive strength *Journal of Neuroscience* **1992**, 12, (3) 818-826.

Letourneau, P. Cell-to-Substratum adhesion and Guidance of Axonal Elongation *Developmental Biology* **1975**, 44, 92-101.

Letourneau, P. C.; Condic, M. L.; Snow, D. M. Interactions of developing neurons with the extracellular matrix *Journal of Neuroscience* **1994**, 14, (3 Pt 1) 915-928.

Liu, Q.; Coulombe, M.; Dumm, J.; Shaffer, K.; Schaffner, A.; Barker, J.; Pancrazio, J.; Stenger, D.; Ma, W. Synaptic connectivity in hippocampal neuronal networks cultured on micropatterned surfaces *Developmental Brain Research* **2000**, (120) 223-231.

Llano, I., Gerschenfeld, HM Inhibitory synaptic currents in stellate cells of rat cerebellar slices *Journal of Physiology* **1993**, 468, 177-200.

Lledo, P., Zhang, X, Sudhof, TC, Malenka, RC, Nicoll, RA Postsynaptic membrane fusion and long-term potentiation *Science* **1998**, 279, (5349) 399-403.

Lopez, J. Don't forget about the presynaptic terminal *Nature Reviews Neuroscience* **2001**, 2, 458.

Lynch, G., Larson, J, Kelso, S, Barrionuevo, G, Schottler, F Intracellular injections of EGTA block induction of hippocampal long-term potentiation *Nature* **1983**, 305, (5936) 719-721.

Ma, W.; Liu, Q. Y.; Jung, D.; Manos, P.; Pancrazio, J. J.; Schaffner, A. E.; Barker, J. L.; Stenger, D. A. Central neuronal synapse formation on micropatterned surfaces *Brain Research. Developmental Brain Research* **1998**, 111, (2) 231-243.

Maccaferri, G., Toth, K, McBain, CJ Target-specific expression of presynaptic mossy fiber plasticity *Science* **1998**, 279, (5355) 1368-1370.

Madison, D., Malenka, RC, Nicoll, RA Mechanisms Underlying Long-Term Potentiation of Synaptic Transmission *Annual Review of Neuroscience* **1991**, 14, 379-397.

Maher, M., Pine, J, Wright, J, Tai, YC The neurochip: a new multielectrode device for stimulating and recording from cultured neurons. *J Neurosci Methods* **1999**, 1, (87) 45-56.

Maher, M., Dvorak Carbone, H, Pine, J, Wright, JA, Tai, YC Microstructures for studies of cultured neural networks *Med Biol Eng Comput* **1999**, 1, (37) 110-118 Med Biol Eng Comput.

Makohliso, S., Valentini, RF, Aebischer, P Magnitude and Polarity of a fluoroethylene-propylene electret substrate charge influences neurite outgrowth in vitro *Journal of Biomedical Materials Research* **1993**, 27, 1075-1085.

Makowski, L., Caspar, DL, Phillips, WC, Goodenough, DA Gap junction structures. II. Analysis of the x-ray diffraction data *Journal of Cell Biology* **1977**, 74, (2) 629-645.

Makram, H., Lübke, J, Frotscher, M, Sakmann, B Regulation of Synaptic Efficacy by Coincidence of Postsynaptic APs and EPSPs *Science* **1997**, 275, 213-215.

Malenka, R., Nicoll, RA Long-Term Potentiation- A Decade of Progress? *Science* **1999**, 285, 1870-1874.

Mallart, A., Martin, AR Two components of facilitation at the neuromuscular junction of the frog *Journal of Physiology* **1967**, 191, (1) 19P-20P.

Mallart, A., Martin, AR The relation between quantum content and facilitation at the neuromuscular junction of the frog *Journal of Physiology* **1968**, 196, (3) 593-604.

Manor, Y., Nadim, F, Epstein, S, Ritt, J, Marder, E, Kopell, N Network oscillations generated by balancing graded asymmetric reciprocal inhibition in passive neurons *Journal of Neuroscience* **1999**, 19, (7) 2765-2779.

Markram, H., Tsodyks, M Redistribution of synaptic efficacy between neocortical pyramidal neurons *Nature* **1996**, 382, (6594) 807-810.

Martin, G., Timpl, R Laminin and other basement membrane components *Annual Reviews in Cell Biology* **1987**, 3, 57-85.

Mauch, D., Naegler, K, Schumacher, S, Goeritz, C, Mueller, E-C, Otto, A, Pfrieger, FW CNS Synaptogenesis Promoted by Glia-Derived Cholesterol *Science* **2001**, 294, 1354-1357.

McMahon, L., Kauer, JA Hippocampal interneurons express a novel form of synaptic plasticity *Neuron* **1997**, 18, (2) 295-305.

Mellitzer, G., Xu, Q, Wilkinson, DG Eph receptors and ephrins restrict cell intermingling and communication *Nature* **1999**, 400, 77-81.

Merz, M., Fromherz, P Polyester Microstructures for Topographical Control of Outgrowth and Synapse Formation of Snail Neurons *Advanced Materials* **2002**, 2, (14) 141-144.

Metherate, R., Ashe, JH Facilitation of an NMDA receptor-mediated EPSP by paired-pulse stimulation in rat neocortex via depression of GABAergic IPSPs *Journal of Physiology* **1994**, 481, (Pt 2) 331-348.

Minota, S., Kumamoto, E, Kitakoga, O, Kuba, K Long-term potentiation induced by a sustained rise in the intraterminal Ca2+ in bull-frog sympathetic ganglia *Journal of Physiology* **1991**, 435, 421_438.

Misgeld, U., Zeilhofer, HU, Swandulla, D Synaptic modulation of oscillatory activity of hypothalamic neuronal networks in vitro *Cellular and Molecular Neurobiology* **1998**, 18, (1) 29-43.

Muller, T., Swandulla, D, Zeilhofer, HU Synaptic connectivity in cultured hypothalamic neuronal networks *Journal of Neurophysiology* **1997**, 77, (6) 3218-3225.

Neher, E., Sakmann, B Single-channel currents recorded from membrane of

denervated frog muscle fibres *Nature* **1976**, 260, 779-802.

Nicholls, J., Martin, RA, Wallace, BG, Fuchs, PA *From Neuron to Brain*, 4 ed.; Sinauer Associates, 2001.

Nicoll, R., Malenka, RC Contrasting properties of two forms of long-term potentiation in the hippocampus *nature* **1995**, 377, (6545) 115-118.

Nusser, Z., Lujan, R, Laube, G, Roberts, JD, Molnar, E, Somogyi, P Cell type and pathway dependence of synaptic AMPA receptor number and variability in the hippocampus *neuron* **1998**, 21, (3) 545-559.

O'Donovan, M. The origin of spontaneous activity in developing networks of the vertebrate nervous system *Current Opinion in Neurobiology* **1999**, 9, (1) 94-104.

Ohno, M., Frankland, PW, Silva, AJ A pharmacogenetic inducible approach to the study of NMDA/alphaCaMKII signaling in synaptic plasticity *Current Biology* **2002**, 12, (8) 654-656.

Otsu, Y., Kimura, F, Tsumoto, T Hebbian induction of LTP in visual cortex: perforated patch-clamp study in cultured neurons *Journal of Neurophysiology* **1995**, 74, (6) 2437-2444.

Ouardouz, M., Sastry, BR Mechanisms underlying LTP of inhibitory synaptic transmission in the deep cerebellar nuclei *Journal of Neurophysiology* **2000**, 84, (3) 1414-1421.

Pfrieger, F., Barres, BA Synaptic Efficacy Enhanced by Glia Cells in Vitro *Science* **1997**, 277, 1684-1687.

Pine, J. Recording action potentials from cultured neurons with extracellular microcircuit electrodes *Journal of Neuroscience Methods* **1980**, 2, (1) 19-31.

Plenz, D., Aertsen, A Neural Dynamics in Cortex-Striatum Co-Cultures- II. Spatiotemporal Characteristics of Neuronal Activity *Neuroscience* **1996**, 70, (4) 893-924.

Poser, S., Storm, DR Role of Ca2+-stimulated adenylyl cyclases in LTP and memory formation. *International Journal of Developmental Neuroscience* **2001**, 19, (4) 387-394.

Pouzat, C., Marty, A Autaptic inhibitory currents recorded from internueorones in rat cerebellar slices *Journal of Physiology* **1998**, 509, (3) 777-783.

Prinz, A. A.; Fromherz, P. Electrical synapses by guided growth of cultured neurons from the snail Lymnaea stagnalis *Biological Cybernetics* **2000**, 82, (4) L1-5.

Ranscht, B. Cadherins: molecular codes for axon guidance and synapse formation *International Journal of Developmental Neuroscience* **2000**, 18, 643-651.

Ravenscroft, M. S., Bateman, K. E., Shaffer, K. M., Schessler, H. M., Jung, D. R., Schneider, T. W., Montgomery, C. B., Custer, T. L. , Schaffner, A. E., Liu, Q. Y., Li, Y. X., ; Barker, J. L. a. H. J. J. Developmental Neurobiology Implications from Fabrication and Analysis of Hippocampal Neuronal Networks on

Patterned Silane-Modified Surfaces *Journal of the American Chemical Society* **1998**, 120, (47) 12169-12177.

Rebel, G., Haynes, L, Lelong, IH *Nerve Cell Culture Methodology: the Medium Environment*; Wiley, J & Sons Ltd., 1999.

Rebiere, A., Dainat, J, Bisconte, JC Autoradiographic study of neurogenesis in the duck olfactory bulb *Brain Research* **1983**, 282, (2) 113-122.

Redman, S. Quantal Analysis of Synaptic Potentials in Neurons of the Central Nervous System *Physiological Reviews* **1990**, 70, (1) 165-198.

Reichardt, L. F.; Tomaselli, K. J. Extracellular matrix molecules and their receptors: functions in neural development *Annual Review of Neuroscience* **1991**, 14, 531-570.

Roberts, A., Tunstall, MJ, Wolf, E Properties of networks controlling locomotion and significance of voltage dependency of NMDA channels: stimulation study of rhythm generation sustained by positive feedback *Journal of Neurophysiology* **1995**, 73, (2) 485-495.

Rosenberg, M. Cell Guidance by Alterations in Monomolecular Films *Science* **1963**, 139, 411-412.

Rosenthal, J. Post-tetanic potentiation at the neuromuscular junction of the frog *Journal of Physiology* **1969**, 203, (1) 121-133.

Rovainen, C. Physiological and anatomical studies on large neurons of central nervous system of the sea lamprey (Petromyzon marinus). II. Dorsal cells and giant interneurons *Journal of Neurophysiology* **1967**, 30, (5) 1024-1042.

Sachs, L. *Angewandte Statistik*, 6 ed.; Springer, 1983.

Sanes, J. R. Roles of extracellular matrix in neural development *Annual Review of Physiology* **1983**, 45, 581-600.

Sanes, J. R. Extracellular matrix molecules that influence neural development *Annual Review of Neuroscience* **1989**, 12, 491-516.

Sanes, J., Lichtman, JW Can molecules explain long-term potentiation? *Nature Neuroscience* **1999**, 2, (7) 597-604.

Schneggenburger, R., Lopez-Barneo, J, Konnerth, A Excitatory and inhibitory synaptic currents and receptors in rat medial septal neurones. *Journal of Physiology* **1992**, 445, 261-276.

Scholl, M.; Sprossler, C.; Denyer, M.; Krause, M.; Nakajima, K.; Maelicke, A.; Knoll, W.; Offenhausser, A. Ordered networks of rat hippocampal neurons attached to silicon oxide surfaces *Journal of Neuroscience Methods* **2000**, 104, (1) 65-75.

Schwartzkroin, P., Wester, K Long-lasting facilitation of a synaptic potential following tetanization in the in vitro hippocampal slice *Brain Research* **1975**, 89, (1) 107-119.

Selkoe, D. Alzheimer's Disease Is a Synaptic Failure *Science* **2002**, 298, 789-791.

Shapovalov, A., Shiriaev, BI Dual mode of junctional transmission at synapses between single primary afferent fibres and motoneurones in the amphibian *Journal of Physiology* **1980**, 306, 1-15.

Shew, T., Yip, S, Sastry, BR Mechanisms involved in tetanus-induced potentiation of fast IPSCs in rat hippocampal CA1 neurons *Journal of Neurophysiology* **2000**, 83, (6) 3388-3401.

Shi, S., Hayashi, Y, Petralia, RS, Zaman, SH, Wenthold, RJ, Svoboda, K, Malinow, R Rapid spine delivery and redistribution of AMPA receptors after synaptic NMDA receptor activation *Science* **1999**, 284, (5421) 1811-1816.

Sil'kis, I. Excitatory interactions in neuronal networks which include cells of the auditory cortex and the medial geniculate body *Neuroscience and Behavioral Physiology* **1995**, 25, (6) 462-473.

Sil'kis, I. Inhibitory interactions in neuronal networks including cells of the auditory cortex and the medial geniculate body *Neuroscience and Behavioral Physiology* **1996**, 26, (1) 62-72.

Son, Y. J.; Patton, B. L.; Sanes, J. R. Induction of presynaptic differentiation in cultured neurons by extracellular matrix components *European Journal of Neuroscience* **1999**, 11, (10) 3457-3467.

Son, Y. J.; Patton, B. L.; Sanes, J. R. Induction of presynaptic differentiation in cultured neurons by extracellular matrix components *European Journal of Neuroscience* **1999**, 11, (10) 3457-3467.

Stenger, D. A.; Hickman, J. J.; Bateman, K. E.; Ravenscroft, M. S.; Ma, W.;

Pancrazio, J. J.; Shaffer, K.; Schaffner, A. E.; Cribbs, D. H.; Cotman, C. W. Microlithographic determination of axonal/dendritic polarity in cultured hippocampal neurons *Journal of Neuroscience Methods* **1998**, 82, (2) 167-173.

Stoeckli, E. T.; Ziegler, U.; Bleiker, A. J.; Groscurth, P.; Sonderegger, P. Clustering and functional cooperation of Ng-CAM and axonin-1 in the substratum-contact area of growth cones *Developmental Biology* **1996**, 177, (1) 15-29.

Suidan, H., Nobes, CD, Hall, A, Monard, D Astrocyte spreading in response to thrombin and lysophosphatidic acid is dependent on the Rho GTPase. *Glia* **1997**, 21, (2) 244-252.

Tai, H., Buettner, HM Neurite Outgrowth and Growth Cone Morphology on Micropatterned Surfaces *Biotechnology Progress* **1998**, 14, 364-370.

Takumi, Y., Ramirez-Leon, V, Laake, P, Rinvik, E, Ottersen, OP Different modes of expression of AMPA and NMDA receptors in hippocampal synapses *Nature Neuroscience* **1999**, 2, (7) 618-624.

Taschenberger, H., von Gersdorff, H Fine-tuning an auditory synapse for speed and fidelity: developmental changes in presynaptic waveform, EPSC kinetics, and synaptic plasticity *Journal of Neuroscience* **2000**, 20, (24) 9162-9173.

Thiebaud, P., de Rooij, NF, Koudelka-Hep, M, Stoppini, L. Microelectrode arrays for electrophysiological monitoring of hippocampal organotypic slice cultures *IEEE Transactions on Biomedical Engineering* **1997**, 44, (11) 1159-1163.

Thiebaud, P.; Lauer, L.; Knoll, W.; Offenhausser, A. PDMS device for patterned application of microfluids to neuronal cells arranged by microcontact printing *Biosensors and Bioelectronics* **2002**, 17, (1-2) 87-93.

Thomas, C. J., Springer, PA, Loeb, GE, Berwald-Netter, Y, Okun, LM. A miniature microelectrode array to monitor the bioelectric activity of cultured cells *Experimental Cell Research* **1972**, 74, (1) 61-66.

Thomson, A. Facilitation, augmentation and potentiation at central synapses *Trends in Neurosciences* **2000**, 23, (7) 305-312.

Thomson, A. Neurotransmission: Chemical and electrical interneuron coupling *Current Biology* **2000**, 10, (3) R110-112.

Traub, O., Eckert, R, Lichtenberg-Frate, H, Elfgang, C, Bastide, B, Scheidtmann, KH, Hulser, DF, Willecke, K Immunochemical and electrophysiological characterization of murine connexin40 and -43 in mouse tissues and transfected human cells *European Journal of Cell Biology* **1994**, 64, (1) 101-112.

van Vreeswijk, C., Abott, LF, Ermentrout GB When inhibition not excitation synchronises neuronal firing *Journal of Comparative Computer Science* **1994**, 1, (4).

Varela, J., Song, S, Turrigiano, GG, Nelson, SB Differential depression at excitatory and inhibitory synapses in visual cortex *Journal of Neuroscience* **1999**, 19, (11) 4293-4304.

Vlkolinsky, R., Stolc, S. Effects of stobadine, melatonin, and other antioxidants on hypoxia/reoxygenation-induced synaptic transmission failure in rat hippocampal slices. *Brain Research* **1999**, 850, 118-126.

Wahle, P., Muller, TH, Swandulla, D Characterization of neurochemical phenotypes in cultured hypothalamic neurons with immunohistochemistry and in situ hybridization *Brain Research* **1993**, 611, (1) 37-45.

Weisskopf, M., Castillo, PE, Zalutsky, RA, Nicoll, RA Mediation of hippocampal mossy fiber long-term potentiation by cyclic AMP *Science* **1994**, 265, (5180) 1878-1882.

Wheeler, B., Corey, JM, Brewer, GJ, Branch, DW Microcontact printing for precise control of nerve cell growth in culture *Journal of Biomechanical Engineering* **1999**, 121, (1) 73-78.

Whittington, M., Traub, RD, Jefferys, JG Synchronized oscillations in interneuron networks driven by metabotropic glutamate receptor activation *Nature* **1995**, 373, (6515) 612-615.

Wyart, C., Ybert, C, Bourdieu, L, Herr, C, Prinz, C, Chatenay, D Constrained synaptic connectivity in functional mammalian neuronal networks grown on patterned surfaces *Journal of Neuroscience Methods* **2002**, 117, 123_131.

Yeung, C. K.; Lauer, L.; Offenhausser, A.; Knoll, W. Modulation of the growth and guidance of rat brain stem neurons using patterned extracellular matrix proteins. [erratum appears in Neurosci Lett 2001 Jun 15;305(3):208.] *Neuroscience Letters* **2001**, 301, (2) 147-150.

Yoshikawa, S., McKinnon, D.R., Kokel, M, Thomas, JB Wnt-mediated axon guidance via the Drosophila Derailed receptor *Nature* **2003**, 422, 583-588.

Zakharenko, S., Zablow, L, Siegelbaum, SA Visualization of changes in presynaptic function during long-term synaptic plasticity *Nature Neuroscience* **2001**, 4, (7) 711-717.

Zeck, G., Fromherz, P Noninvasive neuroelectronic interfacing with synaptically connected snail neurons immobilized on a semiconductor chip *Proceedings of the National Academy of Sciences of the United States of America* **2001**, 98, (18) 10457-10462.

Table of contents